Design of a Proton Therapy Synchrotron

June, 1986

Conceptual Design of a Proton Therapy Synchrotron For Loma Linda University Medical Center

Fermi National Accelerator Laboratory

June, 1986

CONTRIBUTORS TO THE STUDY

LOMA LINDA UNIVERSITY MEDICAL CENTER

J. Archambeau
D. Farley
D. Miller
J. Slater
R. Lee (NBBJ, architects)

FERMI NATIONAL ACCELERATOR LABORATORY

M. Awschalom
D. Bart
F. Cole
C. Curtis
R. Dixon
N. Engler
G. Finstrom
W. Fowler
V. Fox
W. Freeman
A. Gonzales
R. Goodwin
J. Griffin
J. Jagger
M. Johnson
F. Krzich
A. Lennox
R. Lenz
P. Livdahl
C. Miller
F. Mills
A. Moretti
R. Niemann
A. Oleck
C. Owen
M. Palmer
A. Riddiford
M. Shea
S. Snowdon
L. Teng
R. Trendler
D. Young

HARVARD UNIVERSITY

B. Gottschalk
L. Verhey

UNIVERSITY OF WISCONSIN

D. Larson

UNIVERSITY OF CALIFORNIA

W. Chu

FERMI NATIONAL ACCELERATOR LABORATORY IS OPERATED BY UNIVERSITIES RESEARCH ASSOCIATION, INC. UNDER CONTRACT WITH THE UNITED STATES DEPARTMENT OF ENERGY. THIS STUDY WAS CARRIED OUT UNDER THE TECHNOLOGY-TRANSFER PROVISIONS OF THE STEVENSON-WYDLER ACT OF 1982 AND THE WORK-FOR-OTHERS POLICY OF THE DEPARTMENT OF ENERGY.

TABLE OF CONTENTS

1. INTRODUCTION

1.1 Overview of the Study

1.1.1 Summary

This document is the report of a conceptual design study of a proton synchrotron for medical therapy. The study has been sponsored by the Loma Linda University Medical Center and carried out by a group at the Fermi National Accelerator Laboratory. This report discusses the conceptual design of a synchrotron and of the associated treatment facilities. The performance parameters of the accelerator and facility are:

Particle	protons
Energy	70 - 250 MeV
Cycle Time	2 seconds; 0.5 sec acceleration, 1 sec beam spill, 0.5 sec to complete cycle
Beam Intensity	1.2×10^{11} protons per pulse; 10 nanoamperes time-average current
Treatment Facilities	4 treatment rooms with horizontal and vertical beams possible and 1 gantry room to give beam from angles through more than 180 degrees

The photograph on the facing page shows a model of the Loma Linda University Medical Center. The proton therapy accelerator is to be located below ground in the structure at the left side of the building.

The goal of a conceptual design study is to uncover and solve design problems and to demonstrate the feasibility of a complete design. The design presented here meets these goals. We present solutions to the design problems of the accelerator and show that it is feasible to meet the performance specifications given in the table above. No claim is made that the design is optimized; it is an example and further work is needed before construction begins.

A great deal of attention has been paid in the design to safety, flexibility, and reliability, because the facility discussed here is a clinical facility suitable for treatment of large numbers of patients, with large numbers of treatment rooms, not a research facility to treat small numbers of patients with beams limited in energy or adaptability. We consider this accelerator equivalent to the Harvard Cyclotron Laboratory, but with many more treatment facilities, more advanced beam control, and the availability of different energies to treat different depths in tissue.

The possibility of later switching to accelerating helium ions has not been excluded in our design, although a different injector and source would be needed. Doubly ionized helium ions (He^{++}) could be accelerated to the same total energy as protons, that is, to one-

fourth the energy per nucleon. No design effort on helium acceleration has been included in our study.

It should be noted that this conceptual design includes work on both the accelerator and the associated treatment facilities, but that the succeeding design work will not be equally concerned with both these aspects. There are many more Fermilab people expert in the design of accelerators than in the design of medical facilities. Fermilab expects to carry out the design and construction of the accelerator completely, but to work on the design and construction of the associated facility systems under more specific direction from the Loma Linda staff who will be directly concerned in the future with the clinical use of the facility.

1.1.2 Background

Cancer therapy using protons was first proposed by Robert Wilson in 1946 using the Bragg peak to localize the dose to the tissue being treated. The high localizability means that side effects are smaller than with neutrons. Protons also have advantages in high linear energy transfer (LET) to tissue, so that they are efficient killers of the oxygen-deficient cells in tumors. The damage done by a proton to a cancer cell is more uniform and less easily repaired than that of photons or electrons. There have been many years of successful clinical applications at Harvard University-Massachusetts General Hospital, the University of California in Berkeley, Sweden, several institutions in the USSR, and recently in Japan. The history of proton therapy is reviewed in an appendix to this report. All these applications have made use of accelerators originally built for physics research and adapted for medical therapy with great amounts of ingenuity and hard work. In many respects, the development of the field of proton therapy has been ahead of the diagnostic and alignment devices needed to work efficiently with protons, but the introduction of computerized tomography, magnetic resonance imaging, and laser alignment devices have helped the progress of proton therapy. There have been a number of conferences and workshops of physicians and physicists interested in therapy using protons. The clinical success and the development of associated instrumentation have awakened interest in a proton accelerator and associated treatment facility specifically designed for medical work, taking advantage of the high state of development of particle accelerators.

1.1.3 Features of the Design

The conceptual design presented here is based on a synchrotron, a particle accelerator in which the magnetic guide field is increased as the particles gain energy to keep them on a circle of constant radius. Synchrotrons are usually less expensive to build than cyclotrons or other kinds of accelerators of the same energy. Cyclotrons can accelerate many more particles than synchrotrons per unit time, but the accelerated intensity from a synchrotron is entirely adequate for therapy. A synchrotron has the great advantage of easy variability of final energy and it is planned to use this feature to deposit

energy uniformly throughout a given three-dimensional treatment volume.

The synchrotron we have designed is a ring approximately 20 feet in diameter. It is almost entirely built of off-the shelf components. It is perhaps unusual in a medical accelerator, although not in other hospital devices, that we give serious consideration to superconducting guide-field magnets. Successful superconducting synchrotron magnets have been built in large numbers at Fermilab and used in an operating synchrotron. Many of the participants in the study believe that a superconducting magnet system will have significant advantages in reliability, smoothness of beam spill, and operational cost. At the same time, other study participants have carried through the conceptual design of a conventional magnet system, and discuss it in the report. We plan to make the decision on magnet system after building models of the two systems to test them.

Injection into the synchrotron ring is planned to be from a commercially available electrostatic generator, the Pelletron manufactured by the National Electrostatics Company. It is also possible to make use of a radiofrequency quadrupole linear accelerator (RFQ) as an injector. We have not made a decision on whether to utilize a positive-ion accelerator or a charge-exchange system that will give higher injection energy and higher accelerated beam intensity and are planning tests to help in deciding the energy question of injection method.

In neither the magnet style or the injection method is there any question that a workable, feasible system can be built. Rather, we are optimizing the performance and cost of the system. After the magnet and injection choices are made, further detailed optimization of the design will be needed.

The treatment facilities are much larger in physical size than the accelerator itself. Extensive shielding is needed in each of the four treatment rooms and in the gantry room. There have been a number of meetings with the Loma Linda Center architects to work out the design of the treatment areas. The report also discusses the technical equipment needed for dose monitoring, safety, and patient alignment.

We also discuss the design of both foil-scattering (passive) and scanning (dynamic) beam-spreading systems to treat large fields. Traditionally, scattering systems have been used to make large fields, but they are quite inefficient in the use of protons. There have been recent advances in the development of scanning systems at the Lawrence Berkeley Laboratory and the facility design makes use of these advances. It will be possible to use either scattering or scanning systems in each treatment room.

Proper attention has also been paid in the design to the fact that the facility will be built in an area of seismic interest and that pieces of equipment and their mountings must meet the seismic code requirements of the State of California. The accelerator equipment is

not particularly heavy and the seismic code requirements do not have any noticeable impact on costs.

1.2 History of Fermilab Involvement with Particle-Beam Therapy

There has always been deep interest in particle-beam therapy at Fermilab, especially because Robert Wilson, who first proposed proton therapy, was the founding director of the laboratory. Because of the nature of the Fermilab high-energy accelerator system, there is time available on the injector accelerators after they have injected beam and while the main accelerator is carrying out its job. Wilson and his Fermilab colleagues Miguel Awschalom and Donald Young discussed the possibilities of using the linear accelerator injector for therapy. These discussions widened to include local Chicago-area radiation therapists. Together, the group presented a proposal to the National Cancer Institute for a facility in which patients could be irradiated with protons, neutrons, or negative pi mesons. The proposal was not accepted because of its cost and its location far from population centers.

Later, in 1975, the National Cancer Institute funded the operation of a neutron-therapy facility at Fermilab to be used in clinical trials. The facility was built with funds raised from private individuals and foundations. Three successive grants continued for more than ten years and more than 1000 patients were treated in these clinical trials. In September, 1985, the Fermilab neutron-therapy facility became a self-supporting outpatient therapy clinic.

The interest in proton therapy continued at Fermilab and several design studies were carried out, making use of equipment left over from high-energy accelerator development projects. These studies did not in themselves come to fruition, but they engaged the interest of Chicago-area radiation therapists and medical-school leaders. This interest led to a series of workshops on proton therapy at Fermilab and to further accelerator design work by laboratory people. The workshops also led to the formation of a coordination group PTCOG, in which Fermilab people have been active. Following the initial meetings, the Loma Linda radiation therapy group asked Fermilab to carry out design and construction of a proton accelerator to be the basis of a clinical facility. This design report is the first result of that work.

2. FACILITY REQUIREMENTS

2.1 Energy

The peak energy of 250 MeV is chosen for the range of protons in tissue. It is sufficient for irradiation of even obese patients from many directions and it will permit the use of passive beam-scattering techniques to create beams of about 30 cm diameter and a residual range of 25-30 cm.

It is also necessary to deposit energy in smaller tissue depths in order to irradiate a three-dimensional volume uniformly. The energy must therefore also be variable from pulse to pulse and within a pulse. The lower limit of this variation is taken for definiteness to be 70 MeV, although beam could be extracted and used at lower energy if extremely short range were shown to have clinical utility.

2.2 Intensity

The beam intensity is closely related to the treatment time desired for various sites. The numbers of protons needed for different sites also depends on whether passive or dynamic beam spreading is used. This question has been studied in some detail by Awschalom[1]. It is therefore difficult to set a definite criterion for beam intensity. PTCOG[2] has recommended 2 minutes as the desired upper limit for treatment time. If it is assumed that dynamic scanning is used, the number of protons needed in the worst case (Hodgkin's disease) is 8×10^{12} in this time. This corresponds to accelerating 1.2×10^{11} in each 2-sec pulse. This has been adopted as the intensity criterion for this design.

2.3 Extraction Modes

Beam can be extracted from a synchrotron in a very short time (1 revolution, which is 0.1 μsec at 250 MeV) or stretched out over many turns. Slow beam extraction is needed to make dynamic beam spreading possible and the PTCOG meetings have concluded that beam extracted over approximately 50% of the cycle is desirable. A 50% duty factor has been adopted as the criterion for extraction. It is also possible to decelerate the beam to lower energy than that of the flattop and extract it for use at that energy.

It is planned to feed all beam lines from one extraction point, in order to economize on treatment room layout. The synchrotron comes naturally with another long straight section that can be used for extracted beam and we are reserving it in our design for possible future use.

2.4 Treatment Modes

It is desirable to have horizontal and vertical beams available in a treatment room to provide maximum flexibility in utilization. For economy, some treatment rooms with only one beam can also be used. We have taken as our criterion that every room will have the possibility of both horizontal and vertical beams meeting at an isocenter.

Separate from the standard rooms, there should be a gantry room to provide beams from all angles through a series of angles sweeping through more than 180 deg. The treatment rooms and the gantry room should include mechanisms for beam spreading. Dynamic scanning is not well enough developed to base an entire design on, so that passive spreading must be possible, but dynamic scanning has significant advantages in uniformity and in efficiency of beam use, so that it must not be precluded.

2.5 Treatment Rooms

The treatment rooms must be designed so that it is possible to carry out treatment in any room while setup, improvement, or maintenance are carried out in other rooms. Each room must include systems for precise (1 mm) patient alignment and for beam control and patient monitoring from a shielded location near the room.

References for Chapter 2

1. M. Awschalom Unpublished Fermilab Note LL-32, Feb. 4, 1986.
2. PTCOG Utilization Committee Report. Unpublished Note LL-59, Jan. 23, 1986.

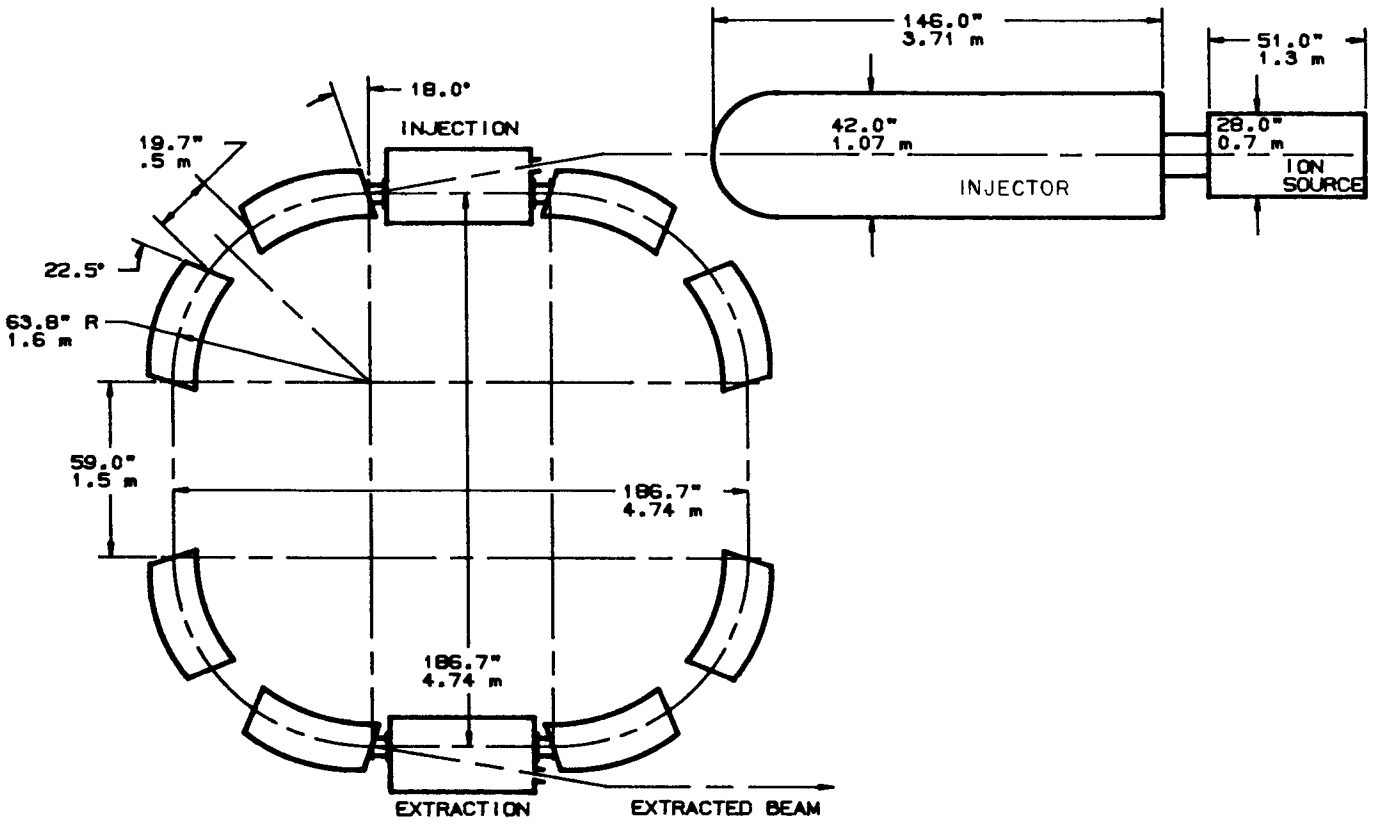

Figure 3.1 General Plan of the Accelerator

3. ACCELERATOR DESIGN

3.1 General Description

3.1.1 Overview of the accelerator

The importance of easy variability of energy in the use of the accelerator, as discussed in Section 2.1 above, leads naturally to a synchroton as the accelerator choice. We have therefore designed a 250-MeV proton synchrotron capable of accelerating at least 1.5×10^{11} protons in a 2-sec cycle with nearly 50% duty factor, that is, with beam spill over a 1-sec flattop. This accelerator is described in the present chapter.

The synchrotron is a ring of pulsed electromagnets interrupted by straight sections used for injection, acceleration and extraction of the beam. There are a total of four quadrants around the circumference, each composed of a 90-degree bend and a straight section, as shown schematically in the layout of Fig. 3.1. The central orbit is approximately 19 feet in diameter, so that the ring will fit into a space 21 feet square. Beam is injected from a Pelletron, an electrostatic generator manufactured by the National Electrostatics Corporation of Middleton, Wisconsin or from a radiofrequency quadrupole (RFQ) linear accelerator. The beam is then accelerated to the desired energy by a radiofrequency system while the magnetic field is ramped smoothly upward to keep the proton beam on the same orbit. The acceleration to full energy takes 0.5 second. After acceleration, the beam is extracted uniformly over a period of 1 second, while the magnetic field is held constant in a ''flattop'', and transported through a beam switchyard to the treatment rooms. The switchyard and treatment rooms are discussed in Chapter 4 below. After extraction, the magnetic field is returned to its injection value in 0.5 seconds to complete the total cycle time of 2 seconds. The magnetic-field cycle and particle energy as functions of time are shown in Fig. 3.2.

More complicated flattops are also possible and will be useful. The magnetic field can be programmed down from its flattop value to any desired intermediate value while the beam is simultaneously decelerated. Beam can then be extracted at this intermediate energy. This multiple flattop capability is inherent in the computer control system and will be developed in detail during commissioning and operation of the accelerator.

3.1.2 Magnet and Injection Design Options

Two options for the magnets have been considered in our study, superconducting and conventional magnets. There is no difference in the field produced by these magnets. The superconducting magnet system has the advantages of much lower power consumption and of great ease in operation of the accelerator and switchyard together at any energy. The two designs are discussed in Sec. 3.3 below.

Another option has been considered in the design. The Pelletron used for injection can be either a 2-MeV single-ended machine or a 3.4-MeV tandem accelerator. Both the 2-MeV and 3.4-MeV machines are standard production models of National Electrostatics Corp. The 2-MeV has lower energy and therefore lower intensity capability. It also has the disadvantage that the ion source is inside the pressure vessel that insulates the high-voltage column and at least an hour is needed to get to it for repair. The tandem machine has the ion source accessible outside the pressure vessel, but stripping at the intensity needed for injection has not been done and some research and development would be needed. On the other hand, the tandem option offers higher injection energy, which will increase the beam intensity possible with the synchrotron, and is also significantly less costly. There are also higher-energy single-ended Pelletrons, but they are costly. If tests show that it can be made a reliable injector, the tandem will be superior to the single-ended Pelletron.

It is also possible to inject at 2-MeV energy from a radiofrequency quadrupole (RFQ) linear accelerator. This new accelerator was invented in the USSR and is being developed at many laboratories. In particular, the Lawrence Berkeley Laboratory of the University of California is building systems that might be appropriate for this use. The difficulty is that the RFQ system usually produces a beam with larger energy spread than can easily be accommodated in a small ring like the one considered here. Recent theoretical work indicates that this difficulty can be overcome in new RFQ designs, but it is not clear at this time that RFQ has advantages over Pelletrons.

3.2 Accelerator Physics Requirements and Design

3.2.1 Magnet lattice

The simplest operation of a synchrotron is obtained by using a magnetic guide field produced and controlled by poleface shaping rather than directly by currents. In order not to operate too close to the saturation field of approximately 1.8 T, the lattice is designed to have a peak dipole field of approximately 1.5 T.

Four long straight sections can be used for injection (less than 1 straight section), acceleration (less than 1 straight section), extraction of two beams (2 straight sections) and various beam monitoring and steering functions. One of the extraction straight sections can be used for a beam-abort system, a fast extraction system that will deposit the beam safely in a dump outside the accelerator if it is mis-steered or otherwise creating undesirable radiation.

On the other hand, the beam parameters are identical in these four long straight sections and we have included four additional short straight sections midway between the long straight sections to be able to measure a different set of beam parameters. The accessibility of two different sets of beam parameters is important in order that one can insert devices to affect the beam characteristics in the

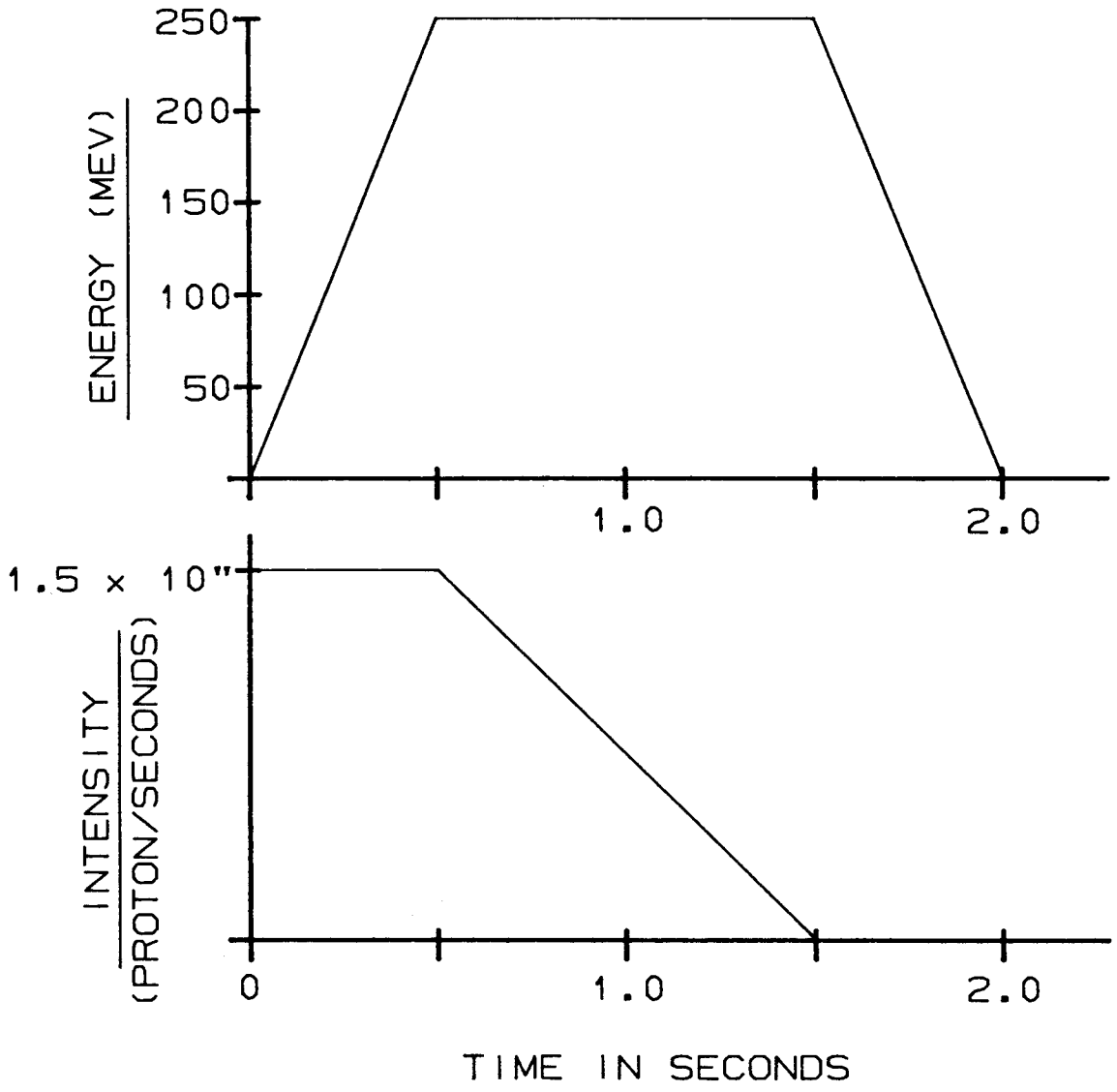

Figure 3.2 Magnetic-Fioeld and Energy Variation Through the Accelerator Cycle

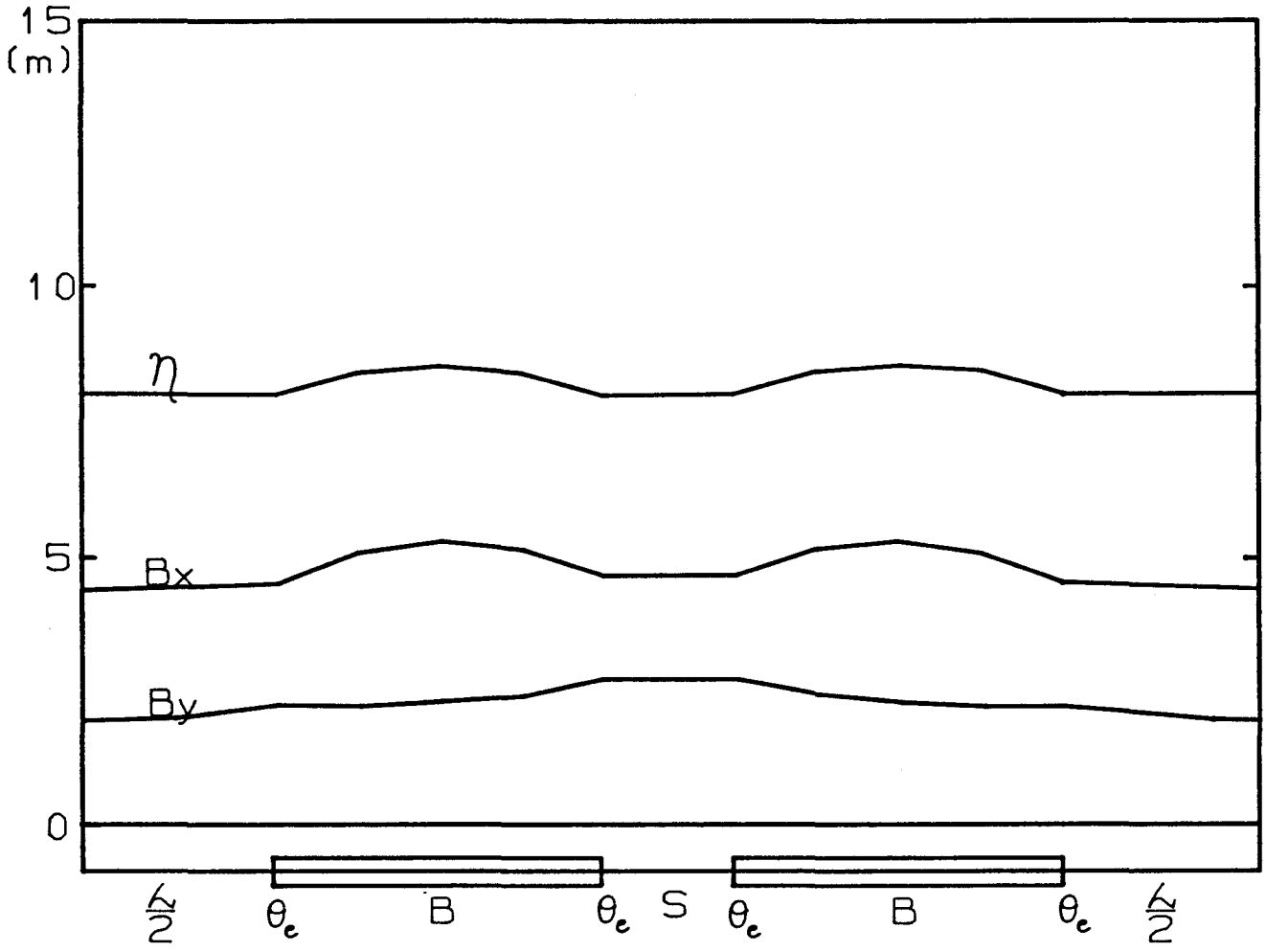

Figure 3.3 Amplitude and Dispersion Functions of the Lattice

horizontal and the vertical planes separately. This then gives eight dipoles, each bending the beam through 45°.

With this ring geometry, one method of achieving proper vertical and horizontal focusing is by the edge focusing of the 16 edge angles of the dipole magnets alone and there is therefore no need for bending magnet gradients or quadrupoles. The properly adjusted edge angle is 0.32 rad. A layout of this ring lattice is shown in Fig.3.1 and the amplitude functions β_x and β_y, and the horizontal dispersion function D of for one quadrant of the ring are shown in Fig. 3.3. The lattice parameters are summarized in Table 3-1.

Table 3-1. Lattice Parameters

Injection energy T_i	3.4 MeV
Extraction energy T_e	70 - 250 MeV
Circumference $2\pi R$	18.053 m
Equivalent radius R	2.873 m
No. of sectors	4
Long straight section (L) length	1.5 m
Short straight section (S) length	0.5 m
Magnet (B) length	1.2566 m
Sector structure	(L/2) BSB(L/2)
Magnet bend angle θ_B	$\pi/4$
Magnet bend radius ρ	1.6 m
Magnet edge angle θ_E	0.32 rad. (18.3°)
Magnet gradient	0
Injection field B_i	0.167 T
Extraction field B_e	0.711 - 1.52 T
Horizontal tune ν_x	0.6005
Vertical tune ν_y	1.255
Horizontal amplitude function β_x	
Mid - L	4.395 m
Mid - S	4.650 m
Maximum (mid - B)	5.298 m
Vertical Amplitude function β_y	
Mid - L	1.967 m
Mid - S	2.722 m
Maximum (end - S)	2.745 m
Dispersion function D	
Mid - L	8.002 m
Mid - S	8.002 m
Maximum (Mid - B)	8.529 m
Transition gamma	0.5865
Magnet good-field aperture	± 2cm (v) by ± 3 cm (h)

A different lattice utilizing rectangular magnet blocks and gradient focusing has been studied in connection with the conventional magnet design. Either lattice can be used to achieve the desired orbit properties.

Effects of field errors and misalignments on orbits have been investigated for this accelerator. For reliable performance, magnet positions should be held within 0.5 mm (0.020 in.) vms. Mounting each quadrant on a strongback, as proposed in Sec. 3.3 below, will easily achieve this alignment tolerance.

3.2.2 Intensity and Injection energy

In order to have a long spill beam with duty factor approaching 50%, the cycle time of the synchrotron is apportioned into 0.5 sec rise, 1 sec flattop and 0.5 sec fall as shown in Fig. 3.2. With proper control of the extraction system, a 0.8-sec good beam spill on the 1-sec flattop and an overall duty factor of close to 50% can be achieved. To get a time-average current of 10 nA, the intensity per pulse needed is 1.2×10^{11} protons. This can be achieved by an injection energy of 3.4 MeV and a good-field aperture of the ring of ± 2 cm (vertical) by ± 3 cm (horizontal). If shorter spill times are acceptable for some treatment modality, proportionality higher time-average intensity is available.

The beam intensity will be limited by space-charge effects in the horizontal direction, where which the amplitude function is largest. The maximum β_x is 5.3 m and at injection and the available horizontal half-aperture is approximately a = 2 cm. With a bunching factor B = 2 and an allowed tune shift $\delta\nu_x$ of 0.25, the space-charge formula

$$\delta\nu_x = \frac{1}{2} r_p \frac{\beta x}{\beta^2\gamma^3} \frac{N B}{\pi a^2}$$

gives, at an energy of 3.4 MeV (with $r_p = 1.535 \times 10^{-18}$ m the classical proton radius)

$$N \text{ (space charge limit)} = 2.8 \times 10^{11} \text{ p/pulse}$$

This is for uniform density distribution across the beam. The density in the real beam will not be uniform and the space charge limit will be slightly lower. Beam intensity parameters are given in Table 3-2.

Table 3-2. Beam Intensity Parameters

Injection beam emittance	40 π mm-mrad
Injection beam momentum spread $\delta p/p$	$< \pm 3 \times 10^{-5}$
Injection beam current	40 mA
Injection pulse length	> 0.7 μsec
Revolution time at injection	0.71μsec
No. of turns injected	1
Maxmum beam width	± 14.5 mm
Space charge limit (bunching factor = 2) (tune shift = 0.25)	approx. 2×10^{11} p/pulse
Expected intensity per pulse	1.5×10^{11} protons

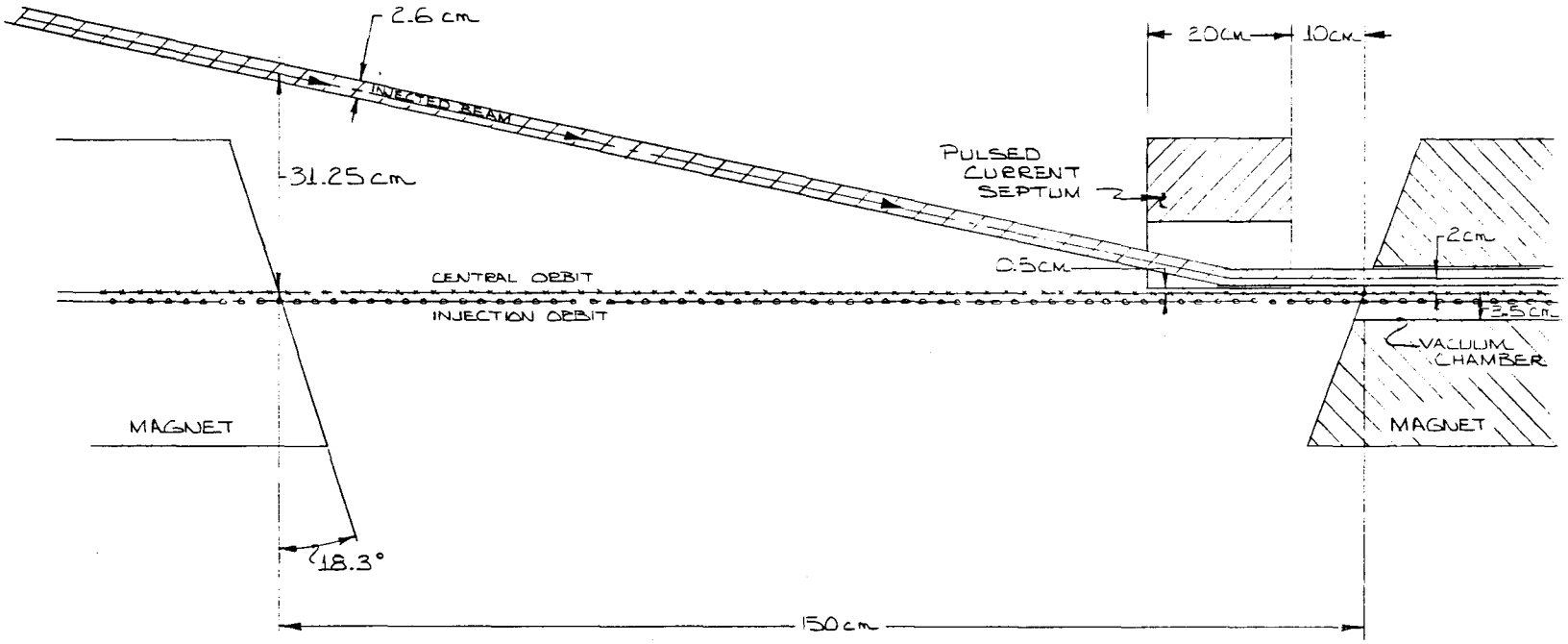

Figure 3.4 Layout of the Ring Injection System

Cycle time	2 sec
Time average beam current	12 nA

If injection is at a lower energy say, 2 MeV, the space-charge limit for a uniform distribution is then 1.7×10^{11} protons/pulse, still adequate to give a time-average current of 10 nA, which corresponds to 1.2×10^{11} protons/pulse at a cycle time of 2 sec.

The revolution period at 3.4 MeV is 0.71 μsec. A pulsed injection current of 35 mA from the injector will fill the synchrotron with 1.8×10^{11} protons in one turn. Single-turn injection will therefore be adequate. If 2-MeV injection is used, the ring can still be filled to the space-charge limit in a single turn.

The beam from the injector is transported by two sets of quadrupole triplets to inject to the injection straight section. The beam clears the outer edge of the upstream magnet at 31.25 cm horizontally outside the central orbit in the synchrotron, as shown in Fig. 3.4. It is then bent by a pulsed-current septum magnet near the downstream end of the straight section to enter the downstream magnet 2 cm outside and parallel to the central orbit of the synchrotron. The septum magnet has a strength $B\ell$ = 3.0 kG x 20 cm and a septum thickness of 1.5 mm.

The injection orbit must be bumped inward 1 cm by small magnets to leave room for the septum. After injection, the septum magnet is retracted to leave room for extraction.

The beam entering the downstream magnet at L1 parallel to and 3 cm outside of the bumped injection orbit (2 cm outside the central orbit) will cross the injection orbit at the upstream end of the opposite straight section at an angle of 3 cm/4.5m = 6.7 mrad. A fast kicker with rise time less than 50 nsec and strength $B\ell$ = 120 G x 15 cm will kick the beam onto the injection orbit. Injection parameters are given in Table 3-3.

Table 3-3. Injection Parameters

Long straight section for injection	L1
Pulsed current septum	
Field B	3.0 kG
Length l	0.2 m
Septum deflection angle	0.225 rad
Longitudinal position of septum mid-point	
From exit of upstream magnet	1.3 m
To entrance of downstream magnet	0.2 m
Horizontal width of beam	± 13 mm
Horizontal displacement of beam center line from central orbit	
At edge of upstream magnet	312.5 mm
At exit of septum	20 mm
At entrance to downstream magnet	20 mm
Angle of beam to central orbit	
Upstream of septum	-0.225 rad

Downstream of septum	0
Horizontal displacement of bumped injection orbit from central orbit	-10 mm
Location of injection bumper	mid - L3
Strength of injection bumper	
Field B	200 G
Length l	10 cm
Injected beam crossing injection orbit	
Location	upstream L3
Angle	6.7 mrad
Fast kicker magnet	
Location	upstream L3 where beam crosses orbit
Strength	120 G x 0.15 m
Fall time	< 50 nsec

3.2.3 Acceleration

The acceleration time from injection to 250 MeV is 0.5 sec. This requires an energy gain per turn of only 78.2 eV. The frequency modulation of 1.41 MHz to 10.19 MHz (harmonic number 1) is large. An untuned ferrite-loaded cavity, which takes up less than 50 cm of straight section length, will be used to produce the voltage needed. A convenient location for the cavity is in L3, the straight section opposite injection. The choice of harmonic number depends only on the availability of rf amplifiers. RF parameters are summarized in Table 3-4.

Table 3-4. Radiofrequency Parameters

Injection kinetic energy	3.4 MeV
Extraction kinetic energy	250 MeV
Acceleration time	0.5 sec
Energy gain per turn	78.2 eV
Harmonic number h	1
Injection rf frequency	1.416 MHz
Extraction rf frequency	10.19 Mhz
Initial bunching factor	< 2
High energy (> 15 MeV) rf values	
Peak rf voltage V	100 V
Synchronous angle $^{\circ}\phi_s$	51.4°
Cavity length	< 0.5 m
Cavity type	ferrite loaded, untuned
Cavity location	L3

3.2.4 Beam Extraction

The two extracted beams could be extracted at 90° from, say, L2 and L3 or at 180°, in opposite directions from L2 and L4. We will discuss extraction at 250 MeV from only one straight section, keeping another reserved for a possible second beam.

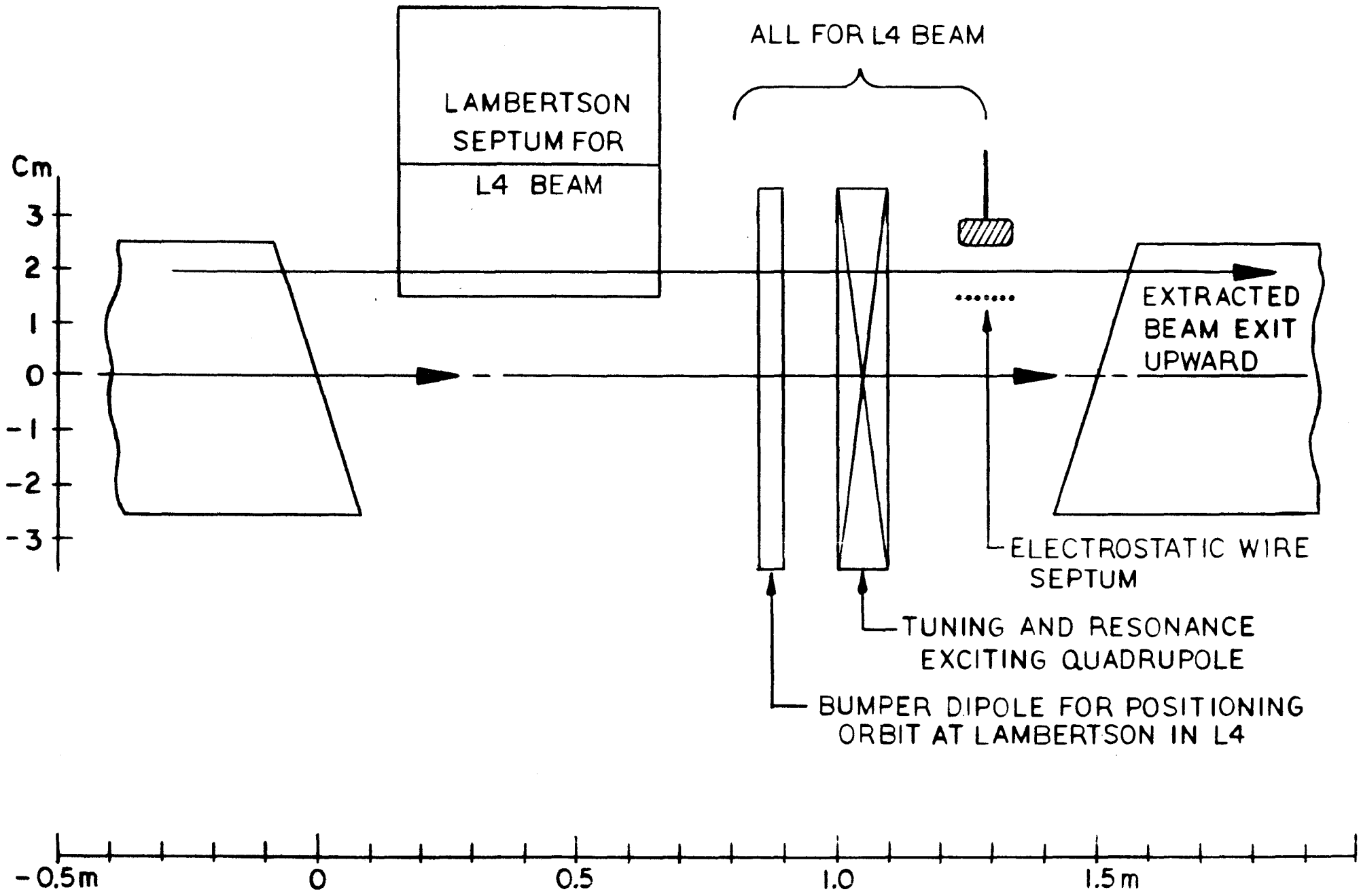

Figure 3.5 Layout of the Ring Extraction System

The standard horizontal half-integer resonant extraction scheme is used. For the beam emerging from L4, the detuning and resonant exciting quadrupole are placed at the midpoint of L2. The quadrupole is horizontally defocusing with a maximum strength $B'\ell$ = 8 T/m x 10 cm. This will put the horizontal tune on the half-integer resonance $2\nu_x = 1$; at the same time the vertical tune will have the non-resonant value $\nu_y = 1.3$. The horizontally broadening beam is sliced off by an electrostatic wire septum located immediately downstream of the quadrupole at 1.5 cm outward from the central orbit. The wire septum has a modest field, 40 kV/cm, and a length of only 10 cm, but the kick received by the piece of beam sliced off by the septum moves it outward 4.7 mm at the upstream end of L4, 90^o phase advance from the wire septum. The 4.7-mm gap is adequate to clear the iron septum of a Lambertson septum magnet placed at the upstream end of L4. The Lambertson magnet has a strength of $B\ell$ = 0.8 T x 50 cm, sufficient to deflect the beam slice upward by 16.4 cm to clear the top of the downstream magnet.

In addition, a small adjustable bumper dipole is placed just upstream of the excitation quadrupole in L2 with a maximum strength of $B\ell = \pm$ 1 kG x 5 cm to position the central orbit in L4 relative to the Lambertson septum. A small octupole magnet to form the extraction separatrices is placed in L3.

The relative arrangement of the extraction elements in L2 is shown in Fig. 3.5 and the parameters of the extraction elements are summarized in Table 3-5

Table 3-5. Extraction Parameters

Extraction resonance	$2\nu_x = 1$
Number of extracted beams	2 (L2 and L4)
Detuning and resonance exciting quadrupole	
(All elements are for extracted beam (L4)	
Location	downstream of L2
Field gradient	80 kG/m
Length	10 cm
Aperture	full
Betatron tune at extraction	
Horizontal ν_x	0.5
Vertical ν_y	1.3
Electrostatic wire septum	
Location	immediately downstream of quadrupole in L2
Electric field	40 kV/cm
Length	10 cm
Aperture	1 cm
Horizontal position from central orbit	1.5 - 2.0 cm
Width of gap in beam at Lambertson septum produced by the wire septum	4.7 mm
Lambertson septum magnet	
Location	upstream in L4
Field	8 kG
Length	50 cm
Aperture	1 cm (h) x 5 cm (v)
Beam vertical displacement at downstream magnet produced by Lambertson	16.4 cm
Bumper magnet to position beam at Lambertson	
Location	Mid - L2
Field	± 1.0 kG
Length	5 cm
Aperture	full
Beam horizontal adjustment	± 5 mm
Extraction octupole	
Location	L3
Strength	small

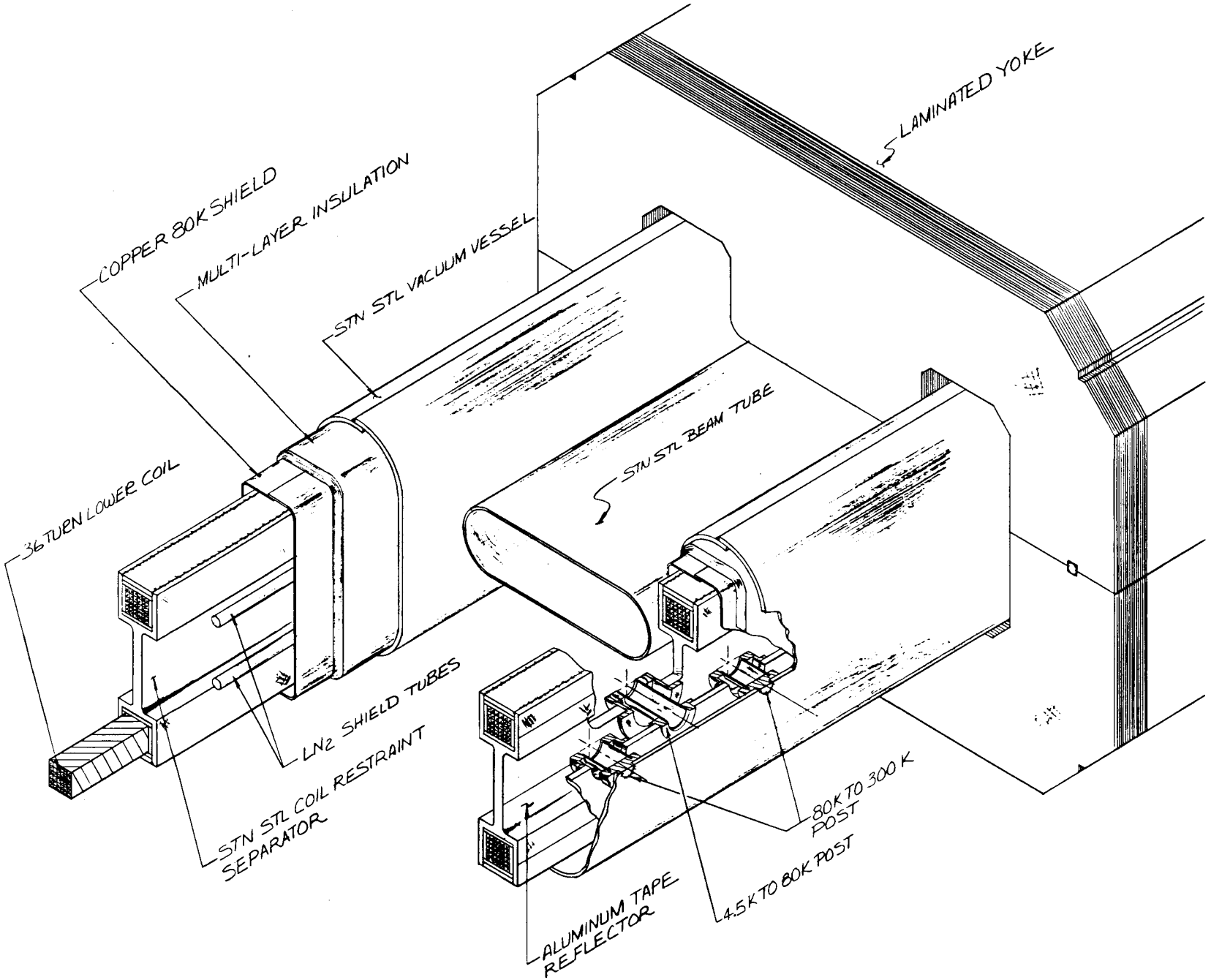

Figure 3.6 A Superconducting Magnet

3.3 Ring Magnets

3.3.1 Superconducting Magnet

3.3.1.1 Introduction. The accelerator magnet system as described in Sec. 3.2 above consists of four magnet quadrants separated by four straight sections used for injection, diagnostics, acceleration and extraction. The physical arrangement is shown in Fig. 3.1. The principal elements of the magnet quadrants are the superconducting magnet coil assemblies, operating in liquid helium at 4.5K, contained in a cryostat assembly. The cryostat is housed in a laminated magnet yoke assembly which also contains the accelerator beam tube. The details of the superconducting magnet are shown in Fig. 3.6.

The four magnet quadrants are connected in series electrically, cryogenically and for vacuum. A single set of two end vessels provides the necessary connections to the ambient surroundings.

3.3.1.2. Magnet Design. The magnetic design utilizes the magnetic fields generated by the superconducting coil and the yoke. The magnetic parameters are given in Table 3-6.

Table 3-6 Magnetic Parameters

Central field		14kG
Number of Turns in Coil		36/pole
Conductor Current		650 A
Inductance		0.026 H/m
Gap Height		1.63 in
Excitation	Aperture(width)	ΔB/B
Low	±1.25in	+0.0021%
		-0.0088%
Full	±0.50in	+0.0000%
		-0.0113%
Yoke size		11.5in. x 16.5in

3.3.1.3 Superconductinc Coil. The superconducting coils of each quadrant consist of an upper and a lower coil wound in a flat pancake configuration. The details of the windings are as shown in Fig. 3.6.

In order to reduce the magnet operating current and thus the refrigeration load associated with current-lead cooling, the coil is wound in a 36 turn, 6 by 6 matrix configuration with all conductors connected in series. The conductor employed is niobium-titanium with copper stabilizer and has a solid rectangular cross section. The conductor composition has been shown by the development and construction experience of the Fermilab Tevatron superconducting magnet system to yield very reliable performance with conservative operational margins.

The conductor electrical insulation system provides the required turn-to-turn and turn-to-ground insulation while at the same time allowing for adequate liquid-helium circulation to maintain the coils at operating temperature and ensure operational stability of the superconductor.

After winding and curing, the coil pancakes are installed in a combined-function coil restraint-separator. The restraint-separator provides the functions of

(i) restraint of the magnet's Lorentz forces within the coil packages and between the coil packages and the magnet yoke,

(ii) containment of the liquid helium that surrounds and cools the conductor, coil-package pressure vessel,

(iii) relative positioning of the top and bottom pancake assemblies and

(iv) positioning of the pancake assemblies relative to the yoke. The restraint-separator is fabricated from stainless steel for rigidity, strength, weldability and favorable low-temperature properties.

The restraint-separator is formed to the curvature of the inside and outside windings.

3.3.1.4 Cryostat. In order to maintain the superconducting coils at their operating temperature and to maintain low thermal loads to the refrigeration system, the superconducting-coil, assembly and the restraint-separator are contained in the magnet cryostat. The cryostat provides the functions of thermal insulation and support of the coil assemblies relative to the yoke. The cryostat consists of thermal-radiation insulation, a cold-mass suspension system, an 80K shield and a vacuum vessel.

In order to reduce heat transfer by thermal radiation between 80K and 4.5K, the entire surface of the restraint-separator is wrapped with aluminum tape. This tape, which has been sucessfully employed in several Fermilab superconducting magnet systems, has a radiant heat transfer rate of approximately 12.5mW/ft^2, which corresponds to 200mW/quadrant.

The restraint-separator is supported relative to the cryostat vacuum vessel (and thus the magnet yoke assembly) by the cryostat suspension system. The requirements of the suspension system are low refrigeration loads, reliability and dimensional stability. The suspension system incorporates individual support assemblies placed along the length of the restraint-separator. The spacing of the supports is determined by the structural properties of the restraint-separator, the static coil-to-yoke position uncertainty

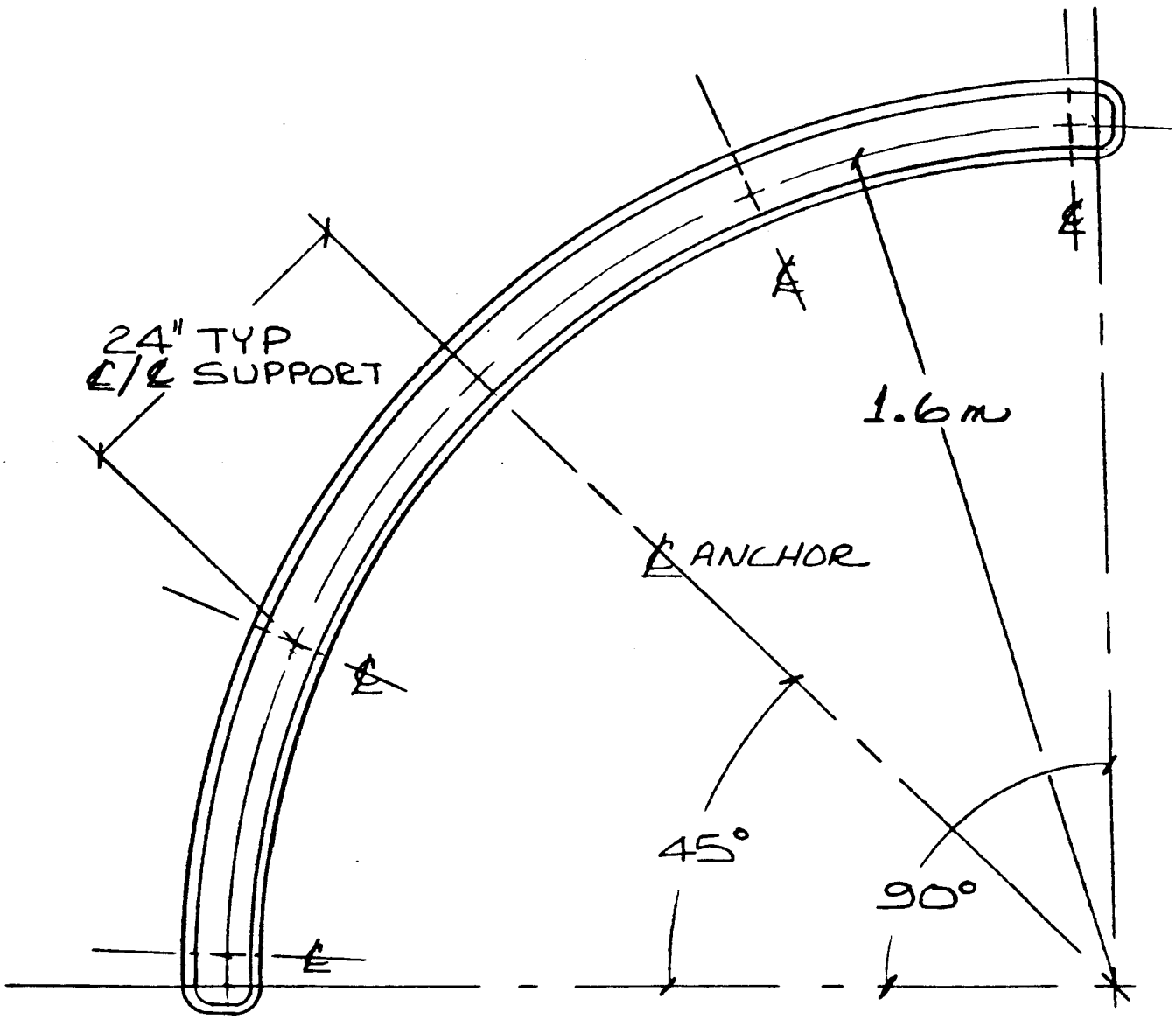

Figure 3.7 Cryostat Support System

(1/16 in.) and the maximum allowable restraint-separator; i.e., coil, deflection (0.020 in.) due to operational loads. The resulting support derived from these criteria is 36 in. A support spacing of 24 in. is employed in the design to improve support at the ends of the coil assemblies. The support locations are shown in Fig. 3.7..

The supports are structurally sized to correspond to the 36-in. support spacing, which results in a structurally conservative design and permits increasing the spacing from 24 in. to reduce support heat leak if deemed necessary.

The supports incorporate FRP tubing with metallic connections. The support is two parts; 4.5 to 80K and 80 to 300K, in order to reduce heat leak while complying to the spatial constraints imposed by the magnet yoke aperture. The restraint-separator is anchored to the cryostat vacuum vessel at mid-span (45°). The support assembly designs allow for relative motion between the 4.5, 80 and 300K members due to differential thermal motions in magnet cooldown and warmup. The heat loads at each support point are 0.028W to 4.5K and 0.86W to 80K.

The restraint-separator is supported from the and surrounded by the LN_2 cooled 80K thermal-radiation shield. This shield is fabricated from copper. The shield is wrapped with a multilayer insulation blanket comprised of alternate layers of aluminized polyester film and fiberglass matting. The radiant-heat transfer rate to 80K of approximately $0.23mW/ft^2$ corresponds to 3.5W/quadrant. The 80K shield is supported from the vacuum vessel.

The vacuum vessel, fabricated from stainless steel, provides the high-vacuum environment (10^{-6}Torr) needed for thermal-radiation insulation systems. The vessel is shimmed into position relative to the magnet yoke.

The ends of the cryostat are designed to permit the electrical and cryogenic connections between coils and quadrants and to continue the insulating function of the cryostat. Connections between quadrants will be by means of vacuum insulated transfer lines.

A set of two end vessels will provide the necessary connections to ambient. These connections include magnet current supply and diagnostics, liquid-helium and liquid-nitrogen supply and return, cryostat instrumentation, insulating vacuum and safety reliefs. Each quadrant cryostat incorporates its own vacuum-space pressure reliefs.

The steady-state refrigeration refrigeration loads for an accelerator consisting of four magnet quadrants, interconnections and end vessels are as given in Table 3-7.

Table 3-7. Accelerator Steady-State Refrigeration Loads

Component	Refrigeration Load to 4.5K (W)	Load to 80K (W)
Support Condition[1]	1.12	34.4
Thermal radiation	0.79	14.1
Current Leads[2]	0.71	--
Interconnection & end vessels	1.00	12.0
Total	3.66 W	60.5 W

1. For supports spaced at 24 in.
2. For one pair of 750A leads.

The corresponding cryogen boiloff rates are 4.9ℓ/hr of liquid helium and 1.5ℓ/hr of liquid nitrogen.

The dynamic refrigeration loads caused by the accelerator cycle have been estimated for the superconductor assuming a copper-to-superconductor ratio of 37:1 with 6μ filament size. The refrigeration load to 4.5K corresponding to one accelerator cycle per two seconds is 2.12W. The heating of the copper by eddy currents has not been calculated, but can be made low by separating the copper to reduce the magnitude of the eddy currents. The dynamic refrigeration loads will require further evaluation as the detailed design of the conductor progresses.

3.3.1.5 Magnet Yoke. The magnet yoke is fabricated from 1/16 in. thick steel laminations with a horizontal parting line separating tops and bottoms. The yoke consists of two sections along the length of each quadrant to permit diagnostics at midspan (45°). The yoke design and fabrication methods will incorporate the techniques that are employed regularly for magnet construction at Fermilab.

The superconducting magnet yoke uses edge focusing, while the coventional magnet yoke discussed in the next section uses rectangular blocks. It should be stressed that either kind of yoke could be used with either conductor.

3.3.1.6 Quadrant Support. Each quadrant is supported relative to ground by a strongback support table. The support table has the necessary rigidity for alignment and position stability. The support yoke to table connections will provide for prealigned positioning and for adjustment and locking during alignment with beam. After alignment, the quadrant and the support table will be as an entity for installation and alignment of the machine.

3.3.1.7 Refrigerator System. The superconducting magnet system is serviced by a refrigeration system to provide the required 4.5K and 80K environments. The system design relies heavily on the extensive Fermilab cryogenic system experience with the Tevatron and in the Experimental Areas. Commercially available refrigerator systems will be used and reliability will be stressed throughout.

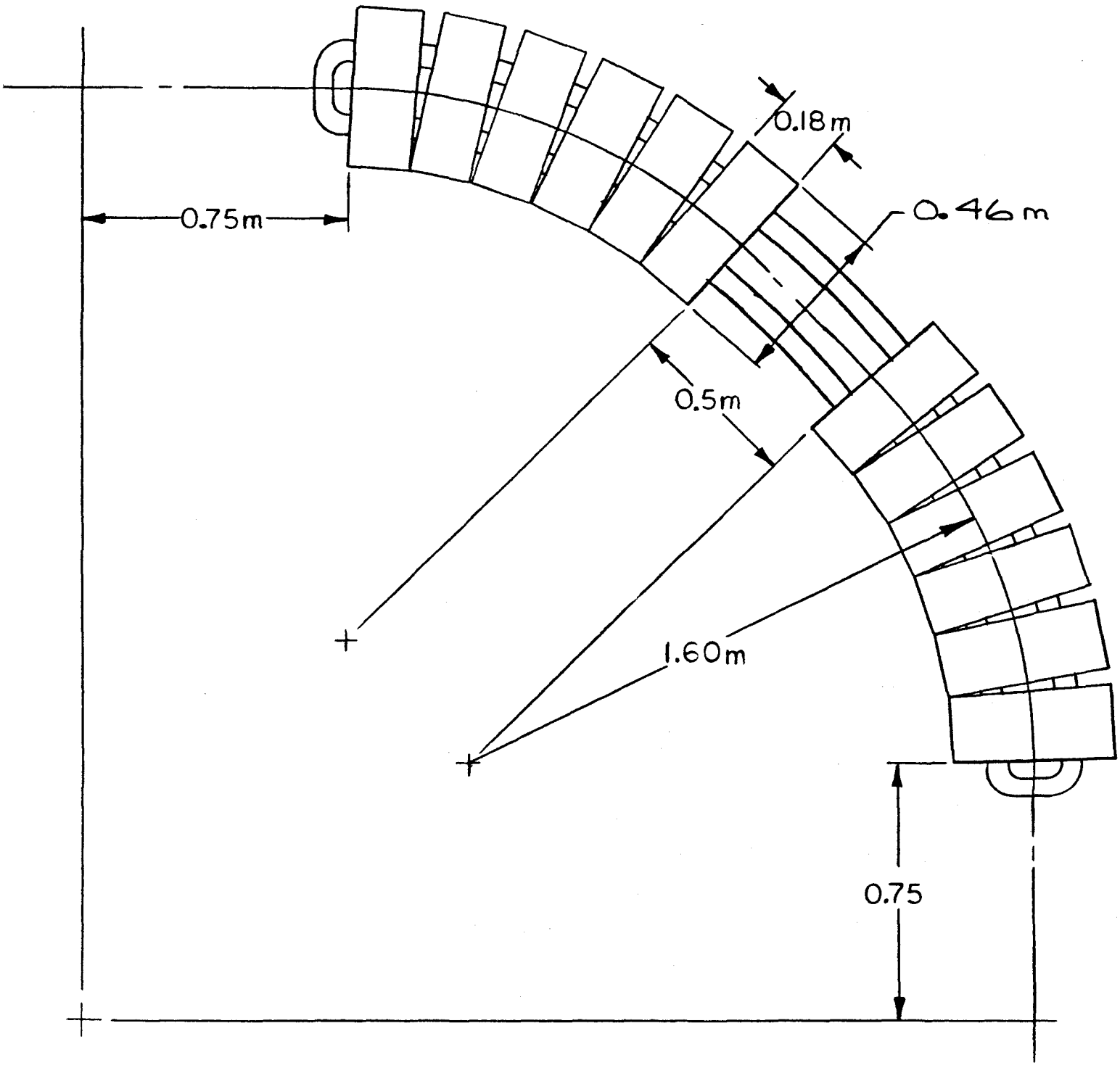

Figure 3.8 Quadrant Layout with Rectangular Block Magnet Cores

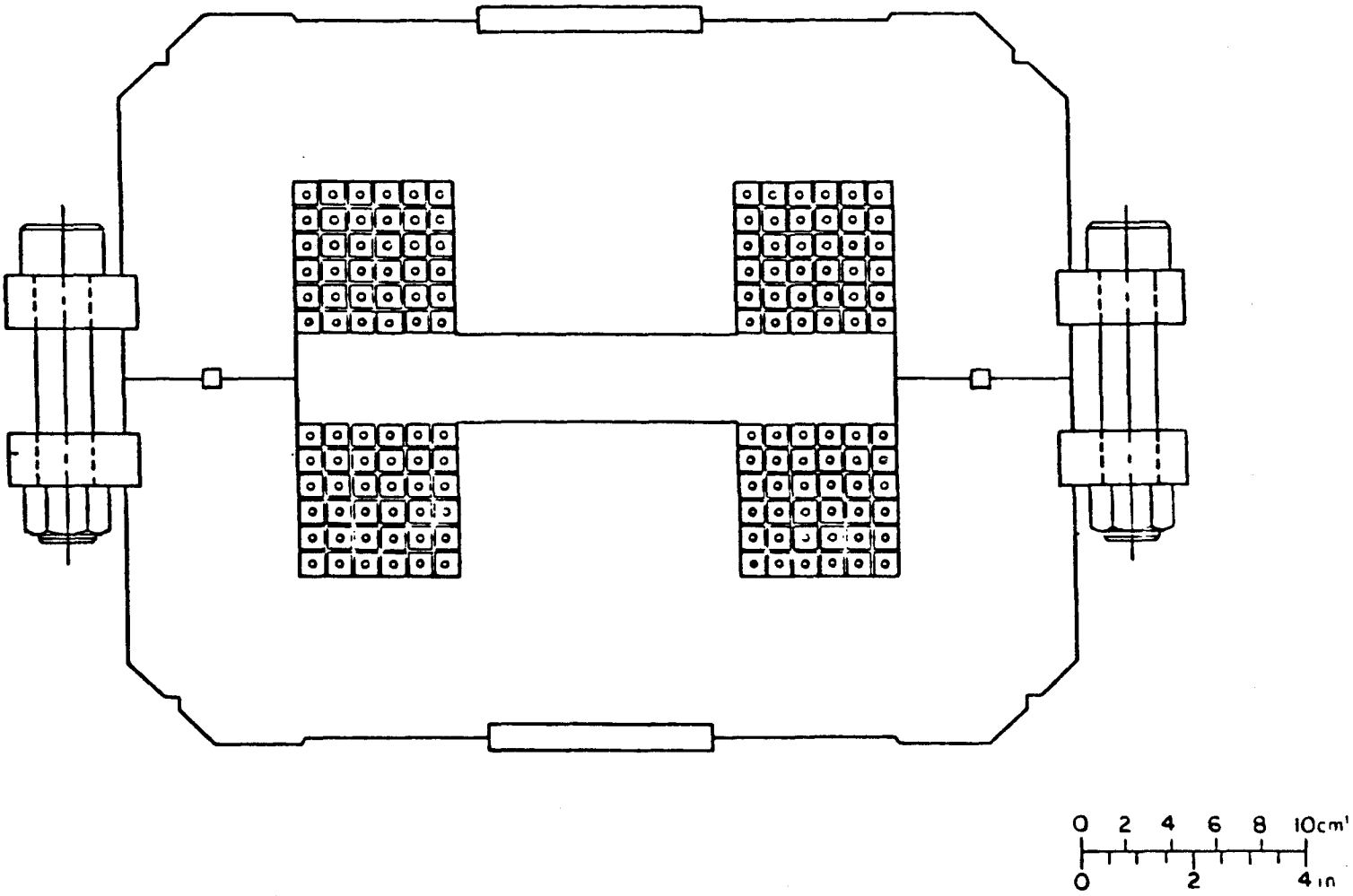

Figure 3.9 Conventional Magnet Cross Section

3.3.2 Conventional Magnet

A conventional copper-conductor room-temperature magnet option has been considered for the accelerator. Since both it and the superconducting version are iron-dominated, overall size and weight are very similar; the main differences in performance are the lower electrical power and voltage required by the superconducting coil and the fact that good current regulation at flat-top (a requirement for a long uniform spill) comes more or less automatically in the superconducting coil. Against these we must weigh the greater complexity of the superconducting cryostat and the liquid-helium requirement.

The conventional main magnet, shown in plan view in Fig. 3.8, has four 90° quadrants each excited by a pair (upper and lower) of large copper windings shown in the magnet cross section of Fig. 3.9. Each quadrant has a 20-in. straight section for beam-position monitors at high-β_y locations. The conventional split-H construction uses (per quadrant) 12 upper and 12 lower lamination packs, each accounting for 7.5° of bend. The wedge-shaped gaps between packs (Fig. 3.8) introduce an effective field index whose detuning effect on the lattice has been estimated to be small; it can be combined into the magnet-gradient specification. Upper and lower packs are keyed together and bolted using cleats welded on after stacking and impregnation. The lower packs have welded and machined feet referenced to the pole face; all the packs in a quadrant are held in position by a single strongback. Depending on the final choice of lattice, there will be either one or two basic poleface profiles. The entire magnet (exclusive of strong-backs) is made of 12 tons of steel (240 lbs. per half-pack) and 1.7 tons of copper.

Each of the two pancake coils exciting a quadrant is wound six-in-hand to simplify insulation and water distribution and obtain a low impedance level. In estimating the electrical requirements, the usual trapezoidal excitation cycle is assumed. Then the maximum inductive voltage LdI/dt is 194V and the resistive drop IR at full current (4480 A) is 215V. Dissipated power is 112 kW; this depends only on the excitation waveform and not on its repetition rate. On the other hand the peak stored magnetic energy is 55J and this must be dissipated, stored elsewhere or returned to the line each cycle. This is equally true in the superconducting case. For a 2-sec cycle, this adds 28 kW if the power is dissipated, which may be the cheapest strategem. The coil is cooled by closed-circuit deionized water, which itself requires further cooling. This system must also handle the beam-switchyard and treatment-area magnet power, which will exceed the synchrotron power.

3.3.3 Magnet Power Supply

3.3.3.1 Introduction. Two accelerator designs are discussed above, a superconducting-magnet version and a conventional-magnet version. In each case, the magnet system consists of four magnets (90 degrees bend each) arranged in a circle. The magnets are to be electrically connected in series. Each case will be discussed separately because of significant design differences.

3.3.3.2 Superconducting Magnets. All calculations are for the accelerator only, i.e., four magnets in series. The relevant parameters are

$$I_{max} = 580 \text{ A}$$
$$I_{inj}^{max} = 30 \text{ A}$$
$$R_{total}^{inj} = 0.001 \text{ ohms } \Omega$$
$$L_{total} = 0.026 \text{ H}$$

The accelerator current waveform consists of a linear rise time of 0.5 sec, a 1.0-sec flattop, and 0.5-sec fall time. Thus the period is 2 sec. Applying the usual circuit equations leads to

$$V_{inj} = 0.03 \text{ V}$$
$$V_{flattop}^{inj} = 0.058 \text{ V}$$
$$V_{(Ldi/dt)}^{flattop} = 301.6 \text{ V}$$
$$V^{(Ldi/dt)} \cong 302 \text{ V}$$
$$P^{peak} = 175 \text{ kW}$$
$$I_{rms}^{peak} = 474 \text{ A}$$

The power supply is designed to have a peak voltage and current capability of 350 V and 600 A. It operates in a pulsed mode with a voltage of nominally 300 V and a current of 580 A. The magnet is center-tap grounded to minimize voltage to ground to about 150 V. Ground-fault protection is also provided. The power supply consists of two power supplies in one with a common regulation system and controls. One power supply is a 12-pulse phase-controlled with power extracted directly from the 12470 V line through an appropriate transformer. This power supply provides the voltage and current necessary to meet the rise time requirement. Additionally, this power supply can be inverted so as to extract the energy stored in the accelerator magnets and return the energy to the line. The power-supply primary transformer is configured to supply the phase shifted ''delta'' and ''Y'' groups for 12-pulse operation. Special consideration for isolation of the primary and secondary is incorporated to minimize the amount of electrical noise on the 12470 V line. The second power supply supplies power for the flattop portion of the accelerator current waveform. This power supply is a low-voltage linear unit capable of supplying the small amount of power needed. The regulation of this supply is designed to meet the stringent ripple and stability requirements.

3.3.3.3 Conventional Magnets. All the calculations are made for four conventional magnets in series. The basic parameters are

$$I_{max} = 1074 \text{ A}$$
$$I_{inj} = 63 \text{ A}$$
$$R_{total} = 0.2 \ \Omega$$
$$L_{total} = 0.096 \text{ H}$$

The desired accelerator current waveform is the same as the superconducting case, 0.5-sec risetime, 1.0-sec flattop, and 0.5-sec fall time. This leads to:

$$V_{inj} = 12.6 \text{ V}$$
$$V_{flattop} = 214.8 \text{ V}$$
$$V(Ldi/dt) = 194.1 \text{ V}$$
$$V_{peak} = 409 \text{ V}$$
$$P_{peak} = 440 \text{ kW}$$
$$I_{rms}^{peak} = 877 \text{ A}$$

This pulsed power supply is somewhat more substantial. To meet these requirements and to supply adequate voltage overhead, the power supply is designed with a peak voltage and current capability of 500 V and 1200 A. As before, a center-tapped ground is employed to minimize the voltage to ground and to provide ground-fault protection. The power supply is a 12-pulse phase-controlled unit with a transformer whose primary is connected directly to the 12470-V line. The phase shifted ''delta'' and ''Y'' secondaries are specially isolated and shielded from the primary to minimize the coupling of phase spikes to the primary line. Additional provision to minimize the effect of the pulsing accelerator load will be implemented.

With the conventional magnet design, more care must be taken to minimize the current ripple that may occur during the flattop portion of the cycle. This can be accomplished utilizing several alternatives. Automatic tap changing of the power-supply transformer during the flattop could be used to maintain sufficient phase advance to minimize ripple. In addition, a series active filter may need to be employed to further reduce the ripple. As before, to meet the fall-time requirements, this power supply must be capable of inversion.

3.3.3.4 Trim Magnet Power Supplies. Any planned trim magnets are expected to be low current and low voltage. These needs can be readily met by any number of commercially available units.

3.4 Vacuum System

3.4.1 Overview of the Style

The medical accelerator is a small slow-cycling synchrotron in which long-time beam storage is not contemplated. The vacuum-system requirements are therefore considerably simplified compared with those

of very large storage rings and a very simple vacuum system will therefore suffice.

3.4.2 Chamber

The chamber will be an all-metal system made of non-magnetic stainless steel. Such chambers are commercially available from many companies. It will make use of metal seals throughout in order to avoid any possible problems with radiation damage and consequent loss of vacuum. This kind of chamber will also present a low impedance to the beam, so that problems of instabilities will be ameliorated.

The system will have separate valves for the injection and extraction straight sections to permit easy working on these components. No other ring valves will be needed.

3.4.3 Pumping System

One roughing pump is needed for the accelerator ring (and a separate one for the switchyard and beam-delivery system). There will also be a need for a turbomolecular pump for the midrange. The basic high-vacuum pumping will be done by small 25 ℓ/sec getter pumps on each accelerator quadrant. It is estimated that this pumping system will bring the chamber down to operating pressure in less than 1 hour, starting from dry nitrogen.

3.5 Source and Injector

3.5.1 Choice of Injector

The synchrotoron accelerates protons and, therefore, one chooses an H^+ or an H^- ion source. The choice of source depends on the acceleration scheme in the injector. The H^+ source is simpler and is based on much experience (one would consider using a duoplasmatron). It is suitable for use on an RFQ (radiofrequency quadrupole) accelerator or in the high-voltage dome of a dc accelerator, such as a singled-ended Pelletron. The RFQ can give an energy of 2 MeV, but at relatively high cost. Some development is needed to produce a small enough energy spread from the RFQ. A 2-MeV single ended Pelletron with H^+ ion source in the dome is conventional, except that the source is inside the Pelletron pressure vessel and therefore not readily accessible for repair. It has low energy spread and the further advantage of being entirely fabricated, including the source, by industry.

The question of injection energy is important because the space-charge limit in the synchrotron scales with energy. The 3.4-MeV tandem is clearly superior in this regard to the 2-MeV single-ended Pelletron. Higher-energy single-ended Pelletrons are available from NEC, but they are larger and more expensive. All are off-the-shelf items and require little or no further work. We shall first describe the tandem option.

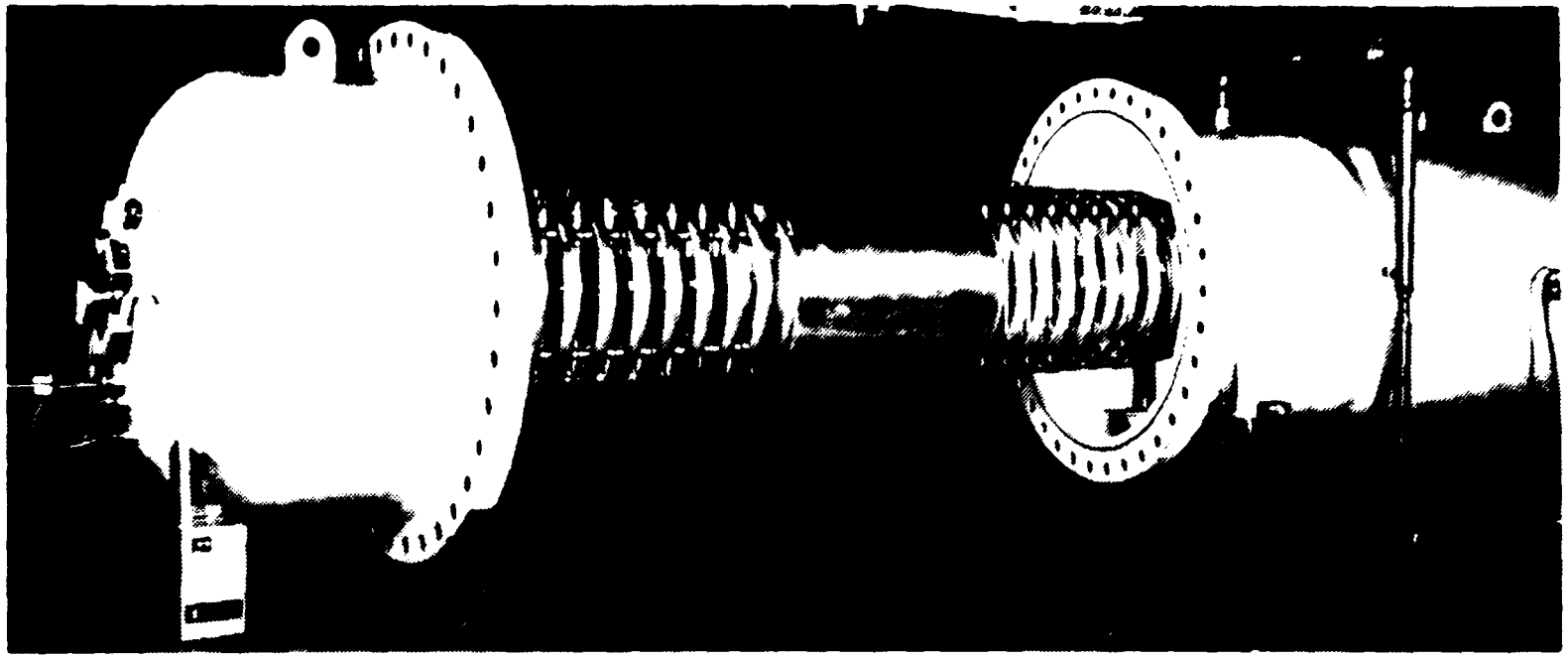

Model 5SDH-2 (above) in operation at Tokyo Institute of Technology, Japan, and Model 5SDH (below), in operation at Nankai University, People's Republic of China. Both are in servicing position to show open, accessible column design. Model 5SDH-2 is high current version of the popular Model 5SDH.

Figure 3.10 Cutaway View of a Pelletron

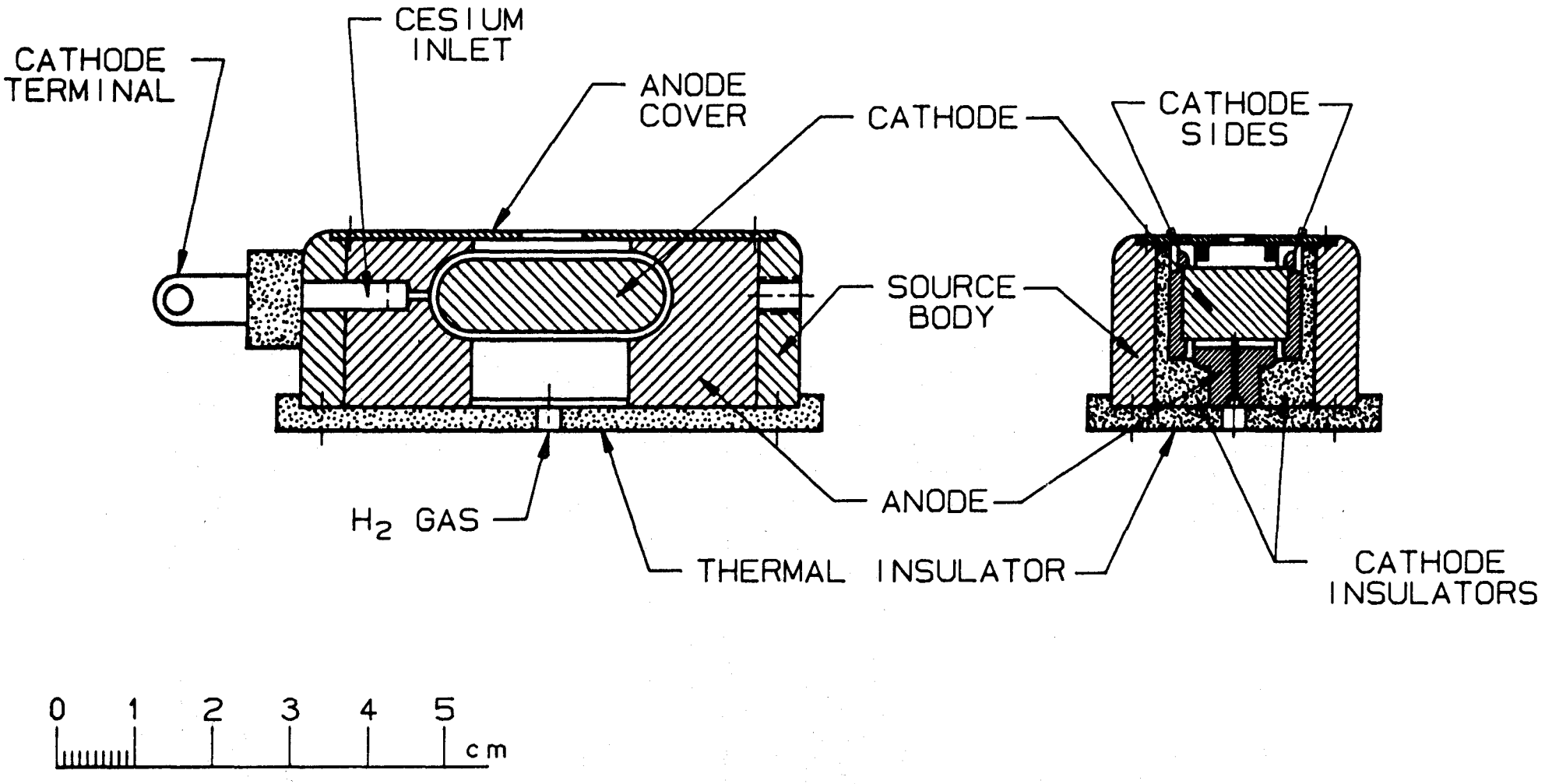

Figure 3.11 Negative-Ion Source

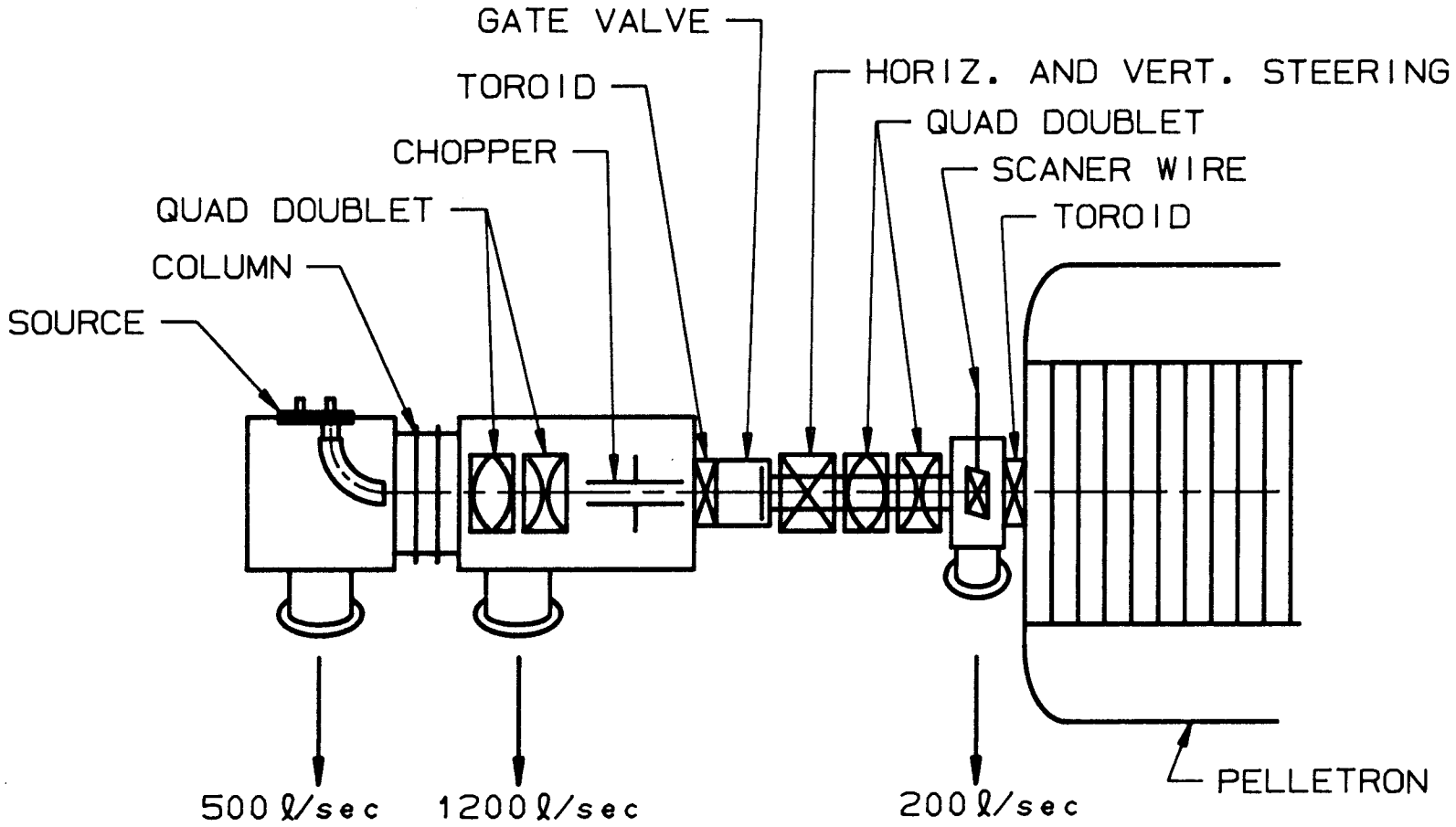

Figure 3.12 Beam Transport from the Source to the Pelletron

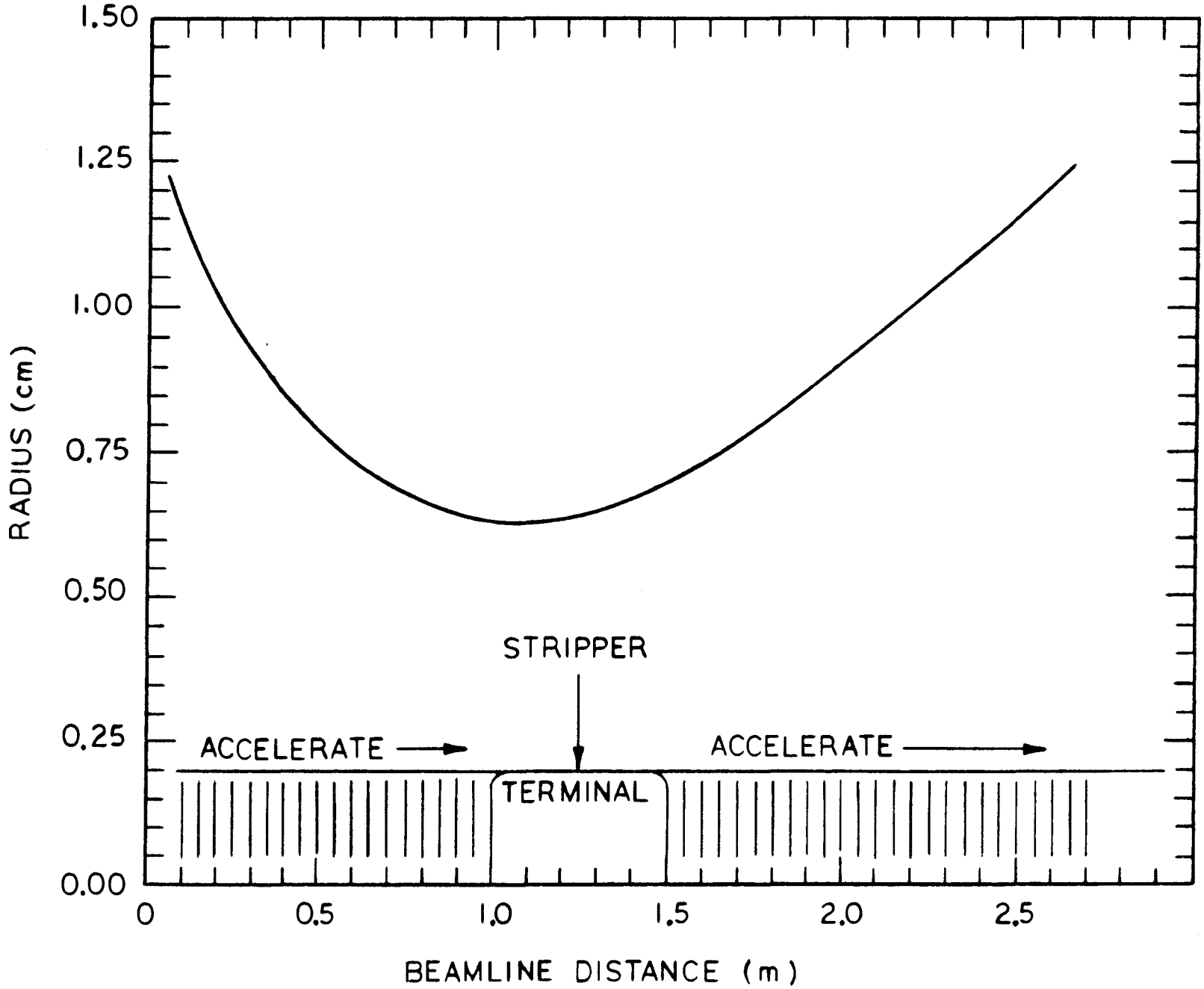

Figure 3.13 Calculated Beam Envelope during Acceleration

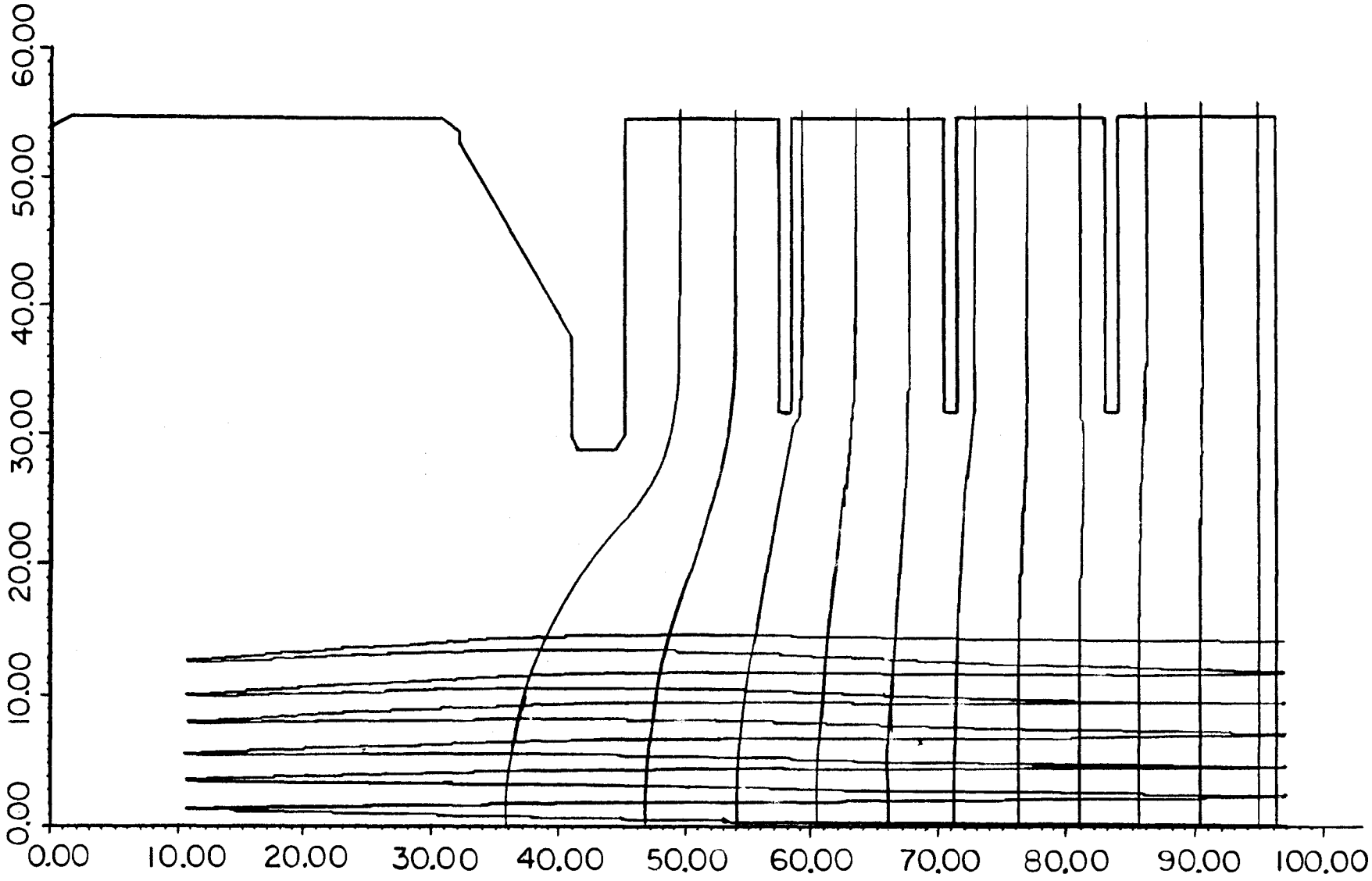

Figure 3.14 Calculated Beam Envelope

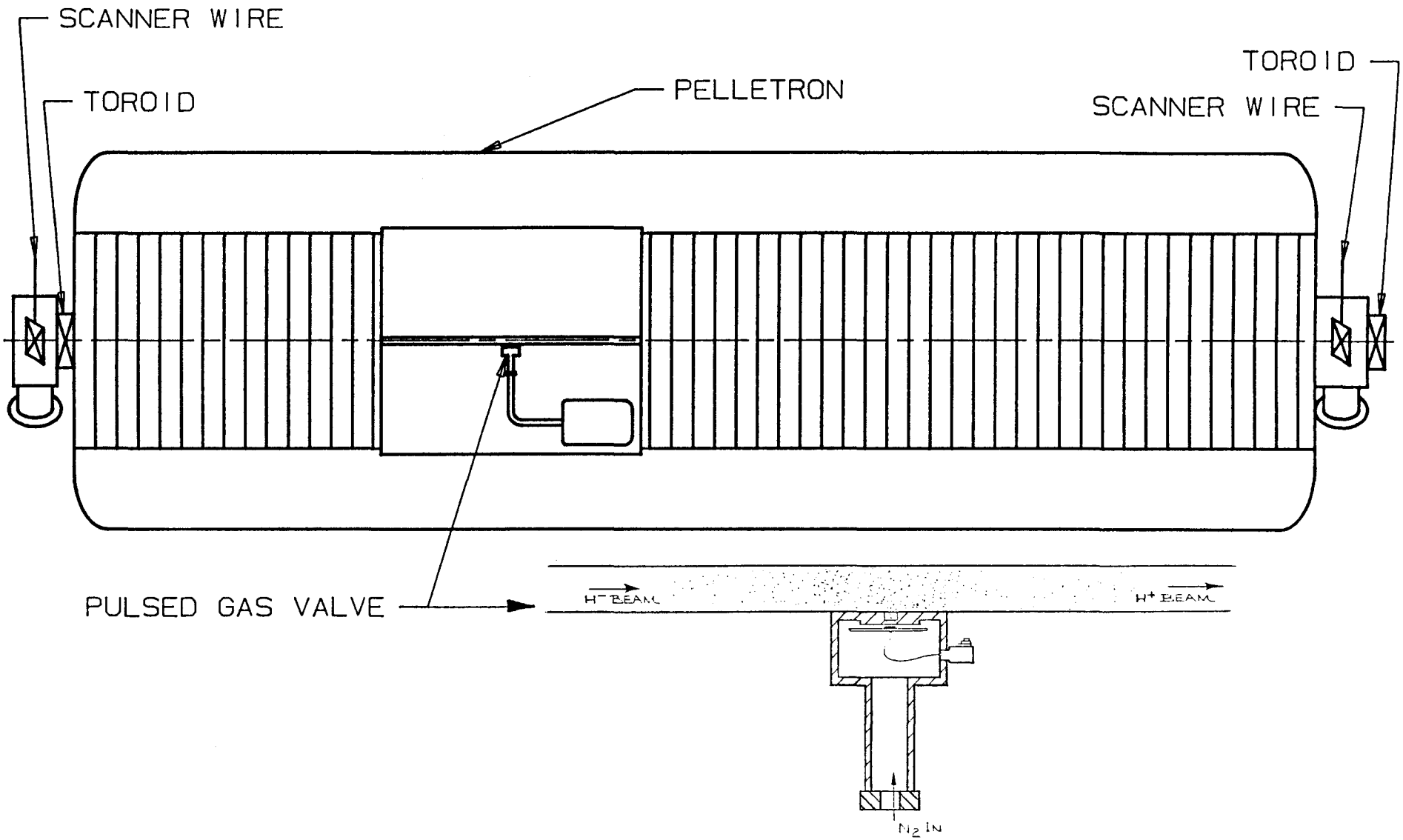

Figure 3.15 The Stripping Canal

3.5.2 Tandem Injector

The standard NEC tandem Pelletron of interest produces 1.7 MV on the dome, delivering a 3.4-MeV proton beam. A cutaway view is shown in Fig. 3.10. Each accelerating column is 1 meter long with 1-in. limiting apertures. The pressurized tank has an outside diameter of 1.07 m and a length of 3.71 m. The dome, where the ion-stripping mechanism is located, is 0.6 m in diameter by 0.75m long and has a capacity to ground of 200pF.

Single-turn injection into the synchrotron achieves the design intensity with a 0.7-μsec beam pulse of 35 mA every 2 sec. We assume an H^--ion source which delivers a beam current of 50 mA. The present operating Fermilab source provides more than 50 mA at 15 pulses per second with pulse length greater than 60 μsec. Replicas of this source are running successfully at other laboratories. Lifetime between source cleanings has been in excess of six months of continuous operation. Beam pulse length will be cut to the requisite 0.7 μsec by a chopper in the beam line. The pulse repetition rate of 15 Hz will be reduced, perhaps to 2 Hz (experiment will determine how much), to reduce the H_2 gas load, which is presently approximately 0.02 Torr-liters/sec.

The source is a surface-plasma magnetron type of small volume (1.4 cc). Cesium vapor flows in from a boiler for reduction of the work function at the cathode, where H^- ions are produced. An 18-kV extractor produces an initially ribbon-shaped H^- beam. A 90^0-bending and focusing magnet shapes the beam and removes unwanted ion species. Details of the ion source are shown in Fig. 3.11. Following extraction, an additional accelerating gap adds 32 keV to provide a 50-keV beam with somewhat reduced space-charge forces.

The low-energy beam transport line matches the 50-keV beam into the Pelletron column. Four small quadrupole magnets control the beam size and angular spread in the horizontal and vertical planes. The line also contains steering coils, the beam chopper and beam current and profile monitors. During the test phase, emittance probes may be added for temporary emittance measurement. The beam-transport configuration is shown in Fig. 3.12.

Computer calculations of the beam trajectory through the Pelletron including finite beam emittance and assumed uniform space charge density show that there are only small problems of transmission. D. J. Larson, using a number of codes and checks, has determined that a 50-mA beam would exit from the first accelerating column with an approximately 6-mm waist radius when entering the column with a beam radius of 1.26 cm and divergence of 0.07 radians. Figures 3.13 and 3.14 show the initial low-energy trajectories and the beam envelope through the complete tandem, including effects of emittance growth from scattering by a 10-$\mu g/cm^2$ carbon stripping foil. For these calculations, a voltage of 2 MV was assumed on the dome to give a 4-MeV proton beam. The normalized emittance of the input H^- beam was E_n = emittance area x $(\beta\gamma) = 2\pi \cdot 10^{-6}$ meter rad.

The simplest stripper is a foil, but there is no experience with thin carbon foils in high peak current, low-average current beams. The concern among those with beam-stripping experience is that foils will not survive long in our application. We therefore plan to use stripping by short puffs of gas released into a stripping canal for temporary confinement. The beam pulse passes through the gas burst while the gas is travelling toward the ends of the canal. The gas then expands into the larger dome volume and is pumped out between beam pulses through the two accelerating columns.

The quantity of gas required to strip 90% of H^- ions to H^+ ions at 1.7 MeV is 700 μcm or 0.7×10^{-3} Torr liters/cm^2 or $0.7\pi \times 10^{-3}$ Torr liters in a 2-cm diameter stripping canal. A fast acting piezoelectric valve can release this gas into the center of a 30-cm long canal in less than 100 μsec (see Fig. 3.15). A thermal-energy molecule of N_2 (1/40 eV) will travel 15 cm toward the end of the canal in 360 μsec (longer if bouncing off the walls). All but a few percent of the molecules have energies less than 0.1eV. Even at this energy they will still require more than 180 μsec to exit the canal. The beam pulse is only 1 μsec in length. The conductance of the two accelerator columns is 33 liters/sec and the volume of the dome is 265 liters. We therefore expect the dome (and top of column) pressure to vary from approximately 3.8 to 2.9×10^{-5} Torr during the 2-sec cycle. Using known stripping cross sections, there will be less than 1% stripping of H^- to H^0 during acceleration in the column. One remaining question is what the transient pressure pulse in the high-voltage end of the accelerator columns arising from directed streaming of gas from the canal will be during the first millisecond. A rough estimate gives a pressure at of less than 10^{-3} Torr, which should not cause voltage breakdown. This question, as well as the overall stripping scheme, needs further investigation with modeling included.

After H^- stripping in the dome, protons are accelerated to 3.4 MeV in the second accelerating column. A transport line directs the proton beam to the synchrotron inflector. This line, shown in Fig. 3.16, has four quadrupoles plus steering coils to match the beam emittance and position to the synchrotron injection orbit. The line also includes beam-profile and current monitors.

Turbomolecular vacuum pumps are planned for the ion source and beam lines at locations shown on the figures. The 500 and 1200 ℓ/sec pumps can be reduced in size by a factor of five or more if the ion source proves to work well at 2 Hz. It is necessary to keep the pressure in the 50-kev beam line to less than 5×10^{-6} Torr for hydrogen and less than 3×10^{-6} Torr for nitrogen to avoid excessive stripping of H^- ions.

The proton beam current arriving at the synchrotron will be subject to control through adjustment of ion source parameters and terminal gas pulser. If one adjusts for a minimum of 90% ion conversion in the gas stripper, one can permit an additional loss of

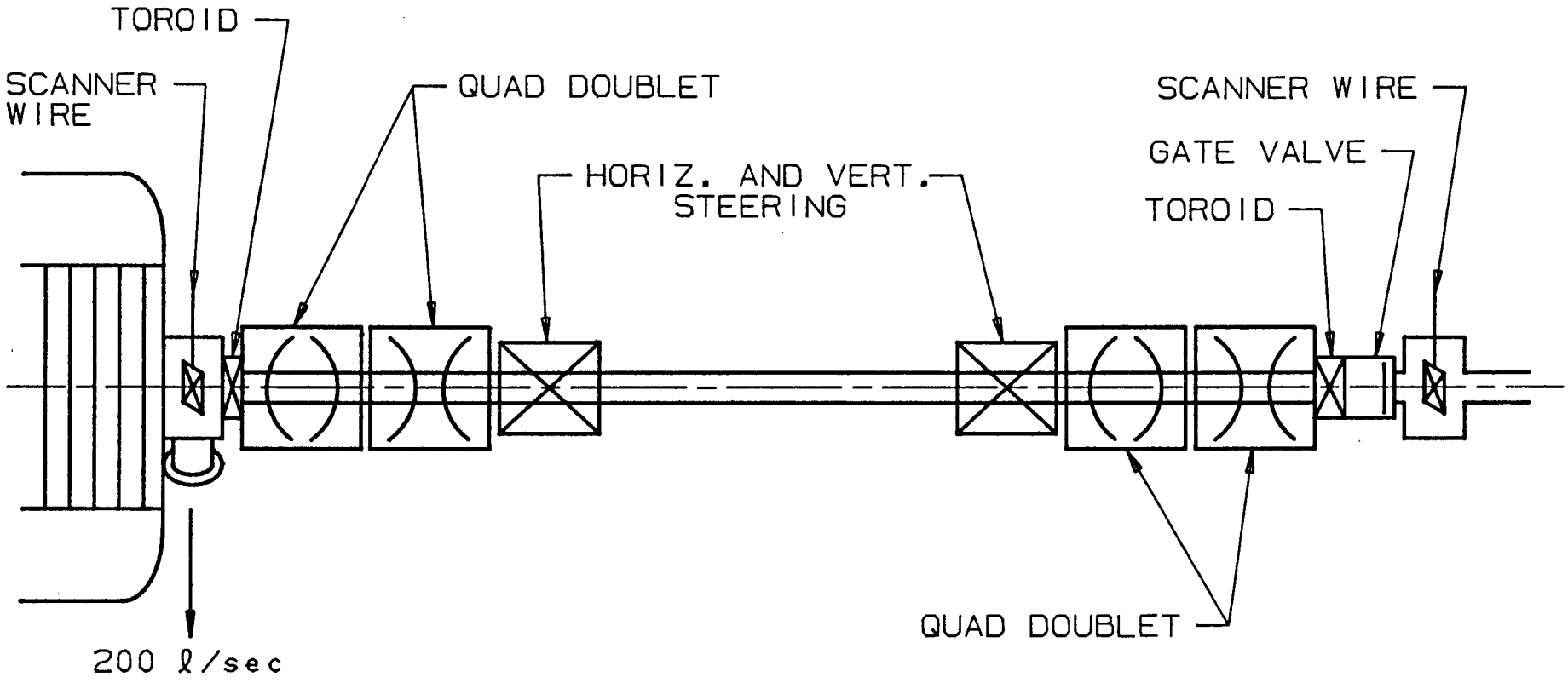

Figure 3.16 Beam Transport from the Pelletron to the Ring

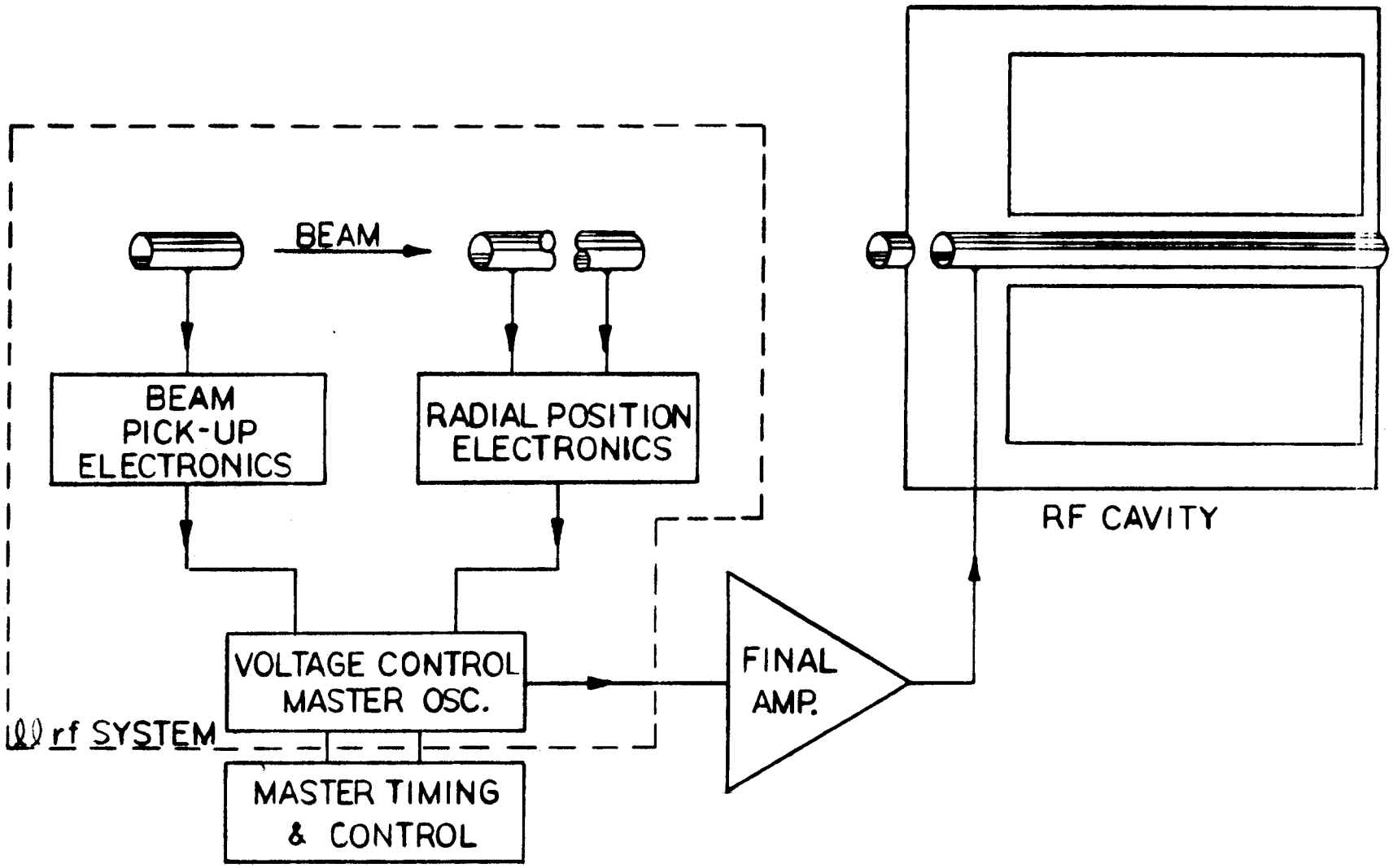

Figure 3.17 Schematic of the Radiofrequency Acceleration System

at least 15% by unwanted gas stripping and scraping in the terminal canal to achieve 35mA into the synchrotron. Table 3-8 lists calculated beam properties throughout the injector.

Table 3-8. Beam Properties in the Injector

	Into Source	Into Pelletron	Into Stripper	Synchrotron
H^- Beam (mA)	53	50	49	mA
H^+ Beam (mA)				40 mA
Energy (MeV)	0.018	0.050	1.7	3.4 MeV
En. Droop (kev)			0.35	keV
E_n (10^{-6} m rad)		2π	$2.3\ \pi$	10^{-6} mrad

3.5.3 Single-Ended Pelletron

The single-ended Pelletron is an alternative to the tandem. With a duoplasmatron ion source in the dome this machine can, with appropriate pulsed extraction equipment added in th dome, deliver short 50-mA proton beam pulses. Less design and development by Fermilab would be required. On the other hand, the system cost exceeds that of the tandem system. Ion source servicing, such as replacement of filaments, requires depressurizing and opening the tank and refilling. NEC has developed procedures for limiting this time to one hour plus repair time. Higher-energy Pellatrons, such as 3 Mev and 4 MeV, are also available at progressively higher cost,if higher energy is important for reaching design intensity.

3.5.4 Radiofrequency Quadrupole Linear Accelerator

The Lawrence Radiation Laboratory RFQ Group has completed a conceptual design of a linear accelerator with radiofrequency quadrupole focusing that will produce an output lower energy spread than previous RFQ's by tapering of the vane contours of the high-energy end. This RFQ operates at 440 MHz and will almost certainly be less costly than earlier, lower-frequency systems. More design work must be done before a decision can be made on the suitability of this system.

3.6 RF Systems

3.6.1 Overview of the System

The beam in the synchrotron is accelerated to its final energy by means of a radiofrequency (rf) accelerating system. The purpose of the rf accelerating system is to supply the required energy gain per turn to the particles synchronously so as to keep the particles on the central orbit as the beam energy and the magnetic field are raised. This is accomplished by the rf accelerating system shown in Fig. 3.17, consisting of a cavity to supply the energy gain per turn in the form

of a impressed rf voltage across an accelerating gap, a final high-power amplifier to excite the accelerating cavity, and a low-level (llrf) system to generate the correct frequency, rf amplitude and phase as functions of time to keep the particles on the central orbit during the accelerator process.

The llrf system is shown inside the dashed line. It consists of a programmable voltage-controlled master oscillator which produces a frequency corresponding to the revolution frequency of the particles as a function of time and also tracks the magnetic field. A small portion of the computer- control system is used to generate this ideal frequency program. Differences between the ideal and actual revolution frequency are detected by the beam pick-up electrode and frequency- comparison circuit. The circuit then produces an error voltage which corrects the master- oscillator frequency. Radial deviations of the center of mass of the particle beam from the central orbit are detected by the radial-position pickup electrode (the obliquely cut cylinder) and radial-position comparison circuit. The circuit then produces an error voltage which is used to correct the frequency to keep the particles on the central orbit of the machine.

Table 3-9 gives the requirements of the rf system. The particles require an energy gain per turn δE of 78.2 eV. This is determined by the rate of rise B of the magnetic field and is given by

$$V_{max}\,\phi_s = 2\pi R\rho B,$$

where V_{max} is the maximum rf voltage on the accelerating gap, ϕ_s the synchronouos phase angle, $2\pi R$ the circumference of the orbit and ρ the magnetic bending radius. The frequency at injection (f_i) and the extraction frequency (f_e) for energy of 250 MeV are also shown in the table.

Table 3-9. RF System Requirements

δE	78.2 eV per turn
ϕs	51.43 degrees
V_{max}	100 Volts
f_i	1.41 MHz
f_e	10.19 MHz
h	1 (Harmonic number)

3.6.2 RF Cavity

Figure 3.18 shows the rf accelerating cavity. The cavity is constructed in the form of a large quarter-wavelength coaxial-line resonator fitted with high-μ ferrite to reduce its overall length. The beam-line length of the cavity proper is 0.46 m; with vacuum flange attachments, its overall length is 0.56 m. Without the ferrite, the cavity be much longer and much less efficient at converting rf input power to accelerating voltage. The beam pipe, the inner conductor of the resonator, contains a ceramic vacuum gap to

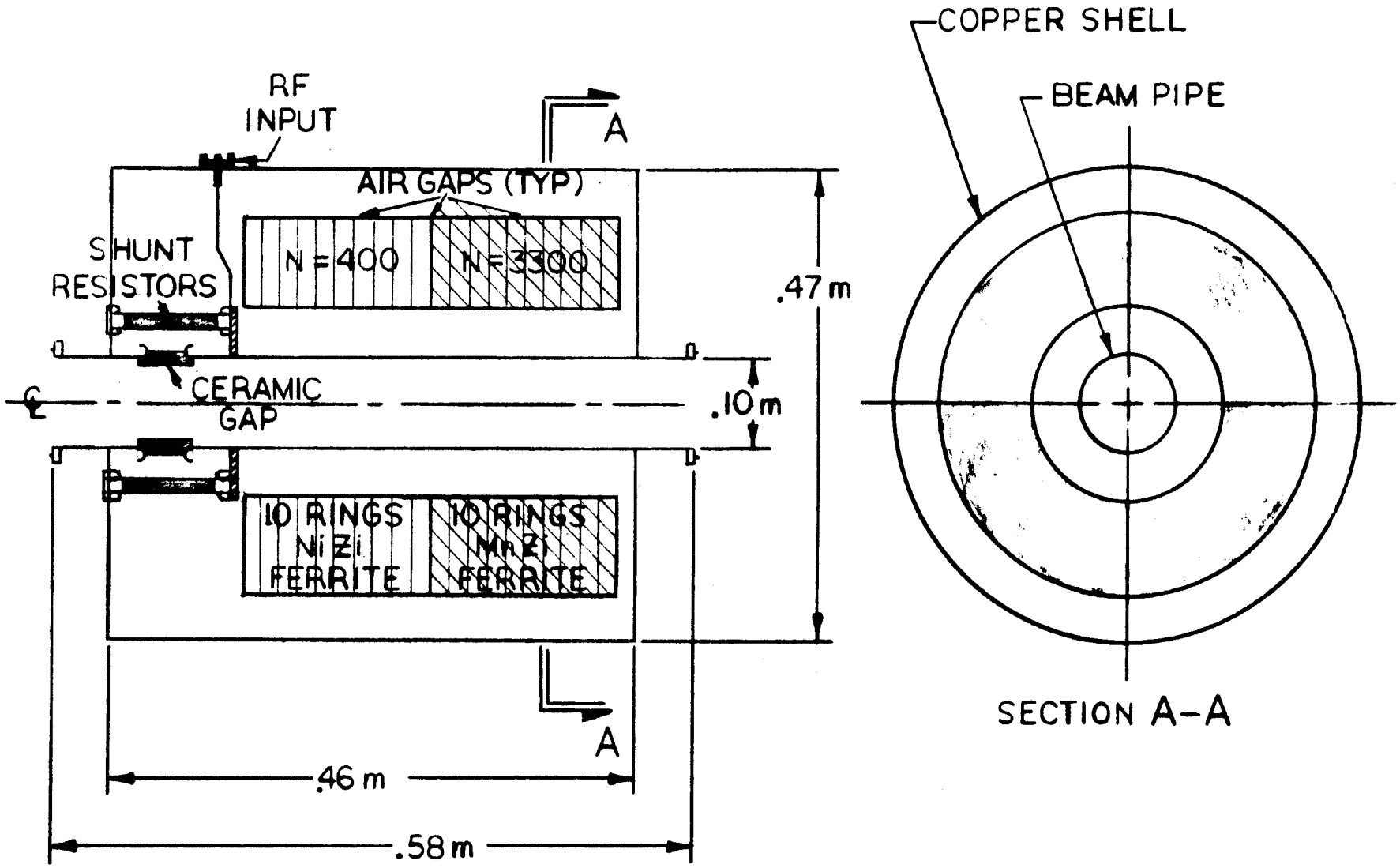

Figure 3.18 RF Acceleration Cavity

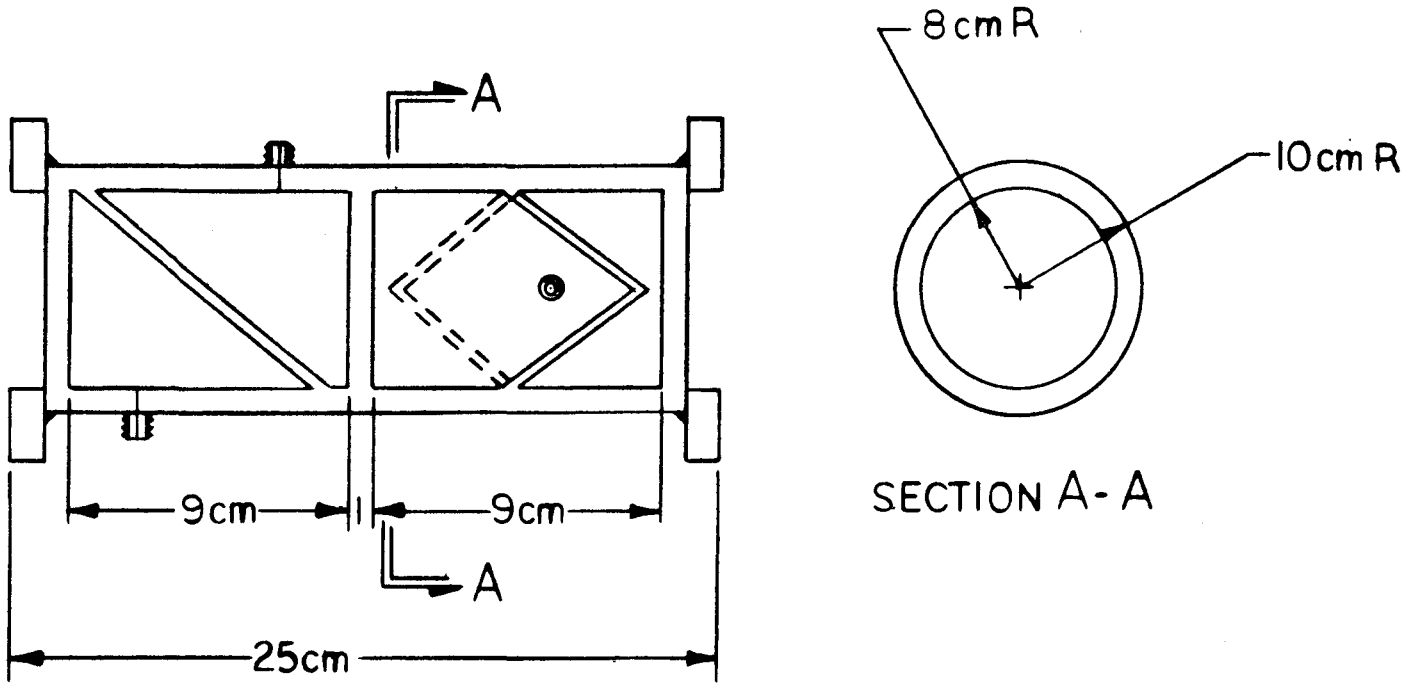

Figure 3.19 Beam-Position Pickups

separate the high-vacuum beam line from the air side containing the ferrite rings. The beam pipe is made of stainless steel to facilate welding to the ceramic gap. The remainder of the cavity is made of copper.

In order to match the cavity to the final rf amplifier, the gap is shunted with resistors so that the combination of resistors and cavity impedance in parallel presents a load of 50 ohms. The high-voltage side of the cavity is attached to the outside shell through a rf input connector by a broad low-inductance metal strip. The final amplifier, a broadband 100-W amplifier, is connected to the cavity at this connector.

An alternative arrangement for matching the cavity to the final amplifier would be by a second rf input connector to the high side of the cavity. To this connector would be attached a matched coaxial 50-ohm load in place of the shunting resistors directly across the gap. This arrangement is feasible only if the cavity impedance is 500 ohms or greater across the rf band of 1.4 to 10.1 MHz. Table 3-10 shows the calculated impedance level of the cavity by itself and the input impedance level when connected to a 50-Ω coaxial load. The calculations indicate that the combination of the 50 Ω coaxial load and cavity impedance are well matched across the board to 50 Ω. Testing on a prototype unit will be done to determine the best arrangement.

Table 3-10. Impedance Level of Cavity

freq (MHz)	Cavity Impedance Amplitude (ohms)	Angle deg	Input Impedance w 50 Ω load Amplitude (ohms)	Angle (deg)
1.4	725	70°	48.8	3.6°
2.0	870	25°	47.5	1.3°
3.0	900	5°	47.4	0.3°
4.0	690	-13	46.7	-0.8
6.0	680	-16	46.7	-1.0
10.0	435	-22	45.2	-2.2

3.6.3 Beam Pickups

Vertical and horizonal beam position monitor (BPM) pickups, shown in Fig. 3.19, are located in each of the short and long straight sections. The pickups are metal cylinders cut along the diagonal into equal electrically isolated half sections. As charged particles pass through the aperture, they induce a voltage on the sections proportional to the distance off center in the direction perpendicular to the direction of the split. The electronics shown in Fig. 3.20 analyzes the signals to produce signals proportional to horizontal and vertical displacements of the beam respectively. The multiplexes are only necessary if the system is expanded beyond 16 channels. An

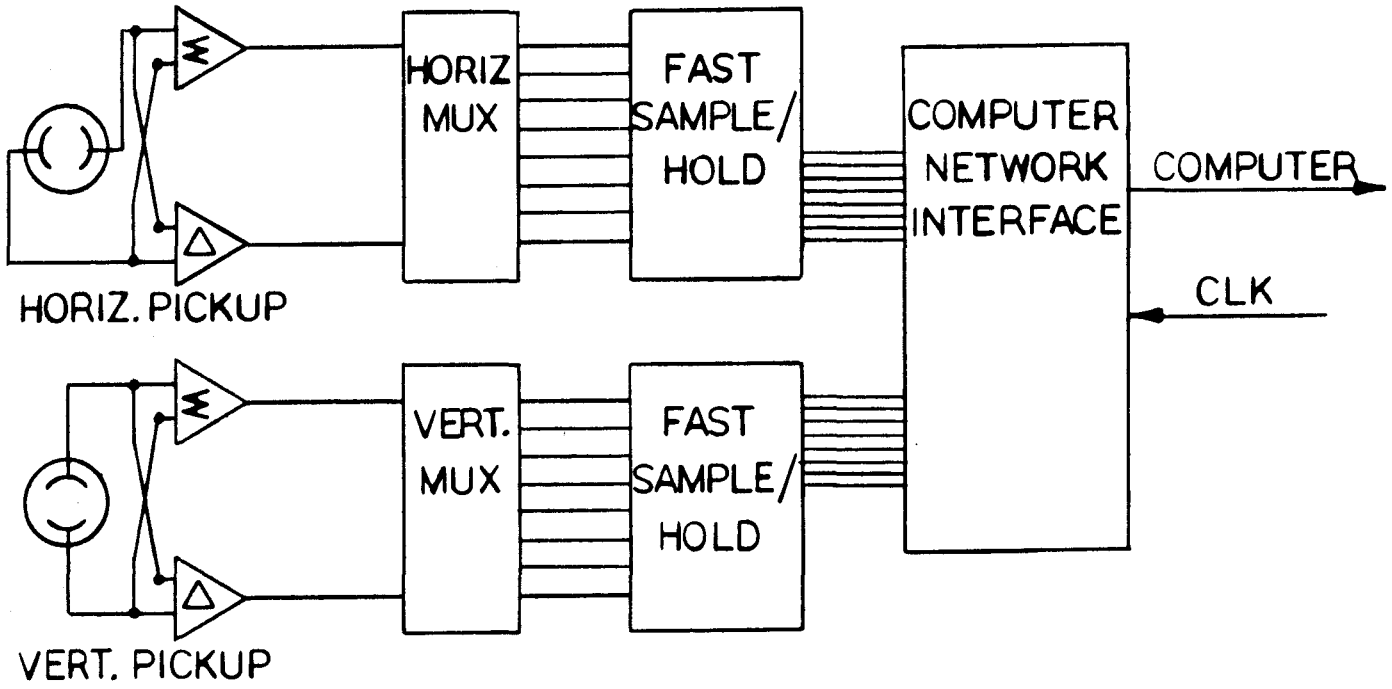

Figure 3.20 Schematic of Beam-Position Electronics

alternative design would use opposed 110° strip lines, one set for vertical and another set for horizontal. Prototype of both types will be built to determine the best pickup design.

3.7 Controls

The accelerator controls will be patterned after the system used at the Fermilab 200 MeV Linac and currently being updated for use in the DO Colliding Beams Detector Facility.

3.7.1 Architecture

The proposed control system consists of multiple distributed microprocessor-based systems networked together and to a MicroVAX II using the IEEE-802.5 Local Area Network (LAN) Standard. This LAN is the Token Ring protocol supported by IBM. Three 68,000-based local stations will be used for the control of the accelerator itself and other local stations are included in the facility control systems (see Section 4.6). The microVAX II performs the centralized coordination of beam requests from multiple treatment rooms and programmed beam-energy control. The microVAX also has disks and printers so it can be used to store operating conditions and copies of the data bases used in the local stations and to make listings as required.

3.7.2 Local Control Stations

The control system will also provide timing pulses to the entire accelerator and facility.

The local control stations will use VMEbus (IEEE-1014) hardware and Motorola 6800 processors. Each local station contains a CPU card, a network adapter and a non-volatile RAM card to store the local data base of descriptors and parameters associated with the equipment controlled by that station. The remaining cards will be the analog and binary input and output interface cards that read and set parameters in the accelerator equipment. The majority of the VMEbus modules will be commercially available to simplify maintenance and spares inventory.

Local stations provide the following functions:

(i) Read analog and binary data
(ii) Make analog and binary settings
(iii) Monitor readings for out-of-tolerance conditions
(iv) Turn off beam, if necessary, based on out-of-tolerance conditions
(v) Send alarm messages to a remote ''Host.''
(vi) Supply requested data to remote requestors.
(vii) Supply requested data to local console.
(viii) Provide the network interface
(ix) Acquire data from other stations, as needed, using the Local Area Network.

(x) Maintain the fixed data base, and the current settings, readings, nominals and tolerances for the local equipment.

The major hardware components controlled by the local stations are the ion source, the injector, injection and extraction-equipment magnet power supplies and rf system.

3.7.3 Consoles

The Fermilab Linac uses small custom-made consoles driven by the local stations to provide local control capability. The local consoles for this accelerator will probably be a personal computer such as an IBM-AT or Apple Macintosh. PC's provide many of the functions normally needed in a console at a cost-effective price.

3.7.4 Local Area Network

The Token Ring protocol is a recent network standard that will be well supported by commercial vendors. This network is used in the DO project at Fermilab. A twisted pair cable forms the physical ring. Wiring concentrators are installed as needed to provide access to the ring by the local stations and consoles.

The 4-megabit data rate for the network should be more than adequate for this accelerator.

3.8 Shielding

Accelerators and beamlines are shielded to reduce the radiation dose received by personnel during beam-on conditions, to reduce exposure to personnel from residual radioactivity present in accelerator components after shutdown, and to reduce contamination to the environment from the creation of radioactivity in uncontrolled locations. The shielding requirements for an accelerator depend on the regulations governing acceptable radiation exposure limits for personnel, as well as on the specific radiation environment around the accelerator. The radiation environment arises from beam loss during acceleration, beam transport, and in targets and beam dumps which generate nuclear cascades in nearby materials. The design of adequate shielding is generally based on the solution of mathematical equations (transport equations) by use of computer codes that predict the behavior of hadronic cascades in different materials and geometries. Semiquantitative estimates can be made by suitable approximations.

3.8.1 Beam-On Conditions

The Loma Linda synchrotron will accelerate protons to 250 MeV with normal intensities of approximately 10^{11} protons pulse, with 1 pulse every 2 sec. The most penetrating component of the secondary radiation that arises from proton interactions in this energy range is the high-energy neutron flux. Shielding that is adequate to attenuate neutrons to safe levels will be more than enough to contain charged particles and high-energy gamma rays.

Estimates of the shielding requirements for the accelerator itself are dominated by local accident conditions in which the full proton beam is lost on a single accelerator component (e.g., a magnet) or, more likely, distributed over the length of a half-cell of the normal lattice. Usually the local-loss scenario leads to shielding constraints that are more strict than for uniformly distributed steady-state losses.

The shielding of the treatment rooms into which the extracted proton beam is ultimately transported must be designed to protect occupied outside areas from neutrons generated not only during normal patient treatments but those that also arise from accidental loss on beam-line components during transport. Which of these loss scenarios dominates the shielding requirements will depend on the actual layout of the accelerator, treatment areas, transport system, and the rest of the facility. Special considerations must be given to the necessary shields associated with beam dumps within the areas. Importance must furthermore be attached to adequate design of access penetrations (labyrinths) and service ducts so that their presence does not impair the integrity of the shield.

The energy dependence of the neutron flux (i.e., the neutron spectrum) that arises in the interaction of protons of a few hundred

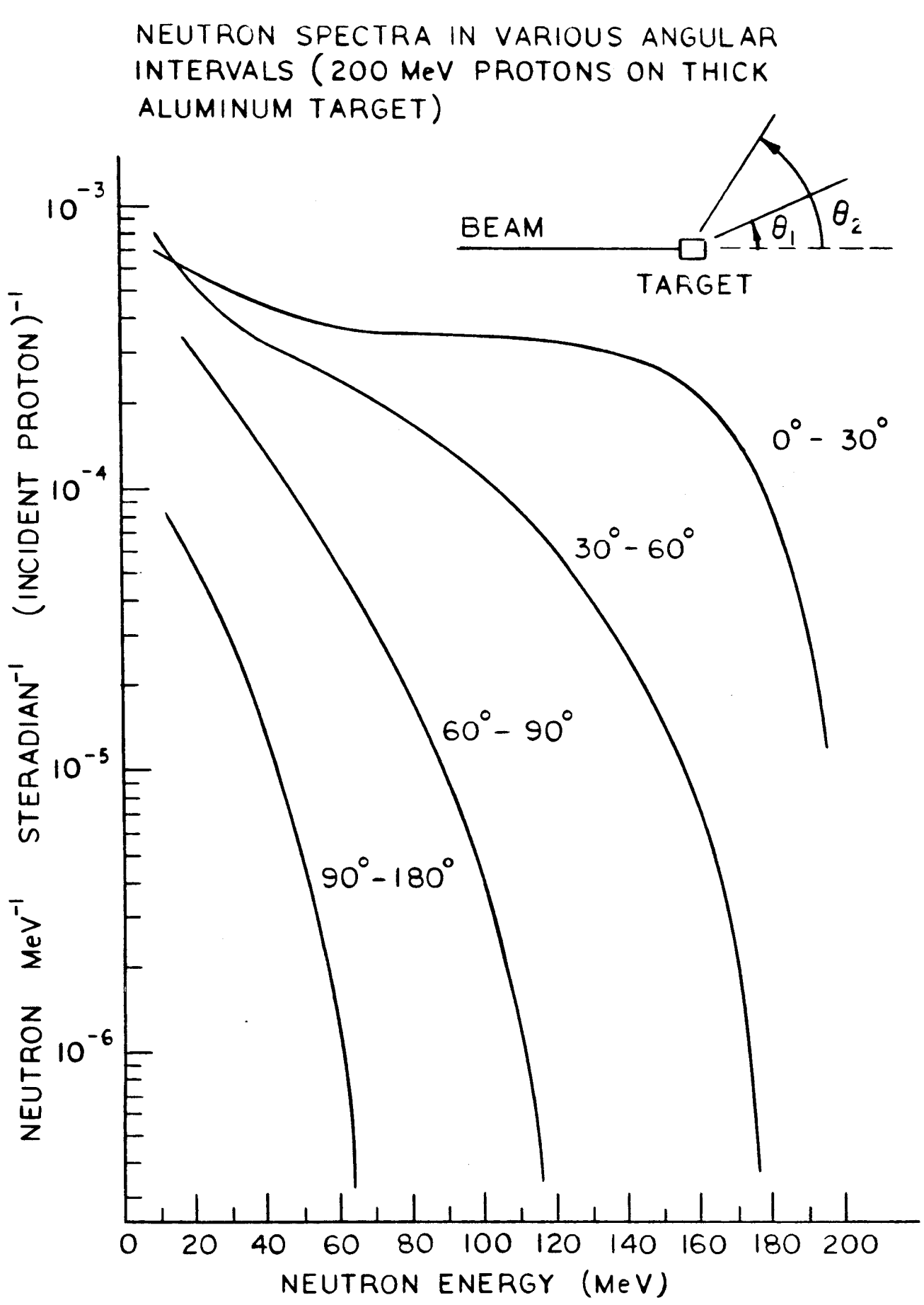

Figure 3.21 Loss of 200-MeV protons in Aluminum

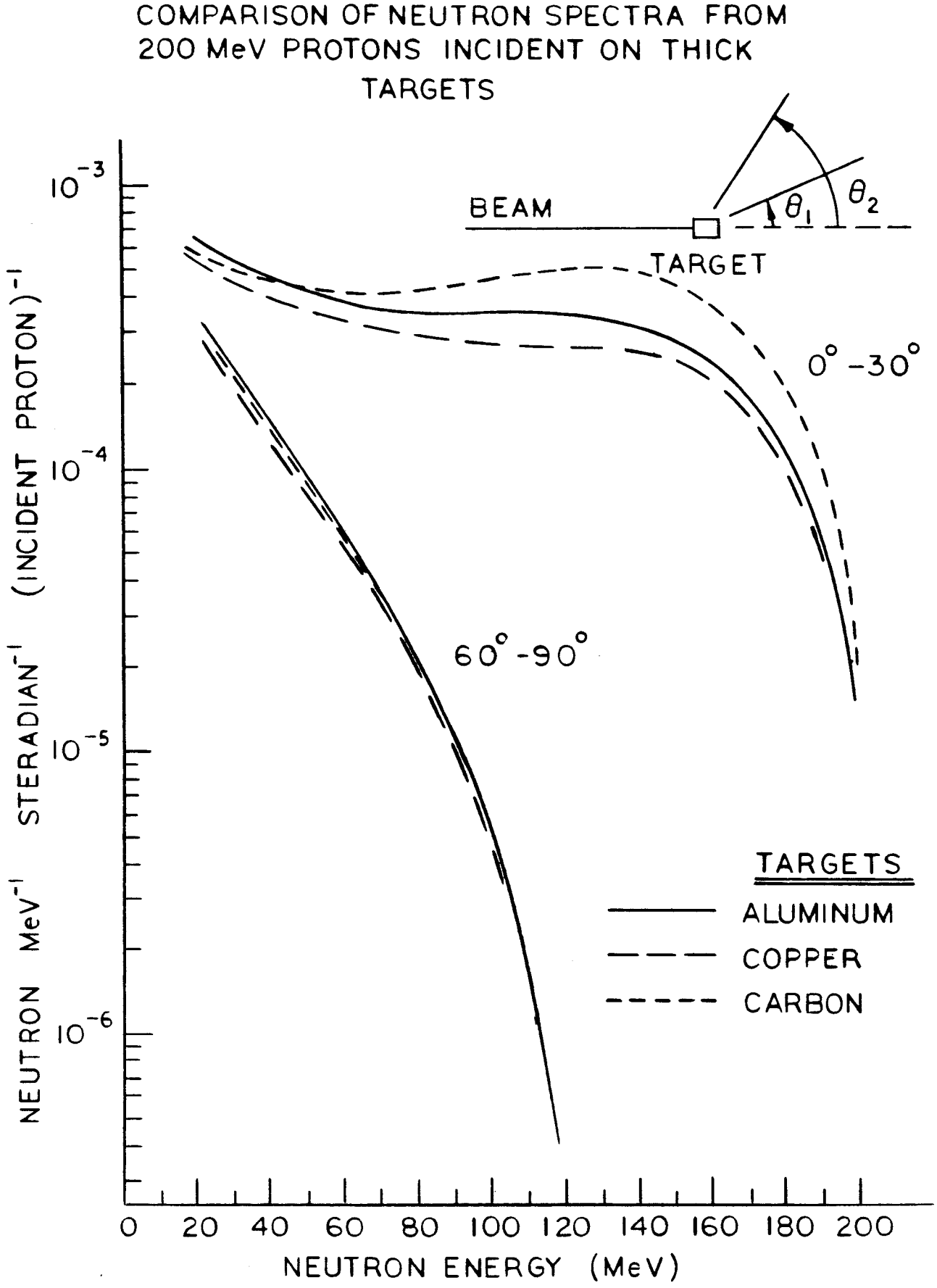

Figure 3.22 Comparison of Loss of 200-MeV protons in Various Materials

MeV with thick targets is strongly dependent on the angles relative to the incident beam at which the neutrons emerge, but only weakly on the target material. This is illustrated for 250-MeV protons in Figs. 3.21 and 3.22; the same general characteristics are expected at 250 MeV. Thus it is apparent that the amount of shielding for different angular regions around loss points will vary. For example, linearly interpolating approximate calculations at 100 and 400 MeV to 250 MeV shielding for the loss of a 1.5×10^{11} proton beam at a thick copper target, placed 100 cm away from the inner shield surface requires about 10.5 ft of concrete shielding at an effective forward angle of 21° (0°-30°) and about 4.75 ft at a back angle of 120° (90°-180°) to reach an exposure limit of 2.5 mrem/hour outside the shielding. At Fermilab, this limit defines a non-posted minimal-occupancy area. For fully occupied locations, the exposure limit is an order of magnitude less. To shield to such a level requires 13 ft of concrete at forward angles and about 6 ft in the backwards direction under the same geometric conditions as above.

The lowest-cost shielding material for facility walls, roofs, and floors is ordinary concrete (or soil where appropriate). The relative high water content (about 6%) aids the slowing down of neutrons and small amounts of heavier material (Ca, Fe, etc.) help to absorb gamma radiation. Special heavy concrete can perform the same shielding task with approximately three quarters the shield volume, but material costs are a factor of ten higher. In other situations in which space is a problem, a shield of steel and concrete allows considerably reduced total thickness compared with ordinary concrete. It must be remembered that steel is almost transparent to neutrons with energies approximately 1 MeV, so concrete must always back up the steel.

3.8.2 Residual Radioactivity and Environmental Considerations

In all accelerators with energies greater than a few tens of MeV, induced radioactivity results whenever beams interact with accelerator or beam-transport components. This typically occurs at injection and extraction elements, collimators, on components in target areas, and beam dumps. These localized regions are consequently the most radioactive areas of the accelerator and work near them constitutes the largest source of radiation exposure to workers at most laboratories. In some situations, local shielding can be used to control photon dose rates from hot spots.

In addition, a large fraction of total residual activity is created by neutrons from cascade and evaporation processes that become thermalized in the hydrogen of water in concrete and earth. These induce radioactivity in the shielding concrete, which accumulates with irradiation time. ^{24}Na is the isotope that dominates the radiation field for about 100 hours after shutdown, although isotopes of Mn, V, and Sc also contribute significantly. The addition of boron to concrete will reduce the thermal flux. Further, the use of limestone concrete, rather than ordinary concrete, on the inside walls of areas such as treatment rooms can reduce the radiation exposure considerably.

Radioactivation of gases may occur in the vicinity of beam dumps and targets from the interaction of both primary and secondary particles with air. Such airborne radioactivity is in general short-lived (e.g., ^{11}C, a major radionuclide produced, has a half-life of approximately 21 minutes), and dilution with inactive air quickly reduces concentrations to acceptable levels. Nevertheless, a program of environmental monitoring should be put in place to assure that concentrations do not exceed appropriate limits.

Monitoring of closed-loop water systems used for cooling magnets, targets, and beam dumps is required to make sure that highly radioactive water is not released into the outside environment. The dominant radionuclides produced are ^{11}C, ^{7}Be, and ^{3}H. The last two are sufficiently long-lived that they could represent as well an external exposure hazard during transport from beam loss point to an outside area. ^{7}Be is highly chemically active and it will adhere to copper piping and filters at the water deionizing facility. Storage of filters for 2 years or less may remove detectable radioactivity. ^{3}H, tritium, presents no hazard as long as the system does not leak. Problems arise once tritium has entered the body through ingestion, inhalation, and skin contact.

Most accelerators are built in close proximity to the surrounding earth. At some locations, particularly near targets and beam dumps, radioactivation of the soil occurs. Some of this radioactivity is leached into the ground water normally present. The rate of production and distribution of activity must be monitored to prevent contamination of nearby drinking water supplies and surface run-off waters.

Estimates of the problem can be made from a knowledge of the chemical composition of local rock and water impurities, radioisotope production cross sections and half-lives, particle spectra and fluxes, and site hydrology, dilution, radioactive decay, and chemical sorption. Radionuclides of greatest concern are those that are produced in large quantities, pass efficiently into the ground water system, do not decay significantly during transport to a public water supply, and have low MPCs (Maximum Permissable Concentrations). At Fermilab, ^{3}H, ^{7}Be, ^{22}Na, ^{45}Ca, and ^{54}Mn are found to be produced in and are leachable from the soil in measurable quantities. The difference in energy and beam power between the Fermilab accelerator and the accelerator considered here is great enough that simple scaling is not likely to apply.

3.9 Radiation Safety System

3.9.1 Introduction

The basic philosophy of any safety system design should be to protect people and equipment from radiation, electrical shock, or other sources of harm.

3.9.2 System Design Considerations

3.9.2.1 Fermilab Installation and Operation. While installed, tested and operated at Fermilab, the accelerator and any associated extraction and transport elements, beam lines, shielding, and interlock or access-control systems will be configured to meet the Laboratory guidelines as given in the Fermilab Radiation Guide, the Fermilab Safety Manual, and applicable DOE requirements.

The system hardware will consist of personnel radiation-safety interlocks, radiation-activated interlocks, and beam-controlling devices such as magnet power supplies, beam stops, and collimators. Because of the potentially serious consequences of an interlock failure, the highest quality materials and workmanship will be utilized in the design and installation of the interlock system. Fully enclosed components will be used whenever practical, and interlock activation mechanisms will be failure-and tamper-resistant.

An important aspect of the system design is the concept of redundancy of devices or duplication of methods to enhance the level of protection for interlocked areas. Redundant hardware design helps ensure that no single component or device failure results in a loss of protection. To accomplish this, two separate independent circuits will be used to detect specific conditions. For example, access-door status will be monitored by two separate switches, each of which is connected to a separate control circuit. Failure of a single switch will not compromise the integrity of the system.

An extension of the redundancy concept will be used in controlling radiation-safety system critical devices. A critical device is one that prevents beam from entering an area. Generally two independent devices will be connected to the safety system to inhibit the beam if the interlocks are broken. In addition, a "failure-mode" critical device will be enabled if the system senses a failure of either primary critical device.

The circuitry of the safety system, which will be hardwired and independent of other accelerator controls will be designed in a fail-safe manner. This will ensure that a failure in the most common failure mode(s) will result in a safety condition, i.e., beam is disabled.

A most important aspect of the system will be the requirement of a search and secure of an area prior to enabling power supplies or

introducing beam into that area. The search of an area will be in a pre-defined sequence that is hard-wired into the safety system to ensure that a thorough search in a logical order is performed.

Once an area has been searched and secured, flashing lights outside any access door will indicate that the area is interlocked and that access is not allowed. An audible warning will be provided immediately prior to introducing beam into the area.

All doors to an interlocked area will be locked and the keys that open these doors will be interlocked in a key tree located in the accelerator control room. There will be basically two types of access to an area, controlled and uncontrolled. A controlled access is defined as one in which a radiation survey of the area has not been performed and power supplies have not been padlocked off. This type of access will present the greatest hazard and only qualified personnel will be allowed to make such accesses. Each key distributed to a qualified individual will be logged out and that individual will be responsible for the proper use of that key. Because these keys are interlocked, beam to an area cannot be enabled until all keys are returned to the key tree.

An uncontrolled access is one in which all power supplies have been padlocked off and a radiation survey has been performed. The level of hazard is thereby reduced and less restrictive access conditions will be used.

As with other areas at the Laboratory, any "power-on" access will require special procedures due to the increased electrical hazards.

The existing Laboratory program for working on and maintaining interlock hardware will be applied. This includes: (1) allowing only authorized individuals to work on the system, (2) documenting the work, (3) maintaining proper control over access keys, (4) periodic testing of the interlock system and, (5) following proper procedures for any jumpering of interlocks. This program is outlined in the Fermilab Radiation Guide as well as in the appropriate Division/Section safety manuals.

3.9.2. Loma Linda Facility.

(i) Accelerator and Beam Lines Enclosures.

The safety system for these areas will be similar in concept to that presented in 3.9.2.1. A good guide for interlock-system design and practice is contained in ANSI N43.1-1969 entitled "Radiological Safety in the Design and Operation of Particle Accelerators."

The following factors should be considered:

•Lines of responsibility
•Proper, up-to-date documentation

•Auditability
•Regular testing and maintenance
•Redundancy
•Fail-safe design
•Designation of critical devices
•Access keys and key control
•Passive versus active barriers (e.g., shielding vs. interlocked detectors)
•Radiation damage
•Instrumentation
•Warning devices
•Jumpering
•Tamper resistance
•Search and secure procedures
•Training

(ii) Treatment Areas

Additional consideration must be given to safety systems in the patient treatment areas. For example, flashing lights and warning horns are not generally acceptable since they will unnecessarily alarm the patient, but it is still necessary to apply proper system design to reduce or prevent exposure to workers in the facility. There will be times when no patient will be present in a treatment room and beam is being brought into the area for set-up, calibration or testing purposes. It is important to reduce the possibility of worker exposure during these times. The basic concepts of critical devices and interlocked access ways will still be used to prevent accidental exposures, and the overall system ideas outlined in Sec. 3.9.2.1 will be applied.

A joint design effort by Loma Linda and Fermilab people will be needed in this aspect.

3.10 Reliability

A highly reliable system is a necessary requirement for a medical accelerator. Reliability comes from a combination of simplicity and conservatism in the design of the electronic and mechanical components with quality control practices vigorously followed in fabrication of the parts of the accelerator system. Substantial derating factors will therefore be used in the design of the individual subsystems and quality-control practices developed at Fermilab in conjunction with the superconducting accelerator project will be adopted for all items to be built at the laboratory.

Simplicity and easy interpretation of displays in the control system are essential ingredients of developing a reliable system. Refrigeration systems required for the superconducting alternative must be conservatively designed systems that are commercially available and backed up with support from the manufacturer.

4. FACILITY DESIGN

There can be many different approaches to the design of the facility external to the accelerator itself, depending on the kind of treatments to be carried out, the number of treatment rooms, and the number and style of beams in the treatment rooms. Given all these treatment parameters, it is still possible to arrange a treatment facility in many different ways, depending on the architectural and functional constraints of the setting. Because of all these variations, we have not attempted to carry through a definitive design of the facility, but to explore and emphasize the feasibility of the technical components and systems. The layouts presented here should be viewed as reference designs or examples, not as proposals.

The purpose of what we have called the facility is designed to transport and deliver the high-energy proton beam from the accelerator to an accurately defined volume in the patient's body.

The Facility components will carry out the following functions:

(i) transport the beam with almost negligible losses from the accelerator (Sec. 4.1) to the entrance of the beam-delivery systems (Sec. 4.2) that carry individual beams to the patients (Sec. 4.3);

(ii) remove any halo from the beam (protons travelling too far from its nominal center (Sec. 4.1.7);

(iii) accurately deliver the proton dose to the aiming volume as prescribed by the radiation therapist (Sec. 4.5.1.4);

(iv) position the patient relative to the beam accurately and use diagnostic x-rays to ascertain that the beam will irradiate the patient as planned (Sec. 4.3);

(v) monitor against beam losses that could harm persons or parts of the therapy system (Secs. 4.5.2.1 and 4.5.2.2).

A computer control system is designed to permit operation of the system by medical personnel who are not expert in accelerator technology.

4.1 Beam Switchyard

The switchyard transports protons from the accelerator to the start of the individual dedicated beam lines leading to the separate beam-spreading systems. An element is defined to be a part of the switchyard if two or more treatment-room beam lines use it. Otherwise, the element will be part of a dedicated treatment-room beam line.

4.11 Location

In our example, the switchyard is located in basement level A, about 2 ft below the floor of level 1 (ceiling of level A) to permit simple and economical delivery of beam to the vertical beam components that carry protons to the horizontal and vertical beam-delivery systems. Some space between the thick concrete floor of level 1 is needed for radiation shielding to avoid occupational restrictions in level 1 (see Sec. 4.7).

4.1.2 Beam-Transport Elements

For economy, the beam bending and focusing should be done by a minimum of magnet types. A satisfactory beam-transport system has been designed using only three types of magnets:

(i) 90-degree dipoles with focusing

(ii) 6 degree dipoles and

(iii) quadrupoles.

The 90-deg dipoles are planned to be identical to the accelerator quadrants. But modifications and higher-field magnets can be used if further development of the architectural design limits the available space. It would be possible to save space, for example, by reducing the length of the short straight section in the center of the quadrant, by redesigning the magnets for 2T operation (which would be very difficult) or by integrating the last 90°-bend magnet with the fast scanning magnet of the dynamic beam spreader. This last idea has been implemented by Dr. W. T. Chu at LBL.

The 6 deg dipoles are be 0.3m long, have a gap of 5 cm, and operate at 0.85 T.

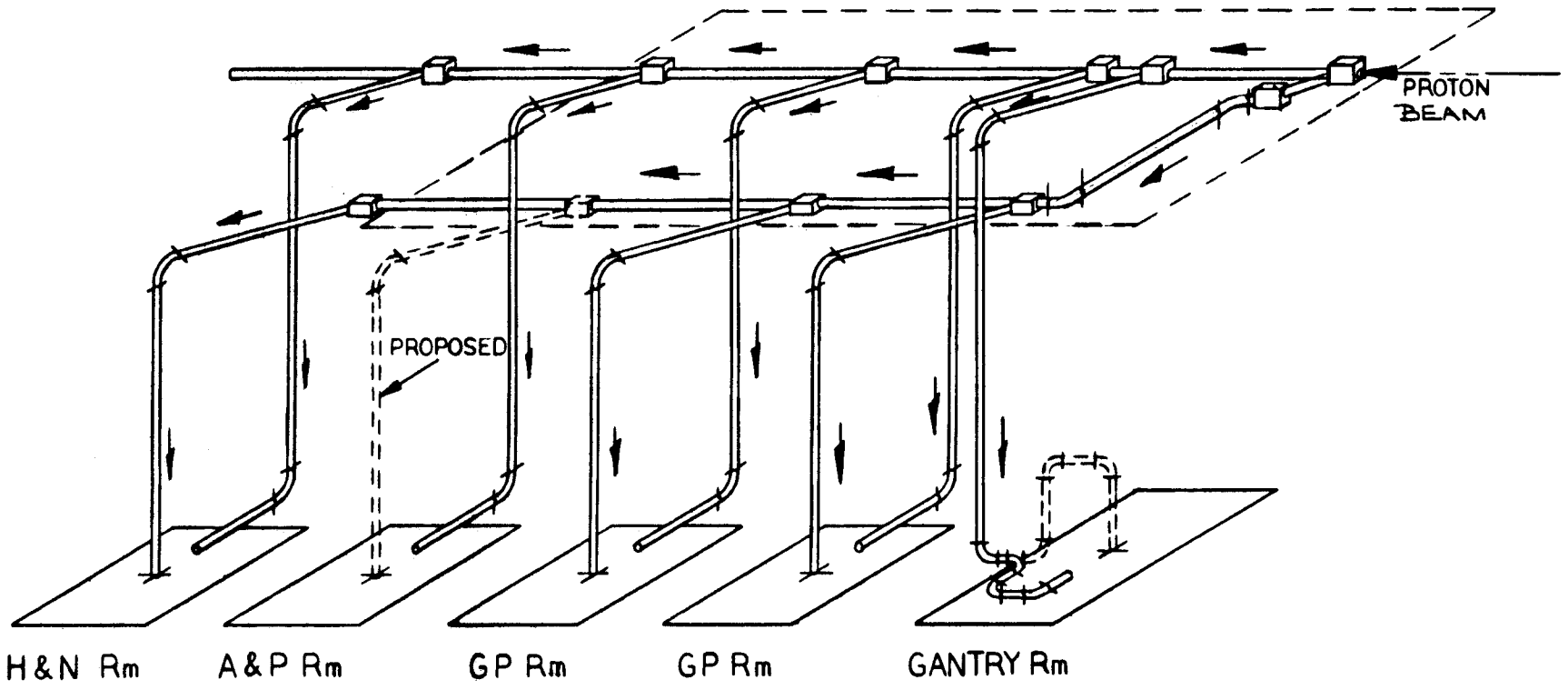

Figure 4.1 Schematic View of Switchyard and Beam-Delivery System

The quadrupoles are needed only to provide a small amount of beam focusing. In our example, it would be possible to utilize quadrupoles that are 0.3m long, have a 5-cm bore and a maximum field of 0.41T at R = 2.5 cm.

A possible arrangement of elements to carry the beam to the beam-spreading systems is shown in Fig. 4.1. For clarity, the quadrupoles are not shown.

As presently visualized, the switchyard has the numbers of magnets listed below. The numbers in parentheses correspond to the case in which the A&P room (see Sec. 4.3.2.2) has with a vertical beam.

(i)	Synchrotron quadrants	2 quadrants
(ii)	6-degree switcher	8 (9) magnets
(iii)	quadrupoles	20 (22) magnets

4.1.3 Magnet Power Suplies

As presently conceived, the switchyard feeds four horizontal, three vertical and one gantry beam-delivery systems. The proton beam is directed to only one system at a time. The 90-deg dipoles can operate in series with the the accelerator.

The quadrupole and dipole magnets and the 6-degree and dipole magnets share power supplies as much as possible, keeping in mind the need for redundancy in operational safety. These power supplies need current regulation of 0.1 - 0.01%, available in "off-the-shelf" supplies.

4.1.4 Beam Diagnostic Instrumentation

In our example, the main beam diagnostic instrumentation (BDI) are SEM's (secondary emission monitors) with two sets of 30 strips each, one vertical and the other horizontal. These BDIs provide information on beam position and shape as projected on vertical and vertical planes. These data are used for beam-position information and to measure beam emittance.

Proven hardware and software exist at Fermilab to extend and retract the BDI's from the beam line, to collect, digitize, display and interpret the charge lost by the two sets of multistrips. This reading, displaying, and interpreting can be done at frequencies of up to 15 Hz.

4.1.5 Beam Loss Monitoring Instrumentation (BLMs)

For the protection of human beings and equipment, two independent networks of detectors are planned. One consists of beam-loss monitors (BLM's) located next to the vacuum pipes (see Sec. 4.5.3.1) and the other of $^{10}BF_3$ counters in polyethylene moderators for neutron detection (see Sec. 4.5.3.2). Either system has the ability to turn off the synchrotron if beam losses larger than preset values are detected.

4.1.6 Number of Radiation Instruments

The system goal is to have the computer start the synchrotron, turn on the beam lines and do all necessary checking and calibration without any intervention by any operator. Therefore a larger than usual number of BDIs is proposed to allow the control computer to detect beam-transport problems and do simple corrections. Furthermore, redundant detectors can be used to diagnose defective detectors. The number of detectors is estimated to be:

(i)	Beam Diagnostic Instruments (BDIs). One per magnet, Thirty three if the vertical beam to the A&P room is installed	30 (33)
(ii)	Beam Loss Monitors (BLMs) one per magnet	30 (33)
(iii)	Radiation Area Monitors (RAMs) One per magnet	30 (33)

The number in parentheses correspond to the case of the option of a vertical beam in the A&P room is executed.

4.1.7 Beam Clean-Up Collimator

In order to remove those protons that are too far from the center of the beam, there is a beam clean-up collimator very close to the accelerator. This collimator makes it possible to transport the proton beam from the accelerator to the beam spreading systems with insignificant losses, provided all magnets and their power supplies are properly placed and powered. The collimator is shielded for radiation safety.

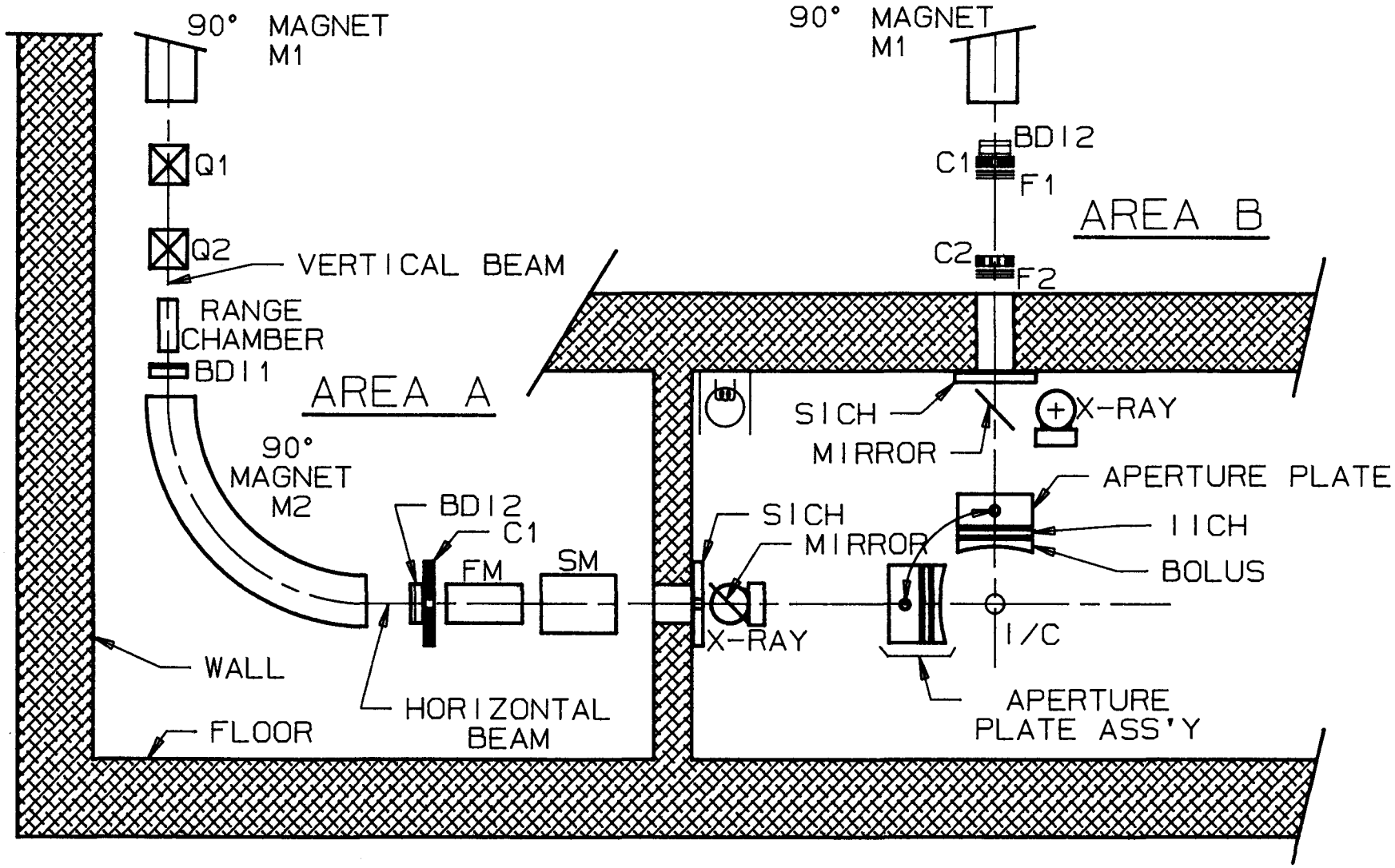

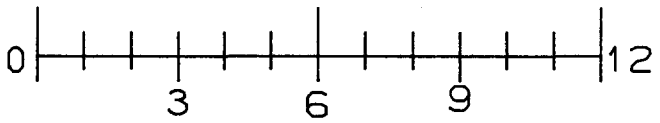

Figure 4.2 Treatment-Room Beam-Delivery and Beam-Spreading Systems

4.2 Beam-Delivery Systems

The beam produced by the accelerator will have small cross section and small divergence. For clinical purposes, it will be necessary to generate beams with cross section as small as 10 mm diameter and as large in size as 40 x 40 cm^2. In addition, these beams must penetrate to depths from zero to 25 or 35 cm of muscle tissue and must therefore be variable in energy. The devices that spread the beam laterally, monitor the beam penetration, measure the proton beam intensity, and shape the beam contour and its distal surface is known as the beam-spreading system.

The part of the beam-spreading system that spreads the beam laterally is the nozzle. There are two types of nozzles, those that:

(i) passively scatter the beam in two metal foils separated by collimators, or

(ii) magnetically "paint" the beam of protons on to a field of uniform intensity by deflecting the beams up and down by one magnet and laterally by another.

These methods are respectively called passive and dynamic beam spreading.

The facility is conceived so that either type of nozzle can be used in any beam-delivery system. The passive or dynamic systems can be mounted in almost all beam-delivery systems. The passive system has a restricted range of beam diameters and residual ranges and possibly only the head and neck room will be initially equipped with passive nozzles.

4.2.1 Component Arrangement

Examples of the two types of beam-spreading systems are illustrated in Fig. 4.2. The drawing shows a dynamic beam-spreading system in area A and a passive system in area B. The drawing shows neither the 90-degree dipoles that turn the horizontal beams from the switchyard into vertical beams nor the range-monitoring ionization chamber in the passive system. The components of the two types of beam spreading systems are described in Table 4-1. References are to Fig. 4.2.

Table 4-1 Passive and Dynamic Spreader Components

		NOZZLE TYPE dynamic (Area A)	passive (Area B)
(i)	90 degree magnet, turns a horizontal beam into a vertical beam	M1	M1
(ii)	quadrupole magnets(only shown in Area A) bring beam to a focus at the appropriate place	Q1,Q2	ns
(iii)	range monitoring ionization chamber, (only shown in Area A) verifies beam penetration	RICh	ns
(iv)	beam diagnostic instrumentation (BDI) upstream of the last 90 degree magnet, (only shown in Area A) shows beam shape and position	BDI1	ns
(v)	last 90-degree magnet, turns a vertical beam into a horizontal one (not needed in the clinical vertical beam)	M2	na
(vi)	BDIs in front of beam collimator upstream from nozzle	BDI2	BDI2
(vii)	collimator upstream from nozzle allows only a properly positioned beam to enter the nozzle	C1	C1
(viiia)	dynamic nozzle, fast and slow deflection magnets	FM,SM	na
(viiib)	passive nozzle, first scattering foil	na	F1
	" " , second collimator	na	C2
	" " , second scattering foil	na	F2
(ix)	symmetry ionization chamber, checks one aspect of nozzle operation	SICh	SICh
(x)	interchangeable x-ray generator and field light mirror, allow visual verification of patient position vis-á-vis the beam	x-ray	x-ray
(xi)	adjustable aperture-plate system consisting of (a) adjustable aperture plate (sets beam cross-section contour), (b) intensity ionization chamber (measures beam intensity), and (c) bolus (shapes distal edge of beam)	Aperture Plate System	

Notes: na = not applicable ns = not shown

4.2.2 Comments on Beam-Spreading Components

(i) The 90-degree magnets are identical to those used in the synchrotron,unless shielding requirements dictate a smaller radius of curvature.

(ii) The quadrupoles are described in Sec. 4.1.2.

(iii) The range monitoring ionization chamber check that the proton beam has the required penetrations (see Sec. 4.5.1.3) before each portal.

(iv) The BDIs verify that the proton is at the correct location for proper operation of the nozzle.

(v) Using suitable power supplies, a raster-scanning dynamic nozzle can operate as a wobbler beam scanner (circular scanning pattern).

(vi) The planned aperture-plate system is quite different in the head and neck irradiation room. That is, it is designed to hold small aperture plates that may be either custom-machined or manually adjustable. In the general-purpose irradiation rooms, a single aperture plate system is used for the vertical and horizontal beams.

4.2.3 Dynamic vs Passive Nozzles

Dynamic and passive beam spreading systems differ in the use of magnets in the first case and an extra collimator and two scattering foils in the second. There are trade-offs between the two modes of lateral beam spreading discussed below.

4.2.3.1 Beam-Spreading Efficiency. Passive beam spreading leads naturally to circular beam contours. When the volume to be irradiated has very different transverse dimensions, a large number of the laterally spread-out protons cannot be used. Even in the case of a treatment volume of square cross-section normal to the beam, a circular beam wastes 36% of the protons. Furthermore, the physical processes leading to a uniform circular beam distribution lead to utilization of only 25 to 32 percent of the beam in making the circular distribution. Hence from the point of view of economy of proton usage a dynamic nozzle is far more efficient.

Because some three-fourths of the protons reaching the passive nozzle will be lost in it, local radiation shielding must also be strengthened.

4.2.3.2 Beam-Spreading Uniformity. At this time, a thorough investigation of proton spreading uniformity has not been completed for dynamic nozzles planned to operate in raster scanning mode. It has been shown that dynamic nozzles working in a circular pattern (wobblers) may produce distributions as good as, if not better than a passive nozzle. Initially passive nozzles can be installed in almost all beam lines. There are two years to decide if this cautious approach is really necessary.

4.2.3.3. Passive Nozzle Limitation. The passive nozzle operation spreads the beam radially with a first scattering foil. This first scattering is the main process to determine the diameter of the disk in which radial non-uniformities are small. A second scatterer and collimator with several circular zones of beam stopping and transmission improve the flatness of the distribution. The first scatterer is dominant and the second one is supportive.

The root mean square scattering angle is

$$\theta_{rms} = \frac{21}{\beta\, p}\sqrt{\frac{z}{\lambda}}$$

where θ_{rms} is in radians, β is the proton speed in units of c, p is the momentum in MeV/c, and z is the foil thickness in the same units as λ, the radiation length. For an energy of 250 MeV, the energy absorbed by the first foil may be so large that the residual proton range is only about 25-30 cm in tissue. That is, with a 3-m spacing between the first scattering foil and the isocenter, and with a range loss of 7 cm in muscle tissue, the useful diameter of the beam is about 30 cm.

4.2.3.4 Nozzle Design. Dynamic nozzles need fast and slow magnets and somewhat sophisticated power supplies.

In raster scanning, the upstream magnet sweeps only in one plane. It usually has a smaller gap and stores less energy than the downstream magnet that has to accommodate both vertical and horizontal sweeps of the beam. Therefore the upstream magnet is the fast one and the downstream one is the slow one. This is satisfactory for raster scanning. Suitable frequencies are of the order of 50 Hz for the fast magnet and 5 to 10 Hz for the slow magnet. These magnets must have good linearity, namely, if B(t) = kt then k should be a constant to within ± 1% at all values of t.

Magnets that are approximately 0.5 m long operate at the following nominal fields:

Source Access Distance	2 m		3 m	
Magnet Type	Fast	Slow	Fast	Slow
Dist to Isocenter (cm)	2.35	1.65	3.35	2.65
Deflection Angle (radians)	0.08511	0.1212	0.05970	0.0754
B (T)	0.2069	0.2948	0.1452	0.1834

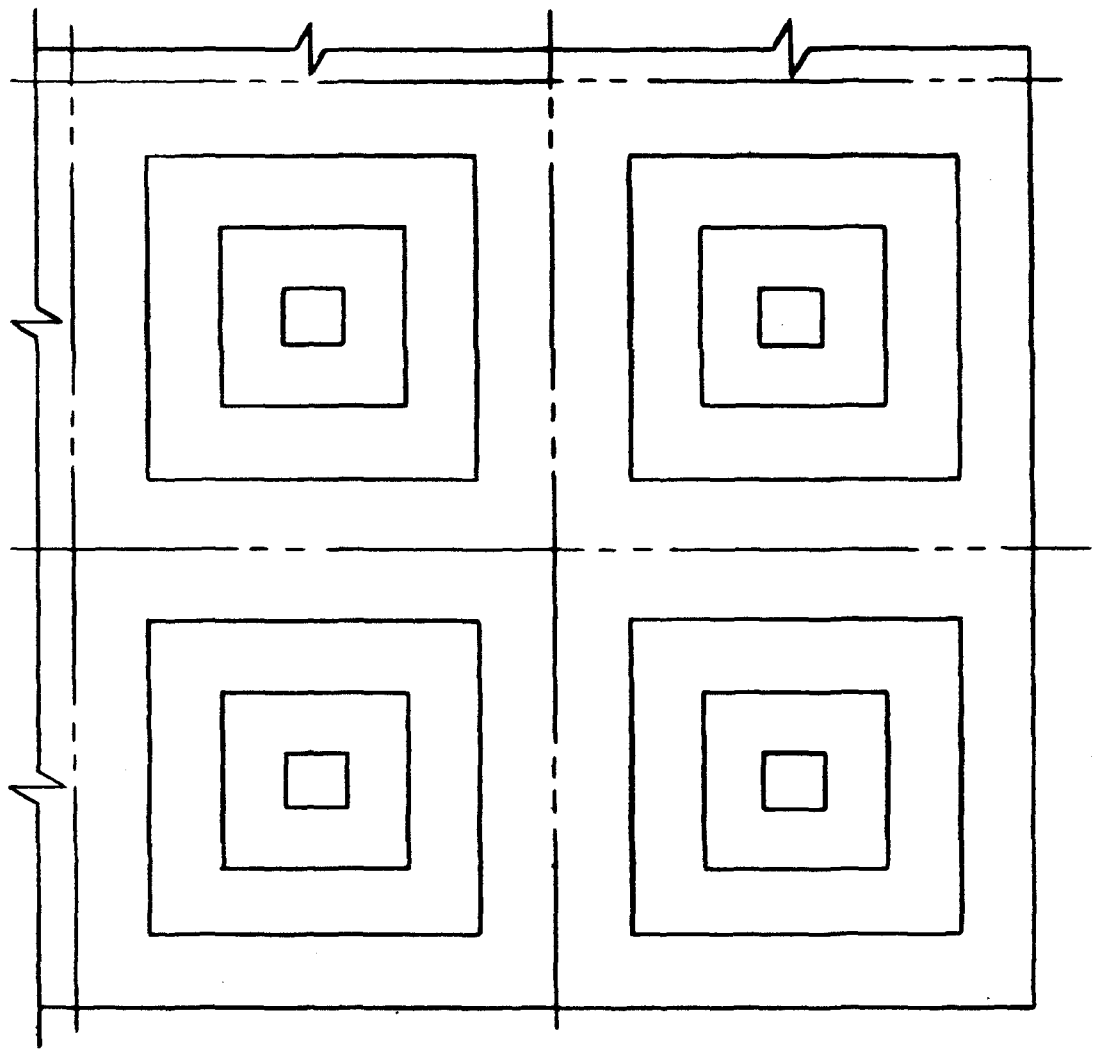

Figure 4.3 Possible Design of a Range Modulator

The passive nozzles need only lead foils of various thicknesses and different second collimators (C2). Optimization of the passive nozzle components requires that the lead foils change thicknesses as the energy of the beam changes. A multiple-foil switching system has been designed. For different field diameters, the second collimator must also be changed.

4.2.4 Beam Depth Dose Uniformity

The adjustment of proton energy for control of the stopping depth in tissue is not done by the beam-delivery system, but by the accelerator. The beam-delivery system will only ensure that it is done correctly before every treatment.

The beam depth dose modulation system has three components, beam energy, range modulation, and shaping of the distal edge.

4.2.4.1 Adjustment of Beam Energy. The penetration of protons in a given medium is primarily dependent on their energy. The primary control for beam penetration is therefore adjustment of the synchrotron output energy. No absorbers are required for major energy degradation. Micro-range modulators can be used to reduce the number of energy steps needed to obtain a suitably uniform depth dose distribution.

4.2.4.2 Diffusion of Proton Stopping Depth. Diffusion can be done with a piece of plastic (lucite) shaped appropriately, as shown in Fig. 4.3. With this micro-range modulator, a monochromatic beam has its range diffused over a distance of several millimeters. Several micro-range modulators may be used in each beam-delivery system.

The purpose of the micro range modulator is to reduce the number the beam energy changes needed to obtain a suitable dose distribution in depth. Basically, the micro-range modulator saves treatment time.

Another type of micro-range modulator uses three dipoles and (possibly) two quadrupoles, which cause beam energy changes by passing the beam through a wedge filter or an echelon. This system allows changing the diffusion function for the beam as needed for deep, medium, and shallow regions of the proximal side of the Bragg curve.

4.2.4.3 Distal-Edge Beam Shaping. A beam transported and spread out laterally stops in a slightly spherical surface in a homogeneous medium. But in clinical work the distal surface of the stopping beam must conform to the shape of the volume under treatment. This is commonly accomplished using a piece of plastic (for example, lucite) shaped to compensate for the patient contour and internal anatomy. These pieces can be machined under computer control using CT-scan information to reproduce the desired shape to very high precision.

4.2.5 Aperture-Plate System

An aperture plate is used to shape the beam contour before it enters the patient. It is usually located as close as possible to the patient to reduce the area in the protected region that is reached by protons scattered from the plate aperture. The intensity ionization chamber and the bolus can be attached to it.

4.2.5.1 Aperture Plate. Since 250-MeV protons are quite penetrating, the thickness of absorber needed is considerable. We show ranges in common metals in Table 4-2.

Table 4-2. 250-MeV Proton Range

Material	Density (g (cm)$^{-3}$)	Range (g (cm)$^{-2}$)	Range (cm)
platinum	21.4	73.8	3.44
tungsten	10.3	72.7	3.76
gold	10.3	73.7	3.82
tantalum	16.6	72.3	4.35
nickel	8.90	53.50	6.01
lead	11.3	75.20	6.63
brass	8.49	57.0	6.72
iron	7.87	53.72	6.83
aluminum	2.70	48.26	17.9

A sketch of a possible manually adjustable aperture plate is shown in Fig. 4.4.

Some of the requirements of the aperture plate are:

(i) It must stop 250-MeV protons.

(ii) To the maximum extent possible, either the proton beam will have little divergence or the aperture must have adjustable edges pointing towards the proton source. A simple arrangement for adjustable finger tips, is shown at the right of Fig. 4.4. These finger tips would be made of tantalum.

(iii) There must be adjustable fingers to allow shaping the contour with suitable resolution. Fingers need not be too thin in a direction perpendicular to the beam direction, since the protons will diffuse by multiple Coulomb scattering inside the patient's body. The minimum finger width is 5 to 8 mm for the aperture plates in the general-purpose treatment rooms.

(iv) In some cases, greater spatial resolution than that provided by the standard set of fingers is needed. In such cases, it

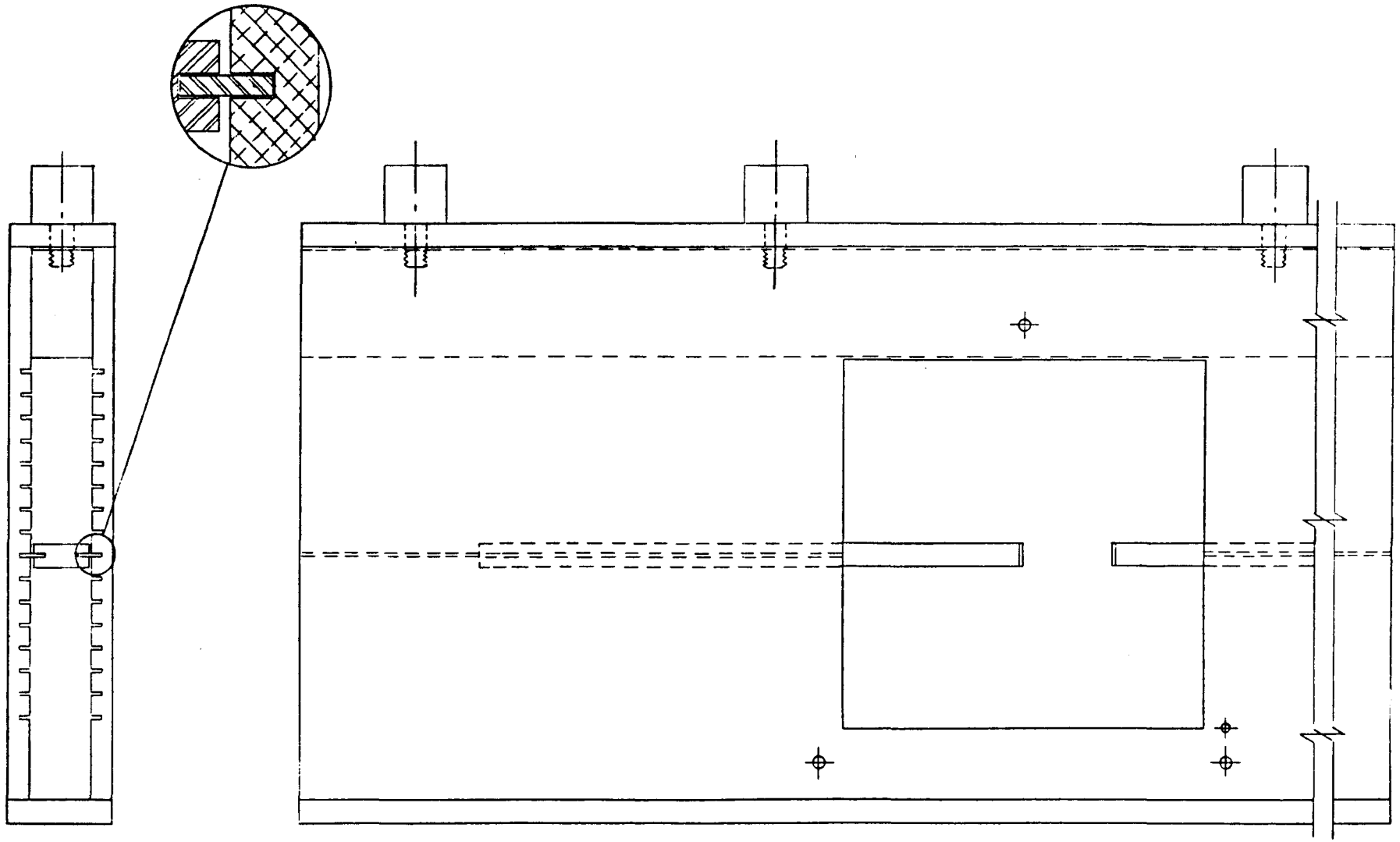

Figure 4.4 Possible Design of an Aperture Plate with Adjustable Finger Tips

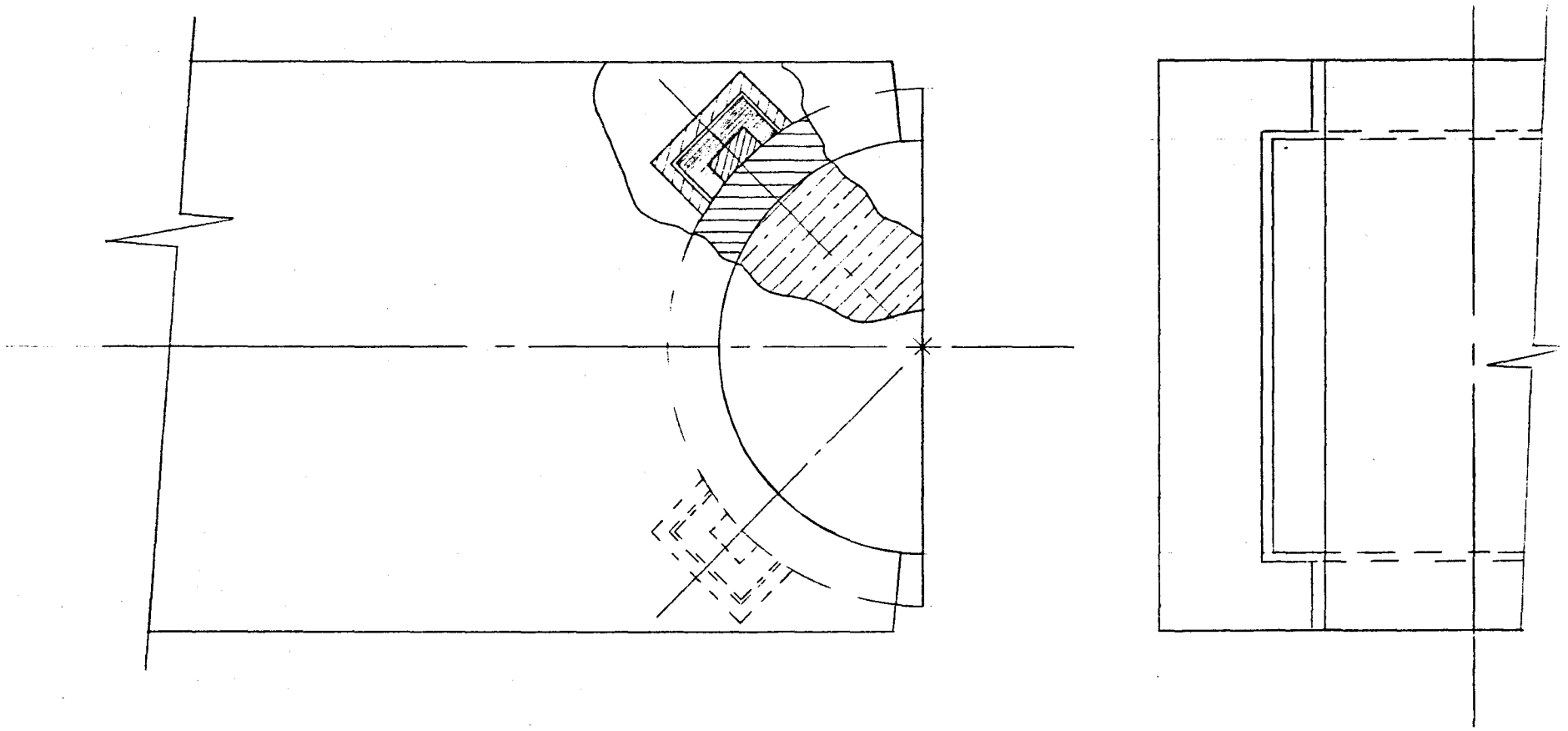

Figure 4.5 Possible Design of Articulated Finger Tips

is possible to machine a custom aperture of brass that can be placed between the standard fingers. This flexibility should be provided for the larger adjustable aperture plates in the two general-purpose rooms and in the head and neck snout of the head and neck room.

(v) There must be a small (or zero) space between fingers to avoid proton leakage into the protected area.

(vi) To get best collimation, the absorber with the minimum proton range would be best, but the metals with the shortest proton ranges also happen to be very expensive. If tantalum is too expensive, then there is little to be gained using anything but steel.

A desirable but not necessary characteristic of adjustable aperture plates is the capability to vary and monitor the opening remotely. This permits reduction of the size of the aperture as irradiation proceeds, reducing the dose absorbed by proximal normal tissues. This feature will be explored during final design.

4.2.5.2 Articulated Finger Tips. Since the planned source access distances is approximately 2 to 3m, it is of interest to design articulated tips for the aperture plate fingers.

Figure 4.5 shows such a design. The tip parallel to the beam boundary is made of tantalum. A steel band is wrapped around its midplane on the cylindrical surface to provide alignment.

4.2.5.3 Dual Beam-Intensity Ionization Chamber (IICh). Because of the characteristics of raster scanning, it is advantageous to mount the beam intensity ionization chamber on the downstream side of the aperture plate. It can be mounted on linear bearings to permit using the field light and then being repositioned easily and precisely. Naturally, for patient safety the chamber is to be double and the digitizing electronics redundant.

4.2.5.4 Bolus Holder. The bolus that is used to shape the distal surface of the beam can also be mounted on linear bearings on the aperture plate downstream from the IICh. The bolus holder should be designed to facilitate placing and removing the boluses which in some cases may be quite heavy.

4.2.6 Beam-Delivery Systems Recommendations

(i) Head and neck room, install passive nozzles for the vertical and horizontal beams.

(ii) General purpose rooms, install both passive and dynamic nozzles. Plan to use the passive nozzle for small diameter

(20 to 30 cm) fields and the magnets for either wobbler or scanning nozzles. The magnets are to be designed for raster scanning but it would also be possible to operate them as wobblers using a resonant 60-Hz power supply. Consideration should be given to placing the "fast" scanning magnet upstream from the last 90^{o} bending magnet of the beam-spreading system.

(iii) A & P room, horizontal and vertical beams as in (ii) above.

(iv) Gantry room, install a passive nozzle for small fields and a dynamic system for large fields (up to 40 x 40 cm^2).

(v) The possibility of beam cross section changing synchronously with a wobbler or a raster scanning nozzle should be explored carefully to see if it is possible to dispense with the aperture plate.

4.3 Treatment Rooms

The common elements of the treatment rooms will be described, then the individual treatment rooms. The components of the dedicated beam-transport system for each room (not in the switchyard) are listed in the section describing the appropriate room.

4.3.1 Common And Diverse Elements

The elements that will be described here are the clinically significant ones such as beam-intensity monitoring or patient-positioning devices. Other elements, such as area radiation monitors, safety interlocks or vacuum gauges, will not be discussed here.

4.3.1.1 Patient-Positioning Aids. The devices listed below help the physicians and technologists position the patient such that the treated volume is within a few millimeters of the aiming volume.

The treatment rooms have been designed keeping in mind that proton beam therapy may be conceived as the treatment of choice in lesions sensitive to low-LET radiation therapy, for two reasons:

(i) highly definable dose localization, and
(ii) reduction of dose to intervening normal tissues.

For lesions distant from critical structures, reduction in complications in normal tissues can be achieved without the extra care needed for precise geographical localization of dose deposition. But if the full potential of proton beam therapy is to be realized, one must also consider the physical demands on the personnel who will place the patient in the proton beam with high precision, avoiding unnecessary sources of fatigue to them and making it easy and simple to position the patient accurately.

To achieve these objectives, the traffic pattern in the treatment rooms for the medical personnel during a day of therapy, is visualized as follows.

(i) As the n^{th} patient leaves the treatment room, the aperture plate opening is set for the $(n + 1)^{st}$ patient, field #1, the bolus is set up, and the calibration ionization chamber for calibration of the beam intensity ionization chamber (see Secs. 4.5.1.4. and 5.) is put in place.

(ii) The beam intensity ionization chamber is calibrated at a depth corresponding to the center of the stretched-out Bragg peak of $(n + 1)^{th}$ patient, field #1.

(iii) If more than one field is to be used, the appropriate ionization chamber will also be calibrated at the appropriate depth in tissue, but possibly using only one aperture plate setting and cross-referencing calibrations using the other apertures at other depths.

(iv) The $(n + 1)^{th}$ patient is set up in the chair or on the couch.

(v) The physicians and technologists return to the local control console where electronic x-rays is used to allow final remote patient-position adjustments of 5 mm or less in each direction.

This traffic pattern reduces the travel between treatment room and local control console to one per patient. This is important because the distance between the local control console and the isocenter will be at least 50 ft and unnecessary fatigue should be avoided.

If no change in beam cross section or bolus is needed, repositioning the patient for other portals will be possible remotely and accurately.

(i) Electronic X-Rays. X-ray generators will be mounted on walls or ceiling to permit viewing the patients' bony structures. Although the x-ray target to ionization chamber distance will not be the same as the source access distance, the distances are long(2 to 3 m) and the difference in perspectives easily manageable in most cases. The receiver is a combination of focused grid, intensifying screen, large aperture short focal-length lens and a high-sensitivity, high-resolution video camera. The signal from the video camera will be analyzed and stored, then passed to high-resolution monitors. A series of scans is performed and the signals added. The signal to noise will increase and the process is stopped as soon as a satisfactory image is obtained. The proton beam and the diagnostic x-ray beam should be coaxial to ± 1 mm or better.

(ii) Laser Beam Crosses. Laser-beam crosses permit rapid initial patient positioning with reference to skin marks. This positioning by skin marks will bring the patient's aiming volume to within 5 mm of the desired position. The line defined by the two laser beams and the center line of the proton beam should be coaxial to ± 1 mm or better.

(iii) Field Lights. Field lights are to be provided for all beam lines to assist in the verification of the correct alignment of beam, aperture plate and aiming volume.

(iv) Computer Remote Monitor. A standard color TV monitor is to be located in each treatment room. It gives the medical personnnel, as well as the patient, a way to verify ID by picture, name, and facility ID number as well as set-up parameters.

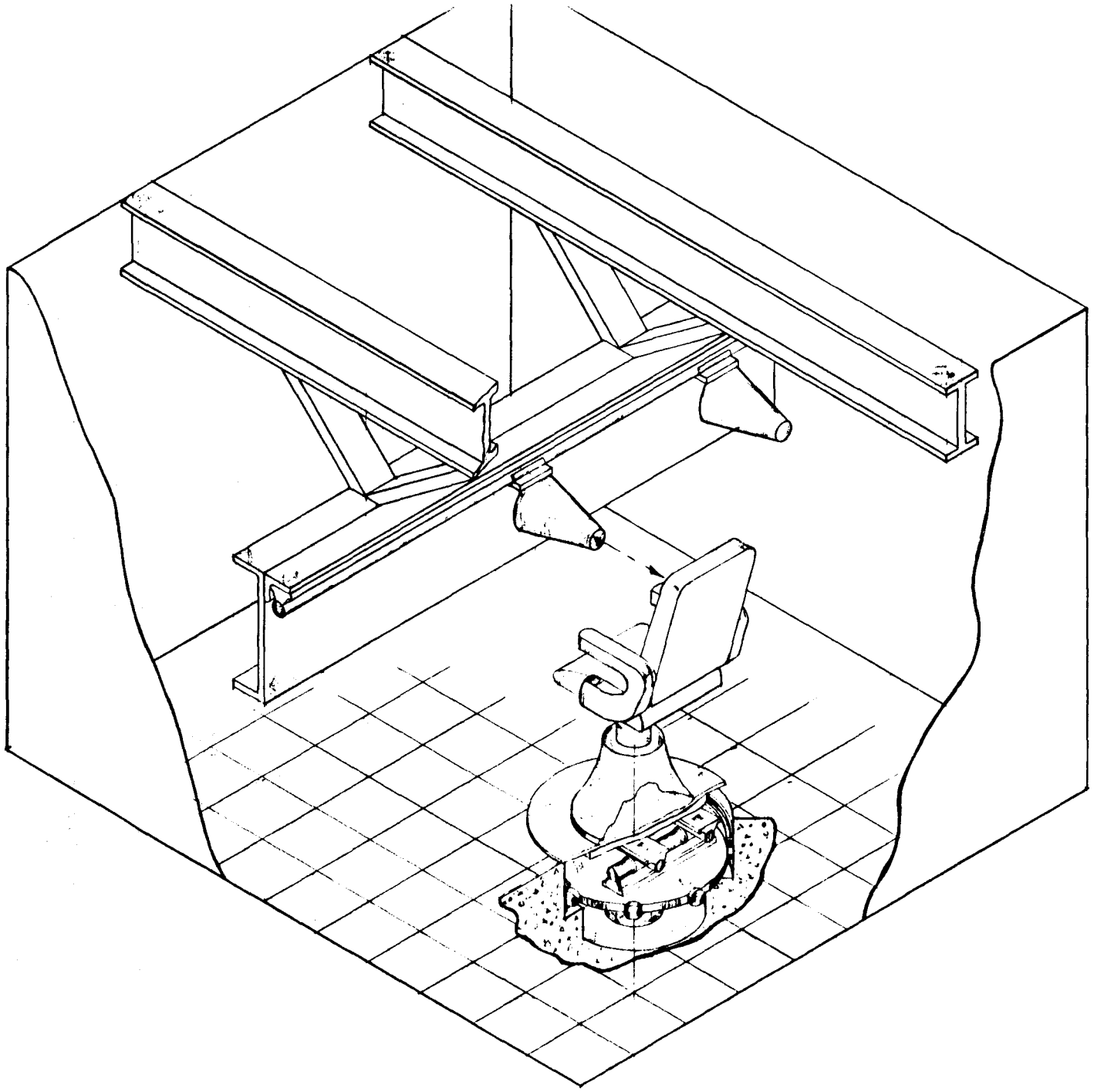

Figure 4.6 Treatment Room with Adjustable Chair

4.3.1.2 Patient Supporting Devices. Patients can be irradiated either in the supine position on a couch or sitting up in a modified barber-shop chair.

(i) Treatment Couch. This couch should have six degrees of freedom, three displacements (up-down, lateral and along patient's long axis) and three rotations (around isocenter (0-360°), roll (±15°) and pitch (±15°). These motions should be remotely monitored and controlled.

The couch top is to be adjustable from approximately 45 inches down to 35 inches above the finished floor. This large minimum height is needed to accommodate the x-ray receivers. The top is to slide 41 inches along the patient axis and ±7 inches perpendicular to that axis.

It is expected that most of each treatment couch will be commercially available and that only the roll rotation may have to be added. For the gantry room, the isocentric couch need only have rotation about the isocenter and pitch variation plus the three orthogonal rectilinear motions.

(ii) Treatment Chair. For treatment of eye melanomas and head and neck lesions, a positioning chair will be used. A barber chair can be modified to serve as a very solid treatment chair. Barber chairs already have vertical adjustment. A modified base will permit x- and y-motions as well as rotation of the chair about the isocenter. In addition, the foot and arm supports can be made adjustable in height and a support adjustable in height and angle will allow immobilization of a patient's head for AVM, pituitary and aneurysm treatments. This immobilization can be achieved using ear plugs and a bite-block. This chair is shown in Fig. 4.6.

For eye melanomas, the patient will lean forward and the head will be held in place by a combination of bite block and contoured plastic mask in a manner similar to that used at the Harvard Cyclotron Laboratory - Massachusetts General Hospital.

For AVMs, aneurysms, pituitary and other head and neck lesions, the patient will lean against the chair back. There will be supports for the bite block and ear plugs at two levels to minimize interference of hardware with the proton beam.

For each type of irradiation, beam-related and visualization hardware are to be housed in specialized ''snouts.''

(iii) Isocenter Height. Loma Linda medical personnel have chosen a height of 48 in. (122 cm) above the finished floor for the isocenter (I/C). This height has been shown to be practical at their conventional irradiation facilities.

A height of 48 inches is also convenient for the chair positioner in the head and neck room because it allows treatment of tall persons without need for uncomfortable and hard-to-maintain slouching positions.

4.3.1.3 Snouts. For the treatment of eye melanomas and other head and neck lesions, protons beams will usually be of energy less than 180 MeV, e.g. ranges of 21 cm or less in tissue (1.53 in. in brass). Higher-energy beams might be used if aneurysms are treated as in the USSR, with the Bragg peak beyond the patient. The snouts must be capable of stopping protons of 80 MeV for the eye system and 180 MeV for the head and neck system.

The fields are small, approximately 5 cm diameter for the eye snout and 20 cm diameter for the head and neck snout. All therapeutic eye and almost all head and neck treatments require accurate beam contouring and positioning. The snouts should therefore carry either machined aperture plates or small adjustable aperture plates.

Snouts must be specifically designed for either eye or head and neck therapy. They should be mounted to allow fast, precise movement in and out of the proper position in the proton beam.

(i) Eye Snout. This snout supports the bite block and contoured plastic mask used in the head-fixation system. It should have places to mount the custom-made aperture plate, an intensity ionization chamber, and a radially and azimuthally adjustable eye-fixation light. It could also carry the CCTV cameras for continuous visual monitoring of the patient's eyes and the taking of electronic x-rays coaxially with the beam.

(ii) Head and Neck Snout. This snout is much simpler than the eye snout. It only need carry the CCTV cameras for visual and x-ray position verification, an intensity ionization chamber and a place to mount a custom-made fixed brass aperture plate or an adjustable aperture plate and a bolus. It must also be heavier, since it must stop 180-MeV protons.

4.3.1.4 Patient Monitoring. Patients can be continuously monitored by CCTV and a high-quality intercom. The CCTV's focus on the irradiated area and on the full patient or room. The cameras should have remotely controllable zooming and focusing lenses and also be able to pan.

4.3.1.5 Gantry. The gantry, now in the conceptual planning stage, is to be a very simple one capable of rotating approximately 270 degrees about the isocenter, although cost considerations could limit its rotation to only 180 degrees. It would then rotate at least from 90 degrees above the horizontal plane to 90 degrees below it. The center line of the gantry must pass within ±1 mm of the isocenter for any gantry angle.

The gantry must carry three 90-deg dipoles, a pair of quadrupole doublets, a range ionization chamber, passive and dynamic nozzles, an x-ray generator, a laser beam cross and a field light. The rate of rotation of the gantry should be 2 to 4 degrees per second. The treatment field size is to be up to 40 x 40 cm^2. A wobbler and raster scan system is planned.

The distance of the source to the isocenter (SAD) has not yet been decided because of cost and architectural considerations, but is expected to be between 2 and 3 m. The gantry should have anti-collision bumpers and, if possible, the counterweight should be part of the neutron shielding system. The support of the aperture-plate system has not yet been designed. A promising scheme is one in which the aperture-plate system is mounted on the floor and tracks the rotation of the gantry within ± 0.1 degree. An isocentric couch with ± 15° pitch capability is provided.

4.3.2 The Treatment Rooms

The Facility is to initially have five treatment rooms. Only two of them are similar. There is to be one room designed for head and neck therapy, one with a gantry to have beams of variable incident angle, one for experiments in biology, physics, and engineering (A&P room), and two general-purpose rooms. It will be straightforward to convert the A&P room to either a head and neck or a general-purpose therapy room, should that be expeditious.

Unless otherwise specified, all treatment rooms will have the following elements in common,

(i) Beams, (a) horizontal and vertical
(b) maximum beam size 40 x 40 cm^2
(ii) Maximum beam energy, 250 MeV
(iii) Nozzle type, passive and dynamic scan planned
(iv) Patient support, isocentric couch with three displacements (x,y,z) and three rotations (around the isocenter pitch and roll)
(v) Patient Alignment Aids,
  (a) electronic x-rays (3 directions, coaxially with beam, vertical and lateral)
  (b) 5 laser beam crosses
  (c) one field light in each beam line
(vi) Patient Monitoring,
  (a) whole body/room CCTV
  (b) irradiation area CCTV
  (c) intercom
(vii) Adjustable Aperture Plate System,
  (a) same system useable for horizontal and vertical beams.

The following abbreviations will be used to describe the magnets, and beam and radiation instrumentation used in the dedicated beam lines and the beam delivery systems,

Magnets

QM = quadrupole magnet
SPQ = special quadrant magnet
SQ = synchrotron quadrant, 90 degree dipole with focusing
SW = 6-degree switching dipole magnet

Radiation Instrumentation

BDI = beam diagnostic instrumentation
BLM = beam loss monitors
CICh = beam intensity calibration ionization chamber
IICh = beam intensity ionization chamber
RAM = radiation area monitors
RICh = range ionization chamber
SICh = symmetry ionization chamber

4.3.2.1 Head And Neck Treatment Room. It will probably be most comfortable for the patients and efficient for the therapy department to treat the eye and head and neck patients sitting up. Eye patients will lean forward into a ''tennis'' racket and patients with lesions elsewhere will lean against the chair back. A special room has been designed for these treatments. In it, the aperture plate is replaced by two snouts and the treatment couch by a chair.

(i) Beams,
(a) maximum size about 20 cm diameter, head and neck snout
(b) 5 cm diameter, eye snout

(ii) Max. Beam Energy, 80 MeV, eye snout,
180 MeV, head and neck snout
(these limits refer to nozzle and snout design but not to radiation shielding design)

(iii) Nozzle type, passive dual scattering

(iv) Patient Support, isocentric chair, with three displacements and two rotations,

(v) Patient Alignment Aids

(a) electronic x-rays (2 directions)
(b) 4 laser beam crosses
(c) field light in each snout

(vi) Patient Monitoring,

(b) irradiation area, one/snout, CCTV

(vii) Aperture-Plate System, specialized snouts on wall (eyes and head and neck on ceiling (head and neck) will have carriers either custom made brass plates or adjustable aperture plates in the head and neck snouts.

(viii) Beam Line Magnets

3 SQ, 2 SW, 10 QM

(ix) Radiation Instrumentation

7 BDI, 5 BLM, 3 RAM
2 RICh, 2 SICh, 2 IICh, 1 CICh

4.3.2.2 Experimental Treatment Room (A&P room)

(i) Beams, (a) a vertical one may be added at minimal cost later on

(iv)Patient Support, none
floor to be prepared for isocenter couch or chair

(v) Patient Alignment Devices, 5 laser beam crosses

(viii) Beam Line Magnets, 2 SQ, 4 QM
for optional vertical beam add 1 SQ, 2 QM

(ix) Beam Line Instrumentation
3(5) BDI, 2(3) BLM, 2 RAM
1(2) RICh, 1(2) SICh, 1(2) IICh, 1 CICh

Note: numbers in parentheses refer to installation of the optional vertical beam.

4.3.2.3 General-Purpose Treatment Rooms

(viii) Beam-Line Magnets,
6 SQ, 12 QM

(ix) Radiation Instrumentation,
8 BDI, 6 BLM, 2 RAM
4 RICh, 2 SICh, 2 IICh, 1 CICh

4.3.2.4 Gantry Room

(i) Beams, (a) one variable angle from horizontal to plus-minus 90 degree vertical beams (180 degree rotation). 270 degree rotation will be optional.
(b) non-standard apparent source to axis distance, 2-3m.

(iv) Patient Support, 180 degree rotation isocentric couch with three displacements and two rotations

(v) Patient Alignment Aids,
(a) electronic x-rays coaxial with proton beam, coaxial with proton beam at all gantry angles;
(b) laser beam crosses, three fixed, one coaxial with proton beam at all gantry angles;
(c) field light

(vii) Aperture-Plate System, non-standard, possibly mounted on special carrier parallel to isocentric couch, aperture plate and peripherals would track gantry to ±0.21 minutes

(viii) Beam Line & Gantry Magnets
1 SQ, 10 QM, 4 SPQ

(ix) Beam Line Instrumentation
6 BDI, 6 BLM, 1 RAM
1 RICh, 1 SICh, 1 IICh, 1 CICh

4.4 Vacuum

The vacuum system will generally follow the concepts presented in 3.4.

4.5 Beam Instrumentation

The Facility is conceived to have two types of radiation detectors, beam-line instrumentation (Sec. 4.5.1) and beam loss instrumentation (Sec. 4.5.2). In addition, a system is provided allowing calibration of certain ionization chambers in a manner traceable to the National Bureau of Standards.

4.5.1 Beam Line Instrumentation

There are to be four types of beam line instrumentation. These detectors measure beam position, clinical-beam symmetry energy, and intensity.

4.5.1.1 Beam Diagnostic Instrumentation (BDI). To ascertain that the proton beam is properly located in the beam pipes and at the entrance to the beam-transport magnets, beam diagnostic instrumentation (BDI) is placed at critical locations.

These instruments are SEM's designed to provide beam position and projected charge distributions on two orthogonal planes. They will also be usable to measure beam emittance.

Because BDIs slightly interfere with the beam and degrade its quality, most BDIs will be retractable. They will be in the beam only as needed during tune-up.

During tune-up procedures, it is planned to read out the BDIs at the end of each beam pulse. There may be several test pulses in one accelerator cycle. It will be possible to read the BDIs at frequencies of up to 15 Hz. Should there be a reason to read the BDIs at a higher frequency, special electronics and software can be designed.

BDI description

(i) beam intensity range, 3×10^9 to 2×10^{11} p/pulse.

(ii) BDI sensitive area, 4×4 cm^2
30 strips/plane on 1.5 mm centers
strip area/total area, about 2/3
mostly retractable

(iii) Estimate of minimum total charge collection,

$$Q_t = \text{efficiency} \cdot N_p \cdot q_p$$
$$= 4\times10^{-2} \times 3\times10^{9} p \times 1.6\times10^{-10} \text{ C}$$
$$= 10 \text{ pC}$$

where N_p is the number of protons, q_p is the proton charge, and 4×10^{-2} is the commonly used ratio of charge collected to charge passing through at relativistic energies. At 250 MeV, this efficiency may be higher by a factor of two.

Assume at the wings of distribution that the charge per strip is 1/100 of total charge. Then Q_s = 0.2 pC = 200 fC. If the integrator has an effective C_{fb} = 20 pF, ΔV_o = 10 mV. An analog-to-digital converter with 12-bit resolution or a gain (x10) amplifier with a 10 bit ADC will each give a satisfactory digital signal to noise of at least 4:1.

(iv). Electronics

The standard BDI package used in the Accelerator Division, including retracting hardware and controls, is to be used. This includes scanner, CAMAC modules, and software.

4.5.1.2 Symmetry Ionization Chambers (SICh). These chambers check that the actual proton distribution will be as planned. Different kinds of geometries are possible. For example, for a passive nozzle, an ICh with four 90-degree sector collectors suffices. Sums and differences divided by the sum of all four collected charges give normalized left-right and up-down asymmetry information. A universal geometry would be an SICh having a mosaic of hexagonal collectors as used at LBL for the heavy-ion symmetry ionization chamber. Then computer analysis gives beam-behaviour analysis in terms of simple asymmetries (L-R, U-D), circles, lines or any other appropriate configurations. An ICh version of the BDI can be used to monitor raster-scanning operations. It could have 60 active strips, 4.5 mm wide on 5-mm centers on each plane. Between -10 cm and +10 cm, all strips are used. From -20 to -10 cm and 10 to 20 cm, every second strip is grounded and the others connected to the scanner.

Assuming an air-filled chamber at 760 Torr and a 2-mm gap, the charge collected per strip per sweep is

$$Q_s = 3\times10^{7} \text{ p} \times \frac{1}{80} \times 4.4 \frac{\text{keV}}{\text{cm p}} \times 10^{3} \frac{\text{eV}}{\text{keV}} \times 0.2 \text{ cm}$$

$$\times \frac{1 \text{ ion-pair}}{34\text{eV}} \times 1.6 \times 10^{-19} \frac{\text{C}}{\text{ion-pair}}$$

$$= 1.6 \text{ pC/sweep},$$

where (1/80) represents the total number of strips. Assuming a feedback capacitor of 20 pF, $\Delta V \approx 0.08V$.

The symmetry ionization chamber is scanned with the electronics used for scanning BDIs. The gas filling of these chambers will be determined later.

Since protons in the 70 to 250 MeV energy range are essentially low-LET (10.6 to 4.33 keV/cm), relatively low polarizing voltages is needed to collect essentially all the charge liberated in the gas by the traversing protons. This low voltage also means that the forces between collected and high-voltage plate are very small. Hence volume distortions will be mainly due to gravitational forces.

4.5.1.3 Range Monitoring Ionization Chambers (RICh). The range of protons in tissue is primarily determined by the energy of the incoming beam. This energy can be measured precisely in the accelerator at the time the beam is extracted. But for patient-safety purposes it is desirable to have an independent means for verifying the penetration ability of the beam. This can be achieved with a range monitoring ionization chamber.

The range ionization chamber is placed in the beam path. To check the beam penetration, a small amount of beam is made to impinge on it. This chamber is made of 150 small IChs having a total thickness equivalent to approximately 40 cm of muscle tissue. Then the place in which the beam stops is a measure of the beam penetration.

This range chamber also performs a safety function. The highest-energy protons will not be able to cross it and as long as it is in place, the proton beam will not reach the patient-treatment room. There will be one such ionization chamber in every therapy beam, upstream from the nozzle. The plates will be made of either conductive equivalent polystyrene or aluminum. The gas filling will be determined later.

The useful aperture will be approximately 4 cm in diameter. The outputs from this ICh will be measured by a scanner similar to the one that will be used for the BDIs.

4.5.1.4 Beam Intensity Ionization Chambers (IICh). These will be dual transmission ionization chambers. They will be mounted behind the aperture plate. Like the other ionization chambers, they have plate separations of 2 mm and will be filled with a suitable gas.

The variable aperture-plate opening may be as large as 40×40 cm^2. Hence this intensity ICh will have a useful diameter of 60 cm. The output from these IChs can be sampled at twice the raster frequency to stop the irradiation at the end of one raster scan line when the required dose has been deposited in the tissues.

4.5.1.5 Intensity-Calibration Ionization Chamber (CICh). There should be two types of calibration ICHs, one used routinely to calibrate the transmission beam intensity ICHs and one suitable as a calibration-transfer standard. The first "ICh" may actually be a Si-diode. The second chamber can be sent on an annual basis to NBS to be calibrated in their ^{60}Cio beam.

The ICh for routine use in beam calibrations is to be mounted in a holder with variable thickness absorbers of polystyrene or teflon upstream. The whole assembly is designed to check either vertical or horizontal beams.

This chamber is used before each portal (or patient, depending on logistics) to calibrate the beam intensity ionization chamber (IICh). For calibration of the IICh, the aperture plate is set at an appropriate opening and an appropriate bolus is mounted behind the IICh. The CICh is mounted at the isocenter at an equivalent depth in tissue equal to the total depth in tissue at the center of the stretched out Bragg peak (SOBP). Then the IICh will be calibrated with respect to the CICh.

It is clear that a system to check the stability (precision) of the CICh will be needed (see Sec. 4.5.2).

The ionization detector might be small. It is to be mounted so that it is always at the isocenter, whether the assembly is set to calibrate a horizontal or a vertical beam. Provision is made for remote "depth" adjustment and verification of beam-line direction. This CICh is to be mounted so that it will automatically store out of the way after a calibration is completed.

The second ICh is to be a parallel plate ICh that will be possible to calibrate easily and reliably at LLUMC in a ^{137}Cs source in a manner similar to that used at Fermilab, but it should also be suitable for shipping to NBS for calibration in their ^{60}Co beam.

4.5.1.6 Faraday Cup. The method discussed in the previous section implies a calibration procedure in which a ^{60}Co calibration of an air-filled ionization chamber is used to calculate its volume. Then, using this known volume, one may interpret the charge collected in the proton beam as absorbed dose to tissue in that part of the beam where the ICh was located.

An independent approach makes use of the proton beam. A Faraday cup is used to measure a proton fluence. A small detector is used to scan and measure the proton beam distribution on a plane perpendicular to the beam. Then the dose that muscle tissue would have absorbed per unit area of beam can be calculated and an ICh or other detector calibrated in terms of rad per unit charge at the IICh, at the calibration energy.

4.5.1.7 Calorimeter. Calorimetry is in some respects an ideal method. The temperature rise in the core of the calorimeter due to a given proton fluence can be related to dose absorbed in muscle tissue. The calibration of the calorimeter does not require a source of radiation. In the case of polyatomic core materials, there may be exoergic or endoergic reactions.

The calorimeter should be designed in such a manner that steel can be added axially downstream and radially outwards. Then, at the time of test-line commissioning, the actual dimensions of the steel can be determined empirically. Since the synchrotron is a relatively high-current one, there will be no special signal-to-noise problems with respect to the support electronics.

It is not recommended that funds and efforts be spent at this time designing and constructing a calorimeter, but Loma Linda University Medical Center is encouraged to participate in AAPM Task Group 20 of the Radiation Therapy Committee. This group owns a calorimeter and would participate at LLOMC in calorimetric dosimetry.

4.5.2 Calibration of Ionization Chambers

A calibration system for ionization chambers similar to the one in use at the Fermilab Neutron Therapy Facility should be considered. During eight years of use, the ratio of the Fermilab calibrations to the NBS calibrations of the same IChs has been found to be 0.9993 ± 0.0030 (one standard deviation).

The system consists of a ^{137}Cs source, a precision irradiation jig, precise digital thermometers and barometers as well as a very stable quartz oscillator.

4.5.2.1 Beam-Loss Monitoring Ionization Chambers. The BLM's that have been designed by the Fermilab Accelerator Division are suitable. They have been used to monitor beam losses around circular accelerators and beam-transport lines. They are very reliable and inexpensive. The output from these IChs is connected to logarithmic electrometer amplifiers which have adjustable discriminators to set the alarm trigger level. These BLMs, amplifiers, discriminators, logic units and computer interfaces can be almost unmodified replicas of the equipment now in use at Fermilab.

4.5.2.2 Area Radiation Monitors. These RAMs are to be placed on the occupational side of the radiation shielding walls. They can consist of $^{10}BF_3$ filled proportional counters in 3-in. wall thickness polyethylene moderators. At the time of commissioning in the test line at Fermilab, the actual length of these proportional counters and their filling pressure will be determined.

To reduce costs, these counters will be run in the current mode and a single coaxial cable will carry both the high voltage and the

output signals. Commercially available fast discriminators will be used to generate standard logic pulses.

4.6 Facilities Controls

The Facility will be monitored and controlled by the control system used for the accelerator, discussed in Sec. 3.8. It has been in use at Fermilab and CERN for a number of years. This control system is based on a widely supported scheme proposed by IBM and known as the "TOKEN ring."

Requirements for the switchyard and treatment room controls are not known in detail at this time. Control system needs will depend upon the type and numbers of diagnostic devices in the switchyard, and the details of the beam-scanning equipment in the treatment rooms.

For purposes of cost estimates, two local stations are included for the switchyard and one for the nozzle in the treatment room. The switchyard system controls steering magnets in the straight line and collect data from the BDIs, IIChs, RIChs, and SIChs.

A beam-scanning system may by be used to deliver the proton beam to the patient. This system is not yet designed, but it is expected that the control of such a system will require a fast processor reading a wire chamber to confirm that the beam is scanning over the intended area. An additional processor board (perhaps a 68020 CPU card) would be installed in the local station to operate and monitor the scanning system. Communication between this processor and the local station can be done using shared memory. Chair or couch positioning and collimator parameters are to be monitored and controlled by this local station.

A treatment room console allows the medical personnel to monitor the treatment. This console includes an IBM-AT computer, four high-resolution, grabber displays to show two current and two reference x-ray views of the patient to verify that the patient's position is correct. This station is also used to enter and record treatment parameters.

A separate console is required for each treatment room.

4.6.1 Operational Description

In general terms, the controls system will provide at least the following support to the Facility.

(i) It will configure the switchyard to carry a given energy proton beam to the selected beam line of a designated treatment room.

(ii) It will set up a table of operational parameters such as raster line position and location of ends, beam energy, required proton charge at each energy step corrected for dE/dx and recent IICh calibration. Note: the beam turn-off at the end of each raster scan (at a given ramp and position) will be via dedicated and redundant hardware under computer control. The information for these tables will be obtained from the patient's floppy disks.

(iii). It will verify that the beam penetrations will be as required by the treatment plan.

(iv) It will calibrate the IICh(s).

(v) It will monitor the symmetry of the charge distributions to ascertain the proper operation of the nozzle in use.

(vi) It will assist in patient positioning via electronic x-ray acquisition support. It will store these x-ray images on request.

(vii) It will display patient's ID, name, and set-up parameters (maybe, it will also display patient's photograph). Then, it will verify that the actual positioning parameters are within acceptable tolerances from the nominal ones.

(viii) It will monitor all other relevant system parameters during patient irradiations.

(ix) At the end of each portal, it will update the patient's chart and state all systems were operating satisfactorily (or which not) during the irradiation.

(x) It will provide information on other treatment room beam requests and forecast time when beam will become available.

(xi) It will produce appropriate reports and summaries of daily, weekly, monthly and annual operations on request.

(xii) It will calibrate ionization chambers and other detectors using the ^{137}Cs source system on a daily basis. It will maintain records of such calibrations.

4.6.2 Hardware

Since the components of the TOKEN ring are relatively inexpensive, it is feasible to avoid links between the controls system and any other computer. The information on treatment plans and patient positioning will be carried on floppy disks. The patient's photograph will be affixed to the external envelope of the disk.

As discussed in Sec. 3.8, the controls system will participate in safety operations such as monitoring the BLM and RAM networks, but these two networks will be able to turn off the beam, if necessary, via dedicated hardware. The controls system will record the events leading to the beam shutdown.

From the point of view of the medical personnel the accelerator, switchyard, beam delivery systems, power vacuum, safety and cooling need not exist. The controls system will only ask for help when it will not be able to correct a parameter out of tolerance by itself. Then, it will ask for the appropriate kind of human help, e.g., vacuum technician, electronics technician, etc.

4.7 Conventional and Radiation Safety

4.7.1 Guidelines

The philosophy on safety will be the same in the whole system, namely, the system shall only operate if it may do so harmlessly to people and to equipment (see Sec. 3.10).

The radiation shielding for the whole system will be based on the following guidelines:

(i) Proton beam energy (everywhere), 250 MeV, even if use of lower energy protons is initially planned for certain areas.

(ii) The shielding walls designed conservatively.

(iii) Beam intensity in each beam line calculated using utilization factors supplied by the LLUMC personnel of normal operations at full intensity plus one full beam pulse loss per day plus eight pulses a day at 10% of full intensity for four tuneups/day.

(iv) Normal operations are defined as 0.1% beam loss at each magnet.

(v) The radiation levels estimated at 30 cm from walls, ceilings or floors as appropriate.

(vi) For shielding design, the Loma Linda University Medical Center Radiation Safety Committee will specify the maximum radiation levels in uncontrolled and controlled access radiation areas.

(vii) Fermilab personnel will provide details of their calculations and required safety factors.

(viii) The conventional and radiation safety systems will be designed by the Loma Linda University Medical Center

personnel. Fermilab personnel will only provide assistance as required by Loma Linda University Medical Center personnel.

4.7.2 Shielding References

There are no good references for shielding calculations or measurements of radiation due to 250-MeV protons incident on various targets.

There is some literature on shielding for 200-MeV protons because of the injector linacs for the Brookhaven AGS and the Fermilab accelerator.

An attempt to combine the available 200-MeV information to estimate shielding requirements for 250-MeV protons for a zero order approach to the problem is given in reference 11, still unfinished (5/6/86).

1. D. J. Hughes and R. B. Schwartz, Neutron Cross-Sections, 2nd Ed. BNL-325 (7-1-58).

2. R. E. Maerker and F. J. Muckenthaler, Calculation and Measurement of the Fast Neutron Differential Dost Albdeo for Concrete, Nucl. Sci. Eng. .u 22, 455 (1965).

3. R. G. Alsmiller, M. Leimdorfer, J. Barish; Analytical Representation of Non-elastic Cross Sections and Particle-Emission Spectra from Nucleon-Nucleus Collisions in the Energy Range 25 to 400 MeV, ORNL-4046 (April 1967).j

4. M. Awschalom, T. Borak, and P. G. Gollon, Chemical Composition of Some Common Shielding Materials, Fermilab TM-168 (5/2/69).

5. R. G. Alsmiller, The Lateral Spread of High Energy ($\leq$ 400 MeV) Neutron Beams and Earth Shine, Nucl. Instr. Math 89, 53 (1970).

6. Basic Radiation Protection Criteria, NCRP Report No. 39, National Council on Radiation Protection and Measurements, Washington, D.C., January 15, 1971.

7. P. J. Gollon and M. Awschalom; Design of Penetrations in Hadron Shields, IEEE Trans. Nucl. Sci NS-18, 741, (1971).

8. R. G. Alsmiller, R. T. Santoro, J. Barish; Shielding Calculation for a 200 MeV Proton Accelerator and Comparisons with Experimental Data, Particle Accelerators 7, 1 (1975), also available as ORNL-TM-4754 (2/1975).

9. J. F. Janni; Proton Range-Energy Tables, 1 keV - 10 GeV, Part I, compounds, Atomic Data and Nuclear Data Tables 27, 150-339 (1982, Part II, elements, ibid, pp 341-529.

10. J. D. Cossairt, J. G. Couch, A. J. Elwyn, W. S. Freeman, Radiation Measurements in a Labyrinth Penetration at a High Energy Proton Accelerator, Health Physics 49, 907 (1985).

11. M. Awschalom, Radiation Shielding for 250 MeV Protons, Fermilab TM-1354 (9/23/85). To be published.

4.8 General References

1. M. Awschalom, R. Goodwin, L. Ghrumboski, I. Rosenbert,

2. M. Shea, High Precision in Dose Delivery: Routine Usae of a Microcomputer in "Biomedical Dosimetry, Physical Aspects, Instrumentation, Calibration," Vienna: IAEA, 1978, pp. 271-280.

3. M. Awschalom, B. Bennett, The Fermilab Neutron Therapy Facility: Performance of the Automatic Photon Calibration System for Ionization Chambers, Fermilab TM-1379 (Aug. 8, 1985).

4. Task Group 20 of the AAPM Radiation Therapy Committee, "Protocol for Heavy Charged Particle Therapy Beam Dosimetry," Draft 8 Sept. 5, 1984.

5. W. Chu, M. McEvoy, M. Nyman, T. Renner, B. Gonzalez. R. P. Single, R. Stradner, "Wobbler Dosimetry for Biomedical Program at the LBL Bevalac" IEEE Trans. Nucl. Sci NS-32, 3324 (1985).

6. A.M. Koehler, R. J. Schneider, J. M. Sisterson, "Flattening of Dose Distributions for Large-Field Radiotherapy Med. Phys. 4, 297 (1977).

7. W. T. Chu, S. B. Curtis, J. Laur, T. R. Renner, R. W. Sorensen, "Wobbler Facility for Biomedical Experiments at the Bevalac," IEEE Trans Nucl. Sci NS-32, 3321 (1985).

8. T. Kanai, K. Kamachi, Y. Kumamoto, H. Ogawa, T. Yamada, H. Matsuzawa, "Spot Scanning System for Proton Radiotherapy," Med. Phys. 7, 365 (1980).

9. T. Kanai, K. Kawachi, H. Matsuzawa, "Three-Dimensional Beam Scanning for Proton Therapy," Nucl. Inst. Meth 214, 491 (1983).

10. D. Kurihara, S. Suwa, A. Tachikawa, Y. Takada, K. Takikuwa, "A 300-MeV Proton Beam Line with Energy Degrader for Medical Science," Japanese Journal of Applied Physics 22, 1599 (1983).

APPENDIX

THE HISTORY OF PROTON THERAPY

Bernard Gottschalk, Harvard Cyclotron Laboratory

This is a synopsis of the rationale, history and present status of proton therapy, to put into perspective the proposal to build a dedicated proton facility at the Loma Linda University Medical Center. An indispensable reference for anyone wishing more detail is Raju's review [1], as of 1980, of proton and other heavy-particle therapy. The most recent work can be found in a special issue of Radiation Research [2] devoted to the proceedings of a Symposium held in Berkeley in May 1985.

R. R. Wilson [3] was evidently the first to point out the potential of high energy proton beams for the therapeutic irradiation of small targets deep within healthy tissue. But protons may also be advantageous in reducing the total dose delivered in the treatment of large fields [4]. The advantages of protons rest on two physical characteristics:

- The dose delivered by a proton penetrating tissue rises as the proton slows down, reaching about 3-4 times the entrance dose near the stopping point ('Bragg peak'), and is zero beyond the stopping point. Protons in a monoenergetic beam have very nearly the same range and therefore deliver maximum dose at the same depth.

- Being heavy, protons do not deviate very much from a straight line as they come to rest.

Special techniques had to be developed to exploit these characteristics, particularly for the treatment of large lesions. A multiple scattering technique [5] for *beam broadening* allows one to treat targets of large cross-section to a uniform dose; nowadays *beam scanning* methods are under development [6] to achieve the same end with greater efficiency and flexibility. *Static range compensators* [7] are used to conform the proton range to the desired distal surface, compensating if necessary for anatomical inhomogeneities such as bone in the proton path. *Range modulation* [8] is used to deliver a uniform dose to targets whose depth exceeds the width of the Bragg peak. *Dosimetry* for protons is basically simple, but the techniques [9] differ from those used for photon beams. To take advantage of the precision possible with protons, correspondingly precise techniques of *patient positioning* [10] are required. Finally, elaborate *interactive treatment-planning* programs [11] allow the options for a given treatment to be explored and the best strategy to be selected.

Using some or all of these techniques it is frequently possible, with protons, to tailor the treatment volume so as to deliver a much higher dose to the target compared to the surrounding tissue. This may be used to increase the probability of tumor control and/or to minimize untoward side effects. This is particularly important when the lesion is near some radiosensitive or critical structure, as in the case of eye tumors or tumors abutting the central nervous system.

Other heavy charged particles (negative pions and heavy ions) may, it is thought, have an additional advantage in terms of improved ability (relative to normal-tissue damage) to destroy certain tumors. A heavy-ion clinical program is underway at Berkeley [12]. Between 1974 and 1981, 227 patients were treated with pions at Los Alamos [13], and pion treatments are continuing at SIN [13] and TRIUMF [14]. These particles share to some degree the dose-distribution advantage of protons and helium ions, but their *biological*

advantage remains to be clinically established. In any event, the advantage of protons over photons rests entirely on dose distribution.

The first work on the biological and medical application of proton beams was done by J. H. Lawrence and C. A. Tobias at Berkeley starting in 1948 [15]; the first patients were treated in 1954 using a high-energy beam and relying on rotation (the 'cross-fire' technique) to concentrate the dose in the target. Initial clinical work at Berkeley used 340 MeV protons; since 1957 work at the 184″ cyclotron has made use of 910 MeV helium ions.* To date some 1630 patients† have been treated with helium ions or protons at Berkeley. They fall into two broad categories.‡ The first (sometimes termed 'radiosurgery') consists of treatments, usually of non-malignant disease, in a single session or a small number of sessions. The Bragg peak is used with a relatively small number of fields to concentrate the dose, or cross-fire may be used with a higher-energy beam and a larger number of fields. Some 1100 patients have received this type of treatment at Berkeley, approximately 900 for disorders of the pituitary or for suppression of pituitary function for other reasons [16] and, more recently, some 200 for arteriovenous malformations (AVM's) in the brain [17].

The second class consists of conventional fractionated therapy using the Bragg peak and a relatively small number of fields. Part of the treatment may be given with photons. In this category the Berkeley group has treated some 240 patients for ocular melanoma and 300 for tumors at various other sites (abdomen, thorax, head and neck...). They report [18] good results for smaller tumors that might be expected to respond well to conventional radiotherapy, but would be difficult to treat because of their location. Patients with larger more 'radioresistant' tumors such as carcinoma of the esophagus and the pancreas have not done well, and are now treated with heavy ions in the hope of a biological advantage.

Another early entry in the field was the Uppsala group under B. Larsson and L. Leksell who started work in 1955 and treated their first patient in 1959 [19] using the 185-MeV cyclotron of the Gustav Werner Institute. This group was active until the early 1970's, treating 69 patients with large-field range-modulated proton beams at a wide variety of disease sites, as well as 25 with narrow-beam irradiation of intracranial structures. The machine was then shut down for an extensive improvement program which is now nearly complete [20]. Plans call for treating malignant ocular melanomas, pituitary tumors, AVM's and small tumors near the base of the skull with narrow proton beams, and larger tumors when broad, modulated beams again become available.

Pre-clinical work on proton therapy was started at Harvard University in 1959 by W. H. Sweet and R. N. Kjellberg (Mass. General Hospital) in conjunction with A. M. Koehler and W. M. Preston (Harvard Cyclotron Laboratory, HCL). The relatively low proton energy (160 MeV) essentially forced the use of the Bragg peak technique. After a

* The biological effects of helium ions are similar to those of protons, except perhaps near end-of-range; that is, they are considered low-LET particles. The physical dose distribution is even sharper than for protons.

† Most patient counts given here are approximate and only meant to convey a general feeling for the clinical experience that has accumulated.

‡ The same categories apply to Harvard and to the proton program in the USSR.

series of animal experiments the first patients were treated in 1961 for advanced cerebral tumors [21]. Techniques for large-field therapy were developed in the early 1970's and starting in 1974, H. D. Suit and M. Goitein (Mass. General Hospital) and their associates have made extensive use of the facility for studies of proton therapy using fractionated treatment schedules. Treatment of choroidal melanomas started in 1975 after preclinical studies on owl monkeys [22]; now carried out by E. Gragoudas (Mass. Eye and Ear Institute) and his associates, this has become the most common procedure performed at HCL. To date some 3400 patients have been treated at HCL. In the 'radiosurgery' category these number 1030 for pituitary disorders, 780 for AVM's and 310 for miscellaneous intracranial lesions. Those receiving fractionated radiotherapy include 820 choroidal melanoma patients, 110 who have had proton boost treatment for prostatic cancer and 240 large-field treatments for malignant disease at other sites (brain, head-and-neck, bone and soft-tissue sarcomas). Approximately 500 patients are treated per year, and the pituitary, AVM and ocular melanoma treatments are performed on a fee-for-service basis.

The literature on follow-up of HCL patients is extensive and we only mention some recent articles. Kliman et al. [23] summarize a 20-year experience with Bragg peak therapy of 510 cases of acromegaly; 435 were followed up, with a long-term cure rate (defined by human growth hormone hGH level) of 75% at 10 years. Complications, mainly visual system disorders of fairly short duration, ocurred in only 3.7% of the cases. Kjellberg et al. [24] have reported observations on 118 patients with Cushing's disease and 29 with Nelson's syndrome treated with Bragg peak therapy from 1964-1984 and find remission rates, with low incidence of side effects, in respectively 85% and 80% of these cases. Follow-up from 2 to 16 years has been reported [25] for 75 consecutive patients treated for AVM's of the brain. Many of these patients were inoperable by other techniques. At the dose levels used, which are selected so as to avoid complications from the proton treatment, protection from death due to hemorrhage appears to develop gradually; among the 75 patients there were two deaths during the first 12 months after treatment, but none thereafter.

Austin-Seymour et al. [26] have reported data on the 965 patients who had received fractionated radiotherapy at HCL through 1984. Among these were 43 patients treated for chordomas or low-grade chondrosarcomas of the base of skull or cervical spine, followed for at least 8 months with a median follow-up of 27 months. The 3-year actuarial local control rate in this group was 89%. In a total of 615 patients with ocular melanomas, tumor regression was seen in 94% of patients followed for more than 2 years, and 66% had vision of 20/100 or better in the treated eye.

Continuing our survey of proton treatment facilities, there is an extensive program in the USSR at three centers: the 1000-MeV synchrocyclotron in Gatchina, a 70-200 MeV proton beam at the Dubna synchrocyclotron and a 70-200 MeV beam from the 10-GeV synchrotron at the Institute of Theoretical and Experimental Physics (ITEP) in Moscow. The Dubna machine had treated 84 patients as of 1975 when it was shut down until 1984; it is now reported [27] to have resumed operation with two proton therapy rooms. As of 1985, 381 patients had been treated at Gatchina [28]; these procedures were all intracranial radiosurgery using crossfire and, usually, a single session. With the exception of 94 AVM's, most treatments were for pituitary lesions or palliation of other conditions (breast cancer,

diabetic retinopathy) by suppression of pituitary function. A dedicated proton beam and two treatment rooms are planned.

The largest and most active Soviet center is ITEP [29]. Beams at five energies from 70 to 200 MeV are available from the synchrotron using an extraction scheme which permits therapy to take place simultaneously with physics research. As of 1981, 575 patients had been treated in a single treatment room, using two treatment setups. One is a rotating stereotactic device for intracranial radiosurgery, and the other, a treatment table for general radiotherapy. A wide variety of conditions have been treated at ITEP: the 575 patients break down into 136 tumors of the uterine cervix, 39 patients with vulvar carcinoma, 196 treatments for suppression of pituitary function in the normal gland, 74 pituitary gland tumors, 59 eye tumors, 17 bone tumors, 35 skin tumors and 19 other cases. Based on this diverse experience the ITEP group conclude that the advantages of proton irradiation of small lesions are proven, and that there are certainly other large fields where proton therapy would be beneficial. Accordingly, two additional treatment rooms already available at ITEP are being fitted with various specialized treatment setups in anticipation of an active program.

Japan has two treatment centers which have only been active for a few years but are distinguished by some rather advanced technology [30]. The National Institute of Radiological Sciences (NIRS) at Chiba features the first 3-dimensional beam-scanning system that has actually been used in therapy, though the limited penetration (3.6 cm) of the 70-MeV proton beam restricts the kinds of cases that can be treated. 29 patients were treated for a variety of tumors from 1979 through 1984. 9 out of 11 patients receiving protons only had local control of the tumor, two with serious complications; of the 18 patients receiving proton boost, 12 had local control, with no complications. The Particle Radiation Medical Science Center (PARMS) at Tsukuba uses a vertical 250-MeV beam obtained from the booster synchrotron of the High Energy Physics Laboratory. Clinical trials were started in April 1983 and 22 patients had been treated for a wide variety of tumors as of February 1984. All but six (five of them glioblastomas) had local control without complications.

We complete our survey of low-LET particle beam facilities by noting that ocular melanomas are now treated at SIN (120 patients over the past two years) using a 70-MeV beam from the injector cyclotron. A 200-MeV isochronous cyclotron at the National Accelerator Center near Capetown, South Africa has just had internal beam, and proton treatments are planned there within the next few years.

The present outlook for proton therapy can be summarized quite briefly. Single-session intracranial radiosurgery is very successful and has all the advantages of a non-invasive technique but must compete, in the case of the pituitary, with improved surgical techniques and drug treatments and, for AVM's, with cross-fire and rotational arc techniques using megavoltage X-rays. In fractionated radiotherapy of cancer, a few sites (e.g. choroidal melanoma and tumors abutting the CNS) have been identified where the dose distribution obtainable with protons is compelling, and where results are excellent. Tumors that do not respond to conventional radiotherapy appear, as expected, not to respond to low-LET beams either. That leaves a large middle ground of common tumors which are managed

fairly well with photons but might be managed even better with the better dose distribution of protons. It will require large numbers of patients to demonstrate gains in this area, and just such a facility as the proposed LLUMC center to take this next step. In the words of Goitein et al. [31] '...We conclude that such therapy has reached the stage at which clinical implementation is practical and that a broader program is needed if the clinical advantages of improved dose distributions are to be determined.'

Bibliography

[1] M. R. Raju, "Heavy Particle Radiotherapy," Academic Press (1980)

[2] Proceedings of the Symposium on Heavy Charged Particles in Research and Medicine held at the Lawrence Berkeley Laboratory, University of California, May 1985: Radiation Research **104**, No. 2, S1-S334 (hereinafter '1985 Symposium')

[3] R. R. Wilson, 'Radiological use of fast protons,' Radiology **47**, 487 (1946)

[4] J. O. Archambeau, G. W. Bennett and S. T. Chen, 'Potential of proton beams for total nodal irradiation,' Acta Radiol. Ther. Phys. Biol. **13**, 393 (1974)

[5] A. M. Koehler, R. J. Schneider and J. M. Sisterson, 'Flattening of proton dose distributions for large-field radiotherapy,' Med. Phys. **4**, 297 (1977)

[6] M. Goitein and G. T. Y. Chen, 'Beam scanning for heavy charged particle radiotherapy,' Med. Phys. **10**, 831 (1983)

[7] M. S. Wagner, 'Automated range compensation for proton therapy,' Med. Phys. **9**, 749 (1982)

[8] A. M. Koehler, R. J. Schneider and J. M. Sisterson, 'Range modulators for protons and heavy ions,' Nucl. Inst. and Meth. **131**, 437 (1975)

[9] L. J. Verhey, A. M. Koehler, J. C. McDonald, M. Goitein, I. Ma, R. J. Schneider and M. S. Wagner, 'The determination of absorbed dose in a proton beam for purposes of charged-particle radiation therapy,' Rad. Res. **79**, 34 (1979)

[10] L. J. Verhey, M. Goitein, P. McNulty, J. E. Munzenrider and H. D. Suit, 'Precise positioning of patients for radiation therapy,' Int. J. Rad. Onc. Biol. Phys. **8**, 289 (1982)

[11] M. Goitein and M. Abrams, 'Multi-dimensional treatment planning: I. Delineation of anatomy,' Int. J. Rad. Onc. Biol. Phys. **9**, 777 (1983)

M. Goitein, M. Abrams, D. Rowell, H. Pollari and J. Wiles, 'Multi-dimensional treatment planning: II. Beam's-eye view, back projection and projection through CT sections,' Int. J. Rad. Onc. Biol. Phys. **9**, 789 (1983)

[12] J. R. Castro, G. T. Y. Chen and E. A. Blakely, 'Current considerations in heavy charged-particle radiotherapy: A clinical research trial of the University of California Lawrence Berkeley Laboratory, Northern California Oncology Group, and Radiation Therapy Oncology Group,' 1985 Symposium S263

[13] G. Schmitt, C. F. von Essen, R. Greiner and H. Blattman, 'Review of the SIN and Los Alamos pion trials,' 1985 Symposium S272

[14] G. B. Goodman, P. Dixon, G. K. Y. Lam, R. Harrison, R. O. Kornelsen, C. M. Ludgate and A. D. Flores, 'Preparatory clinical studies of pi-mesons at TRIUMF,' 1985 Symposium S279

[15] C. A. Tobias, H. O. Anger and J. H. Lawrence, 'Radiological use of high energy deuterons and alpha particles,' Am. J. Roentgenol. Rad. Ther. Nucl. Med. **67**, 1 (1952)

[16] J. H. Lawrence, 'Proton irradiation of the pituitary,' Cancer **10**, 795 (1957)

[17] J. I. Fabrikant, J. T. Lyman and K. A. Frankel, 'Heavy charged-particle Bragg peak radiosurgery for intracranial vascular disorders,' 1985 Symposium S244

[18] W. Saunders, J. R. Castro, G. T. Y. Chen, J. M. Collier, S. R. Zink, S. Pitluck, T. L. Phillips, D. Char, P. Gutin, G. Gauger, C. A. Tobias and E. L. Alpen, 'Helium-ion radiation therapy at the Lawrence Berkeley Laboratory: recent results of a Northern California Oncology Group clinical trial,' 1985 Symposium S227

[19] B. Larsson, L. Leksell and R. Rexed, 'The use of high energy protons for cerebral surgery in man,' Acta Chir. Scand. **125**, 1 (1963)

[20] Börje Larsson, 'Biomedical program for the converted 200-MeV synchrocyclotron at the Gustaf Werner Institute,' 1985 Symposium S310

[21] R. N. Kjellberg, W. H. Sweet, W. M. Preston and A. M. Koehler, 'The Bragg peak of a proton beam in intracranial therapy of tumors,' Trans. Amer. Neurol. Assoc. **87**, 216 (1962)

[22] I. J. Constable and A. M. Koehler, 'Experimental ocular irradiation with accelerated protons,' Invest. Ophthal. **13**, 280 (1974)

[23] B. Kliman, R. N. Kjellberg, B. Swisher and W. Butler, 'Proton beam therapy of acromegaly: a 20-year experience,' in *Secretory Tumors of the Pituitary Gland* (Progress in Endocrine Research and Therapy, Vol. I), edited by Peter McL. Black et al., Raven Press, New York (1984), 191

[24] R. N. Kjellberg, B. Kliman, B. Swisher and W. Butler, 'Proton beam therapy of Cushing's disease and Nelson's Syndrome,' ibid., 295

[25] R. N. Kjellberg, T. Hanamura, K. R. Davis, S. L. Lyons and R. D. Adams, 'Bragg-peak proton-beam therapy for arteriovenous malformations of the brain,' New England Journal of Medicine **309**, 269 (1983)

[26] M. Austin-Seymour, J. E. Munzenrider, M. Goitein, R. Gentry, E. Gragoudas, A. M. Koehler, P. McNulty, E. Osborne, D. K. Ryugo, J. Seddon, M. Urie, L. Verhey and H. D. Suit, 'Progress in low-LET heavy particle therapy: intracranial and paracranial tumors and uveal melanomas,' 1985 Symposium, S219

[27] I. Riabukhin, 'Status of therapy with protons in USSR,' International Workshop on Particle Accelerators in Radiation Therapy, Houston, Texas (1982)

[28] N. K. Abrosimov, A. A. Vorobev, E. A. Zherbin and B. A. Konnov, 'Proton therapy at the cyclotron in Gatchina, USSR,' 1986. Preprint, translated at Fermilab by D. Jovanovic.

[29] I. V. Chuvilo, L. L. Goldin, V. S. Khoroshkov, S. E. Blokhin, V. M. Breyev, I. A. Vorontsov, V. V. Ermolayev, Ya. L. Kleinbock, M. I. Lomakin, M. F. Lomanov, V. Ya. Medved, N. A. Miliokhin, V. M. Narinsky, L. M. Pavlonsky, G. G. Shimchuck, A. I. Ruderman, G. D. Monzul, E. L. Shuvalov, V. N. Kiseliova, E. I. Marova, L. E. Kirpatovskaya, E. I. Minakova, V. A. Krymsky, A. F. Brovkina, G. D. Zarubey, I. M. Reshetnikova and A. V. Kaplina, 'ITEP synchrotron proton beam in radiotherapy,' Int. J. Rad. Onc. Biol. Phys. **10**, 185 (1984)

[30] H. Tsunemoto, S. Morita, T. Ishikawa, S. Furukawa, K. Kawachi, T. Kanai, H. Ohara, T. Kitagawa and T. Inada, 'Proton therapy in Japan,' 1985 Symposium S235

[31] M. Goitein, H. D. Suit, E. Gragoudas, A. M. Koehler and R. Wilson, 'Potential for low-LET charged-particle radiation therapy in cancer,' 1985 Symposium S297